

Evaluation of estrogenic effects of compounds using novel estrogen-responsive genes and elucidation of their mechanisms of action

西, 健太郎

<https://hdl.handle.net/2324/7363913>

出版情報 : Kyushu University, 2024, 博士 (工学), 論文博士
バージョン :
権利関係 :



Evaluation of estrogenic effects of
compounds using novel estrogen-responsive genes and elucidation
of their mechanisms of action

Kentaro Nishi

Contents

Chapter 1: General Introduction

1-1 What is estrogen?	1
1-2 Effects of estrogen on cells	2
1-3 Estrogen-responsive genes	5
1-4 Aim of this Research	6

Chapter 2: Novel Estrogen-Responsive Genes (ERGs) for the Evaluation of Estrogenic Activity

2-1 Introduction	7
2-2 Materials and methods	
2-2-1 Materials	7
2-2-2 Sulforhodamine B (SRB) assay	8
2-2-3 Western blotting	9
2-2-4 RNA-seq analysis	10
2-2-5 <i>Real-time</i> RT-PCR	11
2-2-6 Data analysis for gene expression	14
2-3 Evaluation of cell proliferative activity by 17 β -estradiol (E ₂)	14
2-4 Evaluation of intracellular signals	15
2-5 Identification and analysis of novel estrogen-responsive genes	16
2-6 Evaluation of 30 novel estrogen-responsive genes	18
2-7 Functional analysis of novel estrogen-responsive genes	20
2-8 Characteristics of 30 novel estrogen-responsive genes and classification of ERs	22
2-9 Conclusion	29

Chapter 3: Estrogenic Activity of Fermented Soymilk Extracts and Soy Compounds

3-1 Introduction	30
------------------	----

3-2 Materials and methods	
3-2-1 Materials	31
3-2-2 Fermentation method for soymilk	31
3-2-3 Sulforhodamine B (SRB) assay	33
3-2-4 Western blotting	33
3-2-5 RNA-seq analysis	33
3-2-6 <i>Real-time</i> RT-PCR	34
3-2-7 Data analysis for gene expression	34
3-3 Evaluation of cell proliferation activity by soymilk extracts and soy compounds	35
3-4 Evaluation of intracellular signals	38
3-5 Gene expression analysis by RNA-seq	50
3-6 Gene expression analysis by <i>Real-time</i> RT-PCR	61
3-7 Enrichment analysis using RNA-seq data	65
3-8 Conclusion	68
Chapter 4: Estrogenic prenylated flavonoids in <i>sophora flavescens</i>	
4-1 Introduction	69
4-2 Materials and methods	
4-2-1 Materials	70
4-2-2 Sulforhodamine B (SRB) assay	70
4-2-3 Western blotting	71
4-2-4 <i>Real-time</i> RT-PCR	71
4-2-5 Cluster analysis using <i>real-time</i> RT-PCR data	72
4-3 Evaluation of cell proliferation activity by prenylated flavonoids	72
4-4 Evaluation of intracellular signals	72

4-5 Gene expression analysis by <i>Real-time</i> RT-PCR	78
4-6 Conclusion	87
Chapter 5: General conclusion	88
Acknowledgement	90
References	91

Chapter 1: General Introduction

1-1 What is estrogen?

Estrogens are steroid hormones with a cholesterol skeleton produced in the ovary. Primarily, estrone (E_1), 17β -estradiol (E_2) and estriol (E_3) are synthesized from cholesterol via several processes when luteinizing hormone (LH) acts (Figure 1). Of these three types of estrogen, E_2 has the highest

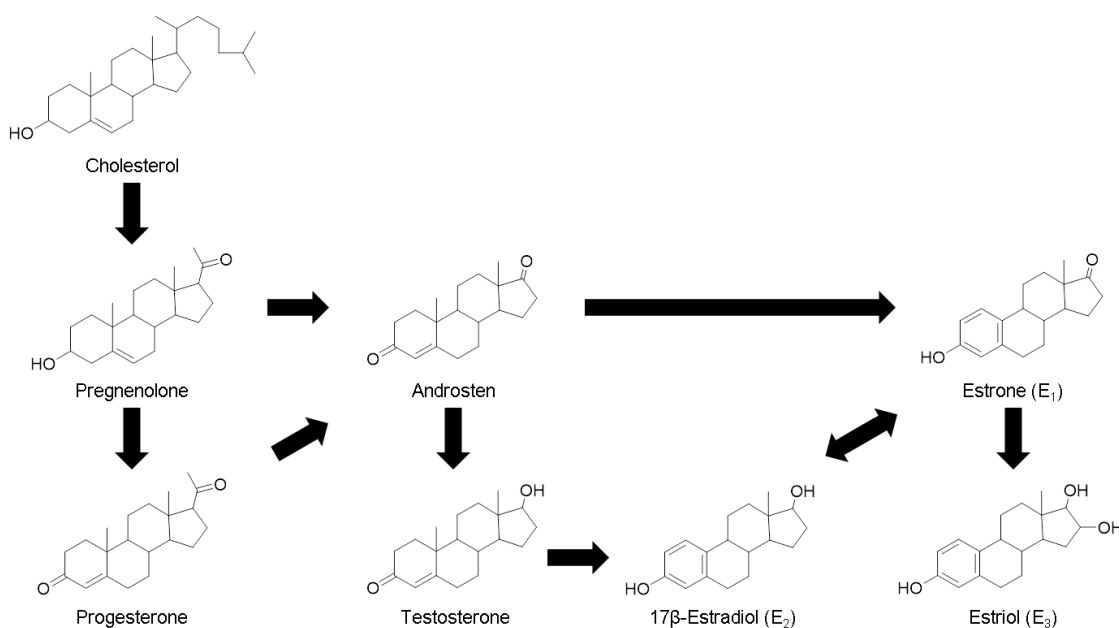


Figure 1 Synthesis pathway of estrogen.

physiological activity, followed by E_1 and E_3 , and its physiological activities include the development of the reproductive organs, regulation of the menstrual cycle, and bone formation [1]. Among them, mammary gland development is promoted by estrogen's binding to the estrogen receptor (ER) of cells, which promotes cell proliferation through intracellular signaling and direct action on the genome. However, estrogen is problematic in the presence of breast cancer because it is a strong cell growth factor [2-7]. In addition, bone formation is based on the balance between osteoblasts and osteoclasts, and estrogen induces anti-apoptosis in osteoblasts and apoptosis in osteoclasts via ER [8]. A deficiency of estrogen can cause osteoporosis, and estrogen is used as a treatment for osteoporosis, but this also has the same problems as mentioned above.

Therefore, there are a number of compounds that exhibit similar functions, called phytoestrogens, as alternatives to estrogen. Typical compounds are genistein and daidzein in soy isoflavones [9-12], which are used as alternatives to estrogen and have anticancer activity against breast cancer [13]. On the other hand, endocrine disruptors such as bisphenol A, a monomer of polycarbonate, are compounds that act at lower concentrations than estrogen and have a strong effect on transcription, and their biological effects are serious [14] (Figure 2).

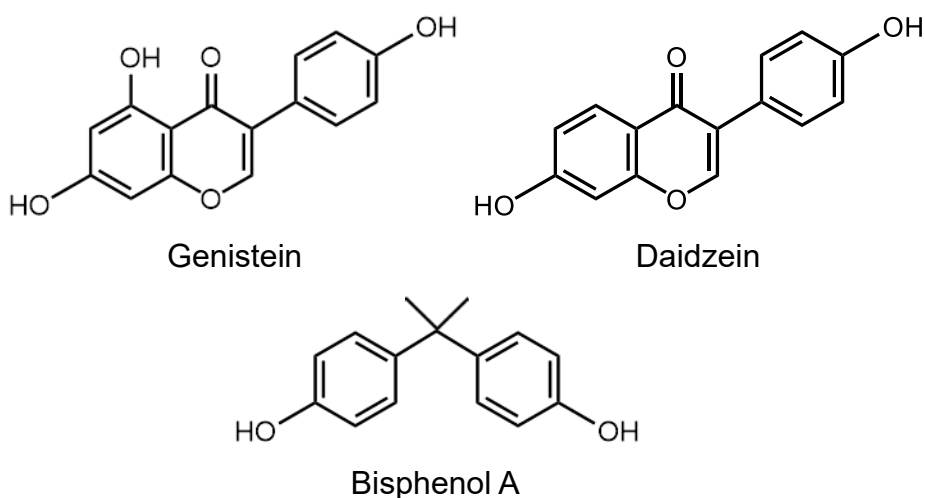


Figure 2 Examples of estrogen-like compounds.

While estrogen is an important hormone for maintaining women's physiological functions, it is problematic for breast cancer, so it is important to clarify its mechanism. Furthermore, although there are many compounds in the world that can substitute for estrogen, clarification of the mechanism of action is expected to lead to develop of safe alternative compounds and drug [15].

1-2 Effects of estrogen on cells

There are two types of estrogen action: a genomic pathway, in which estrogen binds to estrogen receptor α (ER α) and estrogen receptor β (ER β) and directly acts on the genome, and a non-genomic pathway, in which estrogen binds to G protein-coupled estrogen receptor (GPER) and then regulates transcription via signal transduction, affecting various cellular functions [5-7,16-18] (Figure 3). ER α and ER β are nuclear receptors encoded by *Estrogen receptor 1 (ESR1)* and *Estrogen receptor 2*

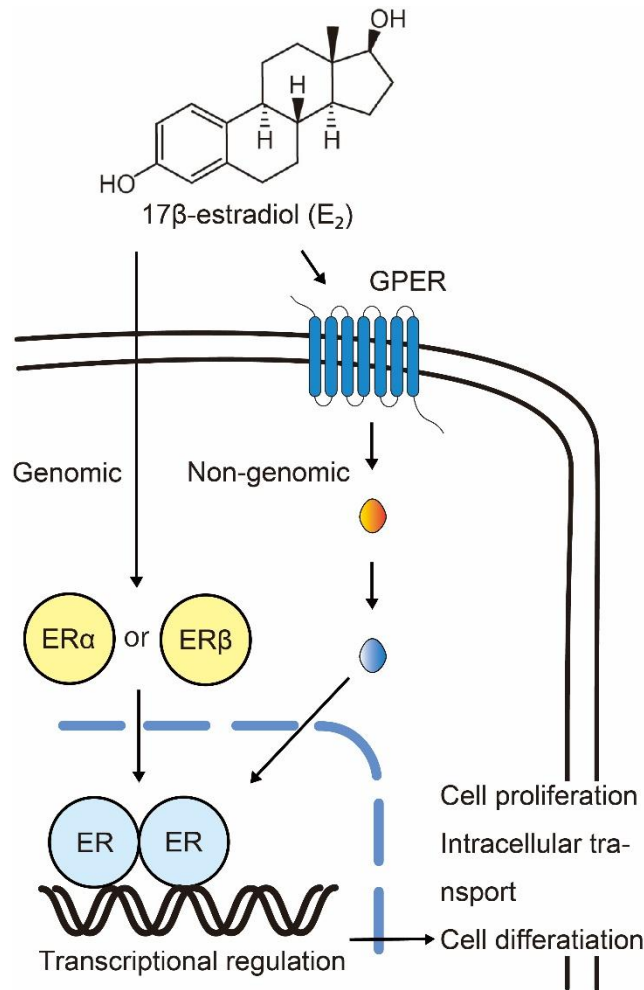


Figure 3 Intracellular pathway of estrogen.

(*ESR2*), respectively, and are located in the cytoplasm. The genomic pathway involving these two receptors is a pathway in which non-water-soluble estrogen is taken into the cell, binds to each receptor, and forms homodimers and heterodimers of each receptor [19, 20], and regulates gene transcription by binding to the genome. On the other hand, GPER is a membrane receptor encoded by *GPER1* that is present in the cell membrane. The non-genomic pathway involving GPER is initiated by the binding of estrogen to GPER, which is then phosphorylated, and the signal is transmitted through the Mitogen-activated Protein Kinase (MAPK) pathway and Phosphatidylinositol-3 kinase (PI3K)/Akt pathway, and then affects various cell functions by acting on genes in the genome [20] (Figure 3). These receptors have been confirmed to be expressed in various tissues, and while they

play a role in maintaining biological functions, as mentioned earlier, they are a problem in breast cancer because estrogen can act as a strong cell growth factor. However, the breast cancer cell line MDA-MB-231 is a triple-negative breast cancer cell line that is immunohistochemically negative for estrogen receptors (ER) and progesterone receptors (PR), and it also does not overexpress or lack human epidermal growth factor receptor 2 (HER2). Therefore, triple-negative breast cancer cells are difficult to treat with hormone therapy or trastuzumab therapy that act through receptors [21]. On the other hand, MCF-7 cells are breast cancer cells that express ER and PR and do not express HER2, so they can generally be treated with aromatase inhibitors or anti-estrogen drugs. Therefore, MCF-7 cells are essential for research into the receptor-mediated mechanisms of estrogen action.

It is known that MCF-7 cells respond very quickly to estrogen in the MAPK and PI3K/Akt pathways [20, 22, 23]. Therefore, one way to check for estrogen activity is to stimulate MCF-7 cells with estrogen or phytoestrogen and then assess the phosphorylation activity of the Extracellular signal-regulated kinase 1/2 (Erk1/2) protein and the Akt protein [15,24]. Estrogen activity can also be evaluated by cell proliferation activity. When MCF-7 cells are stimulated with estrogen or phytoestrogen, they show cell proliferation activity in an estrogen receptor-dependent manner, so by comparing this with experiments using estrogen receptor inhibitors, it is possible to evaluate whether cell proliferation is affected by estrogen or not [15,24]. Furthermore, it is also possible to evaluate estrogen activity by extracting mRNA from MCF-7 cells after stimulation with estrogen or phytoestrogen and examining specific genes [20,24]. Estrogen exerts various effects on cell functions by directly and indirectly regulating transcription through its strong binding to membrane receptors and nuclear receptors in cells. Therefore, there are still many unknown aspects of the intracellular mechanisms related to estrogen, and clarifying these mechanisms is expected to lead to the development of new treatments for breast cancer.

1-3 Estrogen-responsive genes (ERGs)

As mentioned in the previous section, estrogen receptors activated by estrogen affect gene expression as transcription factors that bind to promoter and enhancer regions of genes [25]. In other words, by comparing genes that change significantly in response to estrogen stimulation with those that do not, we can find estrogen-responsive genes (ERGs). The existence and function of estrogen receptors were discovered in the 1960s, which led to the idea of ERGs in the 1970s [26]. Since then, ERGs such as the *TFF1* gene (formerly named *pS2*) have been studied [27]. Since 2000, when DNA microarrays were actively used in research, genes could be analyzed on a large scale, statistically significant ERGs were profiled and used in screening for estrogenic activity [20,28], and a number of ERGs were discovered. A large number of ERGs have been discovered and databases have been created [29]. The development of next-generation sequencers has enabled large-scale analysis of the entire genome, which was not possible with microarrays, and additional ERGs that have not been found so far have been discovered [24,30,31].

ERGs include, for example, *TFF1*, which encodes a secreted protein mentioned earlier and was the first ERG identified in MCF-7 cells, where it is associated with breast cancer metastasis [32]. On the other hand, it has also been reported as a tumor suppressor protein in gastric cancer [33]. As mentioned in the previous section, *ESR1* is ERG encoding ER α [20] and has been studied in the treatment of breast cancer and prostate cancer [34]. Furthermore, *PDZK1* and *GREB1*, which are ERGs, are also important target genes in breast cancer therapy because their proteins are associated with cytoskeleton formation and cell proliferation [35-37]. Profiling ERGs, including these genes, is expected to be applied as a target for genetic testing in mammaprint and blueprint [38], and can also be used to evaluate the activity of new phytoestrogens [20]. Thus, the study of ERGs is important not only to understand the transcriptional mechanism of estrogenic activity, but also because the use of such genes may lead to therapy and drug discovery [31].

1-4 Aim of this Research

The aim of this study is to identify novel estrogen-responsive genes and elucidate the mechanisms of cellular responses to estrogen and phytoestrogens. Specifically, the study seeks to analyze the effects of intracellular signaling and gene expression mediated through the Estrogen Receptor (ER) and G Protein-Coupled Estrogen Receptor (GPER) pathways, and to clarify the stability and significance of expression variations in newly selected estrogen-responsive genes. Additionally, this study aims to uncover the mechanisms of action of phytoestrogens as alternatives to estrogen, demonstrate the utility of estrogen-responsive genes, and facilitate the discovery of novel phytoestrogens. Furthermore, the potential of analyzing mechanisms of action using *real-time* RT-PCR-based expression analysis of the newly identified estrogen-responsive genes will be explored. Through the identification of highly reliable estrogen-responsive genes, this study is expected to contribute not only to the discovery of novel compounds but also to genetic approaches for estrogen-related diseases and the treatment of breast cancer.

Chapter 2: Novel Estrogen-Responsive Genes (ERGs) for the Evaluation of Estrogenic Activity

2-1 Introduction

When describing the effects of stimulating cells with estrogen or phytoestrogen, it is important to use estrogen-responsive genes (ERGs) that always respond to stimulation and have stable expression variations. Furthermore, the use of ERGs improves the reliability of the results in studies on estrogen or phytoestrogen [24, 39]. If the expression of genes is unstable, it is possible that a result could lead to false-positive or false-negative results. Therefore, it is thought that ERGs with stable expression variation will allow us to discover compounds with similar effects to estrogen with a high probability. In addition, if these genes are used as markers, it is expected that they will be useful for improving the accuracy of MammaPrint as described in the previous chapter.

In this study, we identified new estrogen-responsive genes (ERGs) by using RNA-seq to examine all genes from the entire genome and performing statistical analysis. In addition, the reliability of the ERGs identified was assessed by comparing their correlation and coefficient of variation against a previous dataset of a reference set of the ERGs obtained from DNA microarray profiling [39]. We selected 30 novel ERGs based on the coefficient of variation and analyzed their gene functions employing Gene Ontology (GO) and Kyoto Encyclopedia of Genes and Genomes (KEGG). Furthermore, we classified the 30 ERGs to which of the two estrogen receptors they are related to, utilizing the results of ChIP-seq data registered with NCBI.

2-2 Materials and methods

2-2-1 Materials

MCF-7 cells (Japanese Collection of Research Bioresources Cell Bank) were used as human ER-positive breast cancer cells. Normal culture conditions were RPMI 1640 (Gibco, Thermo Fisher Scientific Inc., Waltham, MA, USA) without phenol red, 10% fetal bovine serum (FBS) (Gibco,

Thermo Fisher Scientific) and incubated in an incubator regulated at 37°C, 5% CO₂, and passaged once every 3 days (conditions of temperature and CO₂ are the same below). Antibodies used for Western blotting were Total Erk1/2 (T-Erk, #9102), Phospho-Erk1/2 (P-Erk, #9101), Total Akt (T-Akt, #4691) or Phospho-Akt (P-Akt, #4060) (Cell Signaling Technology, Inc., Ipswich, MA).

2-2-2 Sulforhodamine B (SRB) assay

The SRB assay was performed according to Dong et al. [24,40,41]. MCF-7 cells grown in normal culture were passaged at 1.5×10^4 cells/well in 24-well plates for the experiments. The medium used was RPMI 1640 plus 10% (v/v) dextran-coated charcoal-treated FBS (DCC-FBS) (Gibco; Thermo Fisher Scientific) for 3 days. After incubation, the cells were incubated with 10 nM 17 β -estradiol (E₂; Sigma-Aldrich St. Louis, MO, USA), 1 μ M ICI 182,780 (ICI; Sigma-Aldrich) or 0.1% dimethyl sulfoxide (vehicle; Cont) (DMSO: FUJIFILM Wako Pure Chemical Co). After incubation, all medium in each well was removed, and 10% trichloroacetic acid (TCA; Sigma-Aldrich) solution was added to fix all proteins, and the reaction was carried out in a refrigerator at 4°C for 30 min. After the reaction, the TCA solution was removed, washed three times with ultrapure water, and air-dried. After air-drying, the protein in the cells were stained with 0.4% sulforhodamine B (SRB; Sigma-Aldrich) solution dissolved in 1% acetic acid for 20 min at room temperature, and after staining, all SRB solution was removed. After washing three times with 1% acetic acid, the fixed proteins were dissolved in 10 mM unbuffered Tris-base (pH = 10.5) by shaking for 10 min at room temperature, and finally, the solution was transferred to a 96-well plate. The absorbance was measured at 490 nm employing a Modular-Designed Multimode Reader SH-9000 (Corona Electric Co., Ltd., Japan). The absorbance obtained was calculated by dividing the absorbance of each well stimulated with the compound by the absorbance of Cont to calculate the ratio of cell proliferation. Experiments were performed three times independently, mean and standard deviation were calculated, and *t*-test was used for statistics.

2-2-3 Western blotting

Western blotting was also performed according to the method of Dong et al. [24,40,41]. Normally cultured MCF-7 cells were plated in 6-well plates at 1×10^5 cells/well for experiments. 6-well plates of cells were cultured for 2 days using RPMI 1640 containing 10% DCC-FBS, then replaced with serum-free RPMI 1640 for another day. The cells were then replaced with serum-free RPMI 1640 and cultured for another 1 day. After culture, MCF-7 cells were stimulated with 1 μ M ICI, 10 nM E₂ or 0.1% DMSO (vehicle) for 0 (control), 5, 15, 30 and 60 min (37°C, 5% CO₂). 1 μ M ICI was pre-treated for 1 hour before stimulation with each compound if inhibition experiments were performed. After stimulation, cells were lysed by 1 \times sample buffer to make lysate solution. Each lysate solution, divided by stimulation time, was sonicated for 30 sec and then heat treated at 95°C for 5 min to make samples for Western blotting. Each sample was subjected to SDS-PAGE using e-PAGEL (ATTO Corp., Tokyo, Japan) at a constant current of 20 mA per gel for 1 hour. Next, semi-dry transfer cells (Bio-Rad Laboratories, Inc., Benicia, CA) were used to blot gels to nitrocellulose membranes (Millipore, Billerica, MA) at a constant current of 130 mA per membrane for 1 hour. After blotting, the membranes were cut at the necessary locations, treated with blocking solution for 30 min, and subjected to antigen-antibody reaction using Total Erk1/2 (1000 \times dilution), Phospho-Erk1/2 (1000 \times dilution), Total Akt (1000 \times dilution), or Phospho-Akt (500 \times dilution). Antigen-antibody reactions were performed using Phospho-Erk1/2 (1000 \times dilution), Total Akt (1000 \times dilution) or Phospho-Akt (500 \times dilution) (overnight, 4°C). After the reaction, the membrane was washed 3 times with PBS-T for 5 min, and then reacted with HRP-labeled secondary antibody (Anti-rabbit IgG; Cell Signaling Technology) for 2 hours. After the reaction, the membrane was washed with PBS-T and PBS in sequence, and then immersed in luminescent solution for luminescence detection using WSE-6100 LuminoGraph I (ATTO). After detecting the signal and obtaining the luminance value, the luminance at each time point was calculated as the ratio of Phospho protein to Total

protein (e.g., luminance of Phospho protein at 60 min / luminance of Total protein at 60 min). The obtained values were used to calculate the phosphorylation ratio relative to the control by dividing each time point by the control (0 min). Experiments were performed independently three times, and the mean and standard deviation of the phosphorylation ratios were calculated. Statistical analysis was performed using the *t*-test.

2-2-4 RNA-seq analysis

MCF-7 cells were grown in normal culture and then plated at 1×10^6 cells per 10 cm dish. The medium was RPMI 1640 containing 10% DCC-FBS, and the cells were first cultured for 3 days. After incubation, 10 nM E₂, 1 μ M ICI or 0.1% DMSO (vehicle; Control) were replaced with RPMI1640 (serum-free), respectively, and incubated for another 2 days. After incubation, total RNA was extracted using RNeasy Mini-kit (QIAGEN) [24]. The experiment was repeated six times, each time RNA samples (n = 6) were prepared. The RNA samples were contracted to GeneBay Inc. (Yokohama, Japan) for further preparation for RNA-seq and calculation of FPKM values. First, total RNA was prepared a library for sequencing with Truseq Stranded mRNA Library Prep (Illumina, Inc.) and the MGIEasy Universal Library Conversion Kit (MGI Tech, Shenzhen, China). Next, reads were sequenced with the next-generation sequencer DNBSEQ-G400 (MGISEQ-2000RS, MGI Tech), and reads corresponding to each gene were aligned a splitBarcode (<https://github.com/MGIttech-bioinformatics/splitBarcode>). Reads for all genes in the whole genome were then downsized to 20 M read pairs with seqkit v0.13.0 [42], and adapter sequences in the reads were processed with cutadapt ver. 2.10 [43] and then mapped by HISAT v2.2.1 [44]. Finally, FPKM (reads per kilobase of transcript per million reads mapped) was calculated employing Cuffdiff v2.2.1 [45], and gene expression analysis using FPKM values was performed with Excel software (Microsoft, Seattle, WA, USA) or SPSS 12.0J (SPSS Japan, Tokyo, Japan) [24,39], and *t*-test was performed for statistics. The analysis was first performed with 203 ERGs obtained by DNA microarray [28], and comparisons were made be-

tween each sample ($n = 6$). FPKM data calculated E_2 /vehicle and then converted to \log_2 to calculate the expression profiles (the name are E_2 -1 to E_2 -6). The absolute value (Avg.) and standard deviation (SD) of the mean of six times of the expression variability ratio were then calculated, and the coefficient of variation (CV) was obtained by calculating SD/Avg . The expression profiles were used for the correlation analysis of E_2 -2 to E_2 -6 against E_2 -1, and the CVs were further sorted in ascending order to examine their relationship to the correlation values of the expression profiles [39]. The mean expression profiles ($n = 6$) of E_2 was then sorted in descending and ascending order to select the top 150 genes each for a total of 300 genes. Furthermore, for the 300 genes, the top 30 genes (Table 1) with stable expression profiles were selected in ascending order of CV value [39]. The RNA-seq data were uploaded to the Gene Expression Omnibus database at NCBI, and the accession number was GSE205784.

2-2-5 *Real-time* RT-PCR

The 30 genes selected in the previous section were again evaluated with *real-time* RT-PCR. The same procedure as in the previous section was performed until RNA sample extraction, and a sample of RNA different from the total RNA of RNA-seq was prepared and used [24]. Reaction mix was prepared by iTaq Universal SYBR Green One-Step Kit (Bio-Rad) and evaluated with the CFX Connect *Real-Time* PCR Detection System (Bio-Rad). The first step [28] was performed by reverse transcription reaction at 42°C for 10 min to produce cDNA, followed by inactivation of the enzyme at 95°C for 1 min. Next, the *real-time* PCR reaction was performed at 94°C for 10 sec, 57°C for 30 sec, and 72°C for 20 sec for 46 cycles. In addition, DNA dissociation reactions were performed at 65°C to 95°C to generate melting curves after the PCR reactions. *Real-time* RT-PCR was performed three times independently, the mean and standard deviation were calculated by CFX Maestro Software (Bio-Rad), and statistics were performed by *t*-test. The 30 genes were primer set with the sequences shown in Table 1, including *EGR3* [39], *LOXL2* [46] and *SYNE1* [47], primers were pre-

pared based on the paper.

Table 1 Primer sets for 30 estrogen-responsive genes.

No.	Gene name	Forward primer (F) Reverse primer (R)	Sequence
1	<i>EGR3</i>	F	CCATGATTCCTGACTACAACCTC
		R	GTGGATCTGCTTGTCTTTGAATG
2	<i>ACOX2</i>	F	AACCAGACCACTGTCATACACCT
		R	GAGAAAGTCACCCGAGTTAGTCA
3	<i>GATA4</i>	F	CTCAGAAGGCAGAGAGTGTGTCAAC
		R	CAGGCATTGCACACAGGCTCGCC
4	<i>SUSD3</i>	F	CATTGTGAGCTGTGCCATCATC
		R	GTCTCCAAGTCCTCATCTTTCAG
5	<i>IL20</i>	F	AAGACACAAAGCCTGCGAATCG
		R	GCGAGGCTGCTGATCTTCCG
6	<i>ZNF521</i>	F	CCACCTGATAGAGCACAGCTT
		R	GGGCAGAGAAAATATGCTGCT
7	<i>PDLIM3</i>	F	CTCTCAGGGGGCATAGACTTC
		R	TTGAGACACAGCTGGTGAGC
8	<i>IGSF1</i>	F	ACGTTCTGAATGAAGCTATCAGG
		R	CTATCAATACCCCATTCACAGT
9	<i>RAPGEFL1</i>	F	ACCAGGACCTGCTGTCTTTCTAC
		R	ATCACTTCTCGGTAGCTTTTGTG
10	<i>LOXL2</i>	F	ACATGTACCGCCATGACATCGACT
		R	TGAAGGAACCACCTATGTGGCAGT
11	<i>CTSD</i>	F	GACACAGGCACTTCCCTCAT
		R	CTCTGGGGACAGCTTGTAGC
12	<i>TMPRSS3</i>	F	TGAAGAGAACTTCCCCGATG
		R	GAGATGATGCCACCGTACAC
13	<i>FDFT1</i>	F	TCAATCAGACCAGTCGCAGT
		R	GTTGTGTAACAGCGGGACCT
14	<i>PKIB</i>	F	ATCCCGGTGGACTGTAGAGG
		R	GCACAGGGTTTTCTGCTTCT

15	<i>INSYN1</i>	F	CGGATTCGACAGCGCATGAAG
		R	CTTGTCACTGCTAGAGGTGCTGC
16	<i>DOK7</i>	F	AGCTTCCTGTTCGACTGCAT
		R	CTCCAGCTGTAGGGTTTCCA
17	<i>SPOCD1</i>	F	ACCCCTTCTACCCCTCCAAGAAG
		R	CGAGTCCATAGTACCTCCTGCAT
18	<i>B4GALT1</i>	F	GGAGCACCTCAAGTACTGGCTA
		R	GAGGTCCACGTCATAAACACA
19	<i>BARX2</i>	F	GGAGACCTGCGATTACTTTGAG
		R	GACCAGGTGGGAGATGACAG
20	<i>LINC02593</i>	F	AAGCTCACGATCTGGGAGAA
		R	CAGCCATGAGGCTCTGTAC
21	<i>SYNE1</i>	F	CTAGATGAGCTCCGACGGTAC
		R	CCCAGCAGTTTCATGTAGCCT
22	<i>RAB26</i>	F	ATTCAAGGATGGTGCTTTCTG
		R	GGTAGTAGGCATGGGTAACACTG
23	<i>RAP1GAP</i>	F	GAGTCCCTAATGTTGTCCAGATG
		R	CTTCTGATAAATGACGCCAACTT
24	<i>CRISP3</i>	F	CATTATTCCCAGTGCTGTTGTTCC
		R	CATTTGCTGCAGCCTCTTTGTTC
25	<i>MATN2</i>	F	CATCTCTAGGGGCAGACACG
		R	GAAGGTCTTGAGGGAGAACTCA
26	<i>CYP1A1</i>	F	CAGCTGTCAGATGAGAAGATCATTA
		R	AATCACTGTGTCTAGCTCCTCTTG
27	<i>CCDC68</i>	F	GAGTCTACGTCCGCTCACATTA
		R	AGAGCCCTGTTGAAGGTTTCC
28	<i>SRGAP3</i>	F	AGTATGTGAATGGCAGTAACCTCA
		R	CTTCCATACTGCCGTTAAAGAGTT
29	<i>CSTA</i>	F	TGATAAGGTTAAACCACAGCTTGA
		R	AAGTACCAAGTCCTCATTTTGTCC
30	<i>FRY</i>	F	GAATACAGACCAAGAACAAGC
		R	CTGTCTATTACAGGATGAAGTGG

2-2-6 Data analysis for gene expression

The FPKM values of all genes obtained by RNA-seq were converted to expression profiles (\log_2), p -values were calculated, and the data were organized according to whether the expression variation showed a statistically significant increase or decrease ($p < 0.05$) [24]. Two Volcano plots were created, using the expression variation value for the X-axis and the p -value and the coefficient of variation converted to $-\log_{10}$ for the Y-axis, respectively. Pathway analysis was performed with WebGestalt software (WEB-based Gene SeT AnaLysis Toolkit) (<http://www.webgestalt.org/>[49]) using statistically significant ($p < 0.05$) gene sets and Gene Ontology (GO) (www.geneontology.org/) and Kyoto Encyclopedia of Genes and Genomes (KEGG) (www.genome.jp/keg/) were determined. Q value was calculated by the Benjamini-Hochberg method, and the determined GOs and KEGGs were utilized to create a bubble chart using the top 10 entries that resulted in an FDR < 0.05 .

2-3 Evaluation of cell proliferative activity by 17β -estradiol (E_2)

For estrogen-responsive gene (ERG) profiling, MCF-7 cells were initially evaluated for cell proliferative activity by E_2 , ICI, and $E_2 + ICI$ employing the SRB assay [15]. E_2 showed approximately 2-fold proliferation compared to Cont, and its growth was inhibited when ICI was added (Figure 4). Equal proliferation was observed when cells were stimulated with ICI and $E_2 + ICI$, suggesting that MCF-7 cells proliferated by ER-mediated E_2 signal.

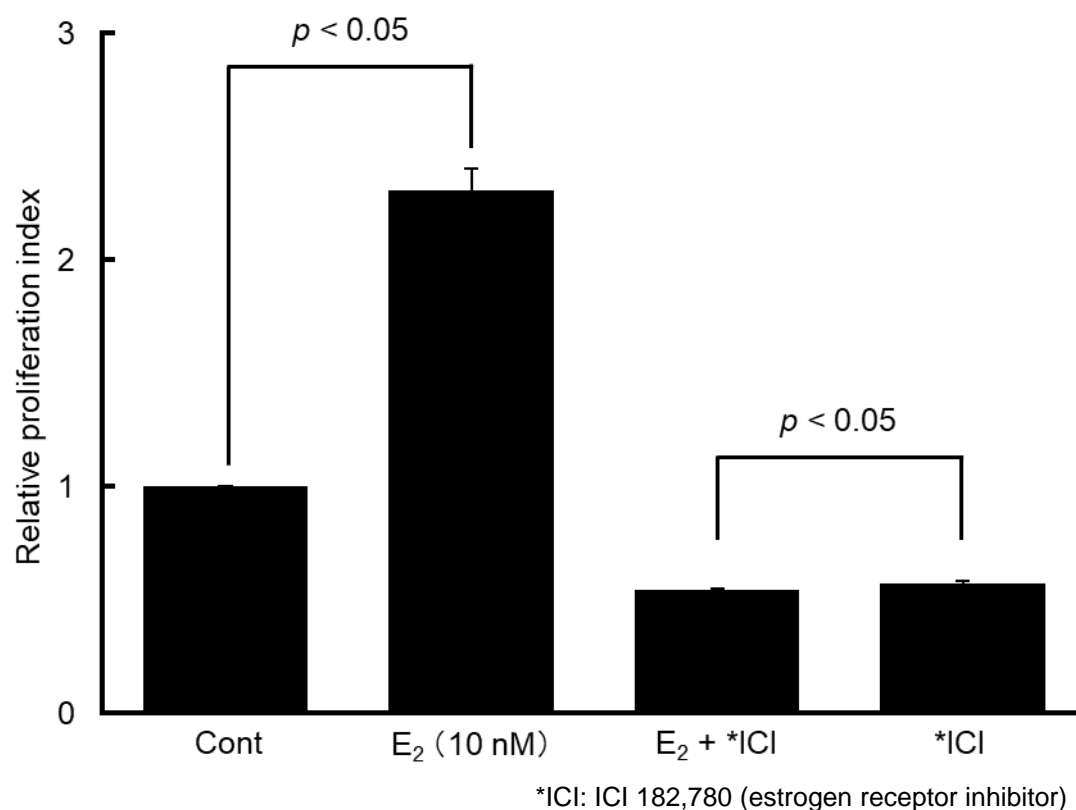


Figure 4 Evaluation of cell proliferation activity.

2-4 Evaluation of intracellular signaling proteins

The phosphorylation of intracellular signaling proteins Erk1/2 and Akt was confirmed by Western blotting to evaluate the phosphorylation activity in cells by E₂ signal [15]. The reaction times were set at 0, 5, 15, 30, and 60 min. The phosphorylation activity of Erk1/2 and Akt was highest at 5 and 15 min, respectively. Furthermore, inhibition experiments with ICI suppressed the phosphorylation of the two signaling proteins. Therefore, the data suggests that the phosphorylation of the two signaling proteins was promoted by E₂ signaling via ER (Figure 5).

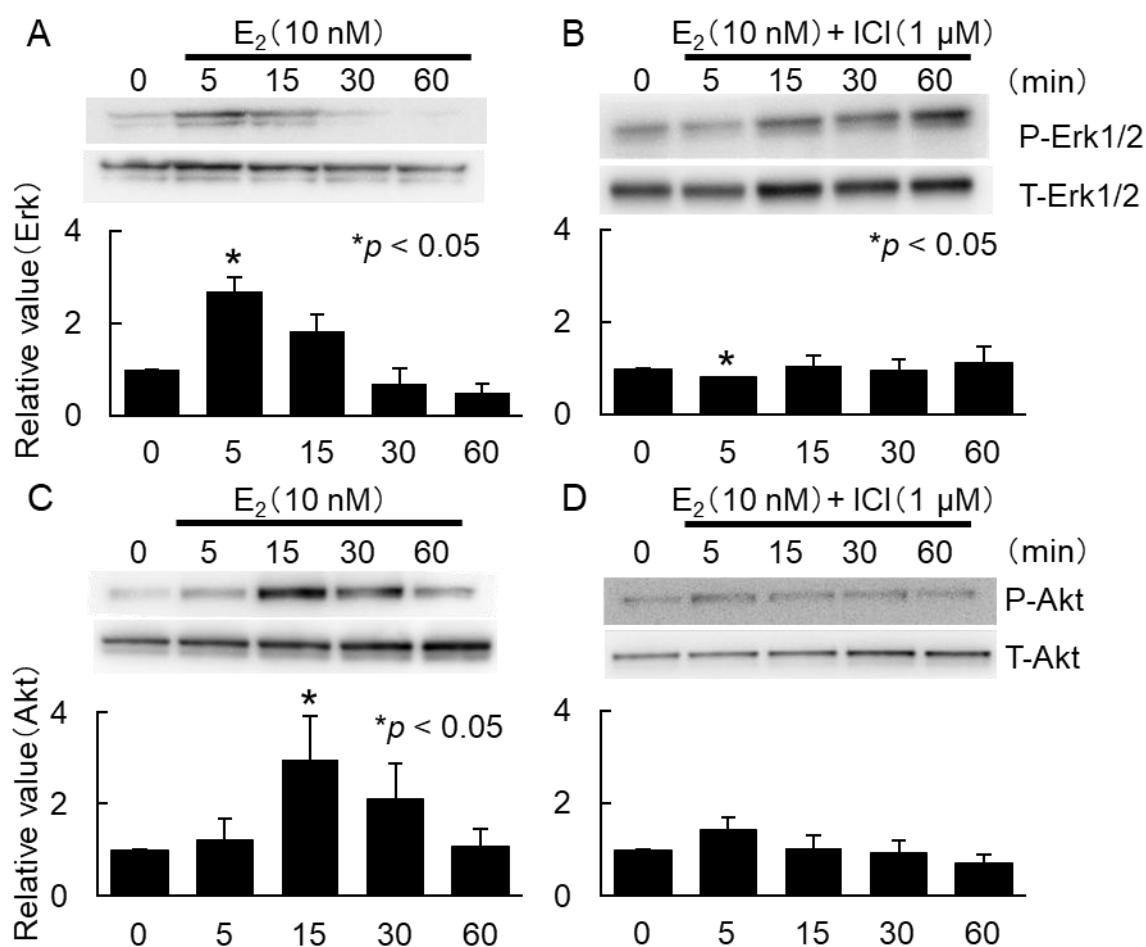


Figure 5 Evaluation of phosphorylation activity of E_2 .

2-5 Identification and analysis of novel ERGs

The two analysis methods described so far indicated that the MCF-7 cells used promote cell proliferation and phosphorylation of signaling proteins by E_2 . Therefore, we next performed gene expression analysis with RNA-seq. The expression profiles (\log_2) was calculated from the FPKM values of all genes in the genome obtained by RNA-seq, and correlation analysis was performed on 120 ERGs [15, 20, 28] selected by DNA microarray (Figure 6). The experiments were conducted 6 times independently, and the analysis compared E_2 -2 to 6 against E_2 -1 and also E_2 + ICI. The results showed a high correlation value of 0.83 to 0.95 for E_2 -2 to 6,

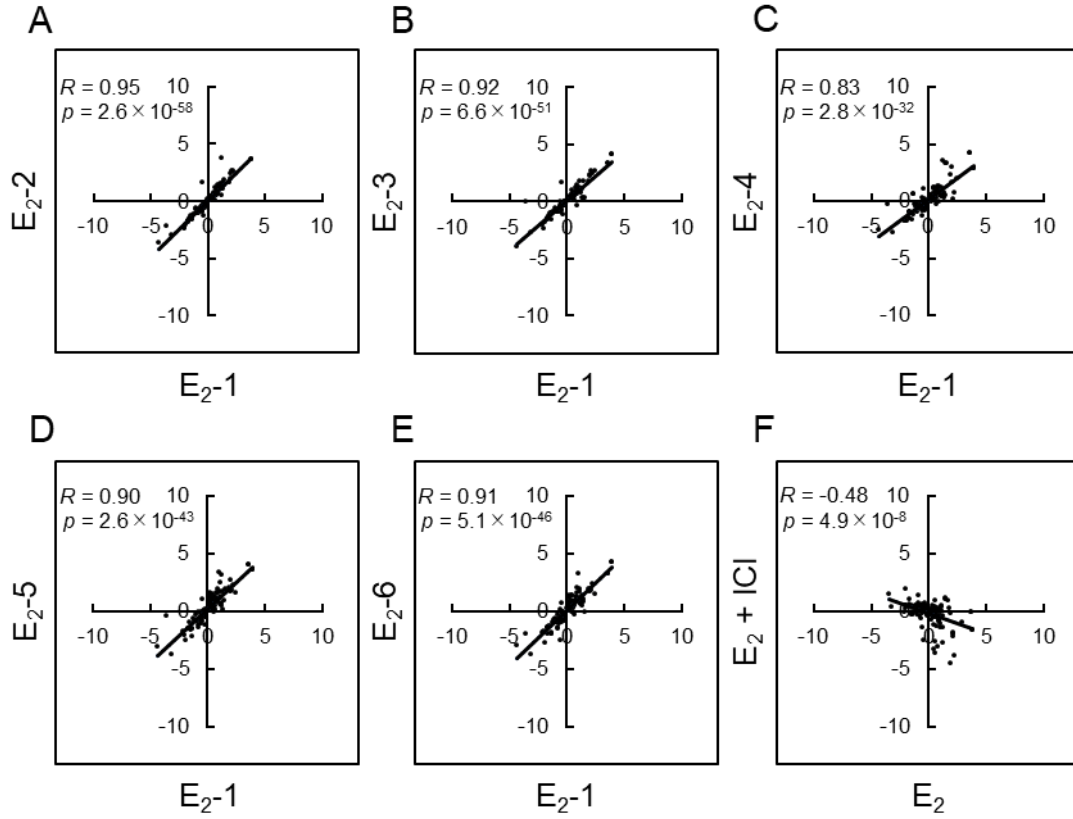


Figure 6 Correlation analysis of estrogen-responsive genes (1).

while there was no correlation between E_2 and $E_2 + ICI$, suggesting that ERG expression was regulated by the E_2 signal. Thus, it appears that RNA-seq can be used for profiling ERGs. Furthermore, to perform a quality check of ERGs obtained by RNA-seq, the mean (Avg.) and standard deviation (SD) of the expression profiles (\log_2) for the six times described above were calculated, and the coefficient of variation (CV) was calculated as $SD/Avg.$ [39]. Based on the obtained CVs, the 203 ERGs [20, 28] were sorted in ascending order, and the CVs for 174, 150, 120, 90, 60, and 30 genes were averaged, respectively. Then, based on each averaged CV, the correlation values of E_2-2 to 6 against E_2-1 were analyzed again for each number of genes (Figure 7). The results showed that, similar to the previous study [39], the correlation value increases with decreasing the number of genes in RNA-seq, and furthermore, the CV value of the selected genes becomes lower. In other words, if genes with a large change in expression profiles and low CV values are selected, it is possible to se-

lect estrogen-responsive genes that are stably expressed in RNA-seq. Furthermore, in the case of 30 genes, the correlation was found to be 0.97 to 0.99 in the present study, whereas it was 0.93 to 0.97 in the previous study [39]. Therefore, the data were statistically more reliable for RNA-seq than for DNA microarray.

2-6 Evaluation of 30 novel estrogen-responsive genes

To select genes with high gene expression variation and low CV values (stability) when MCF-7 cells are stimulated by estrogen, we analyzed the genes of the whole genome again using data obtained by RNA-seq method (n = 6). First, the expression variability ratios of the genes in the whole genome were ascended, and a total of 300 genes (150 with high expression variability ratios and 150

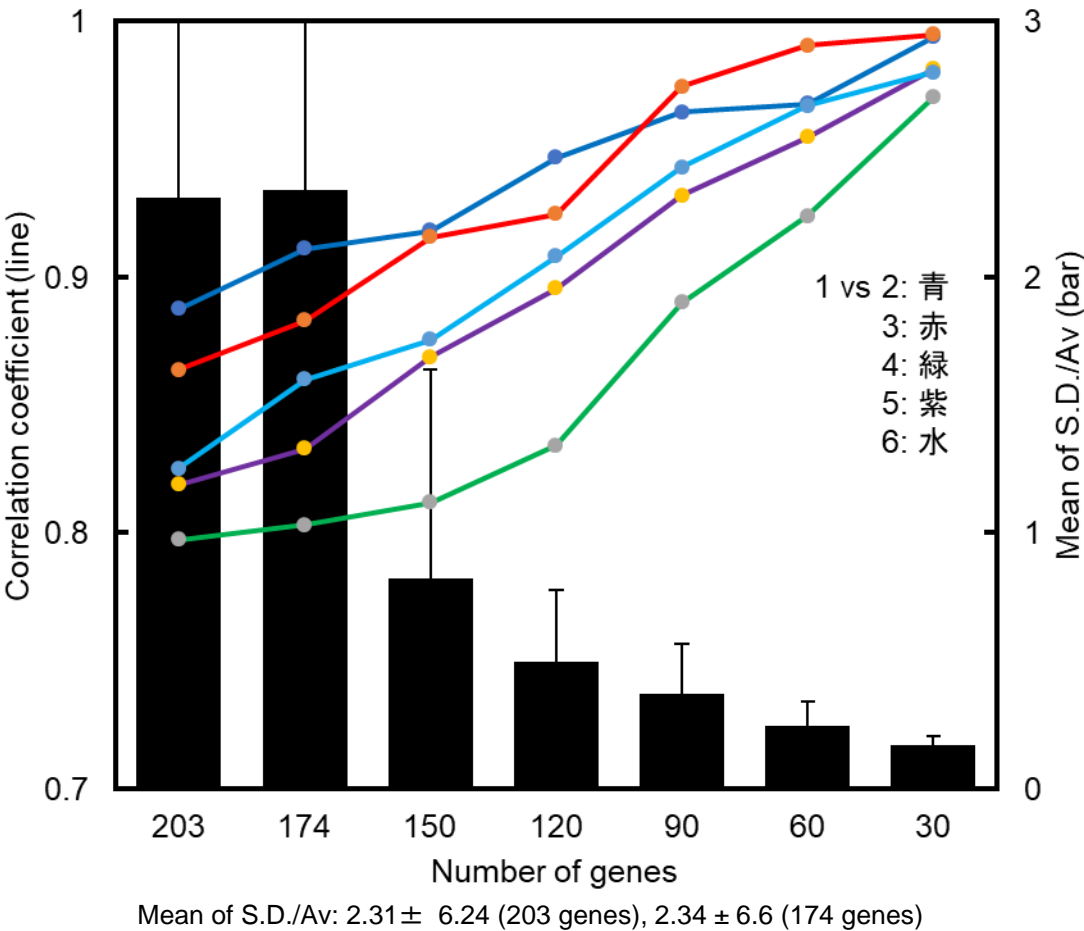


Figure 7 Correlation analysis of estrogen-responsive genes (2).

with low expression variability ratios) were selected, and then the CV values were further ascended. Then, we were able to select the 30 estrogen-responsive genes with the highest expression variability and the most stable among them [24]. This gene set is characterized by 19 genes having an increasing gene expression profiles and 11 genes having a decreasing ratio (Figure 8 bottom). Primers for this gene set were generated (Table 1), and its expression variation pattern was further examined using *real-time* RT-PCR method. Statistical (n = 3) analysis of gene expression variation showed that all genes exhibited a pattern of gene expression variation similar to the graph of the RNA-seq data (Figure 8 upper). Thus, the 30 selected estrogens maintained their gene expression characteristics and remained stable when another experimental method was used. Therefore, it is suggested that when MCF-7 cells are stimulated with estrogens and phytoestrogens, this gene set can be used to study their activity without using expensive experimental methods such as RNA-seq methods.

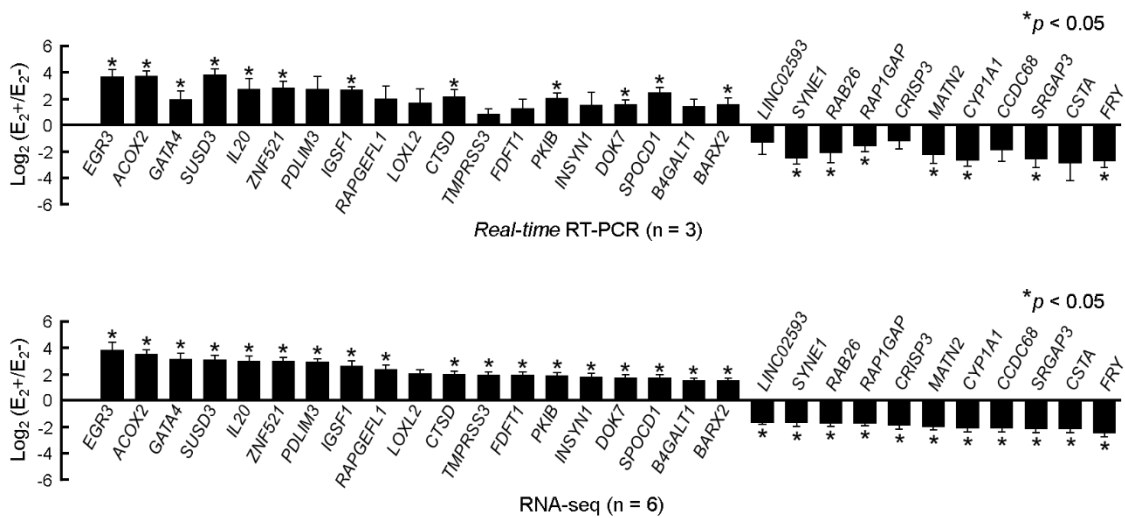
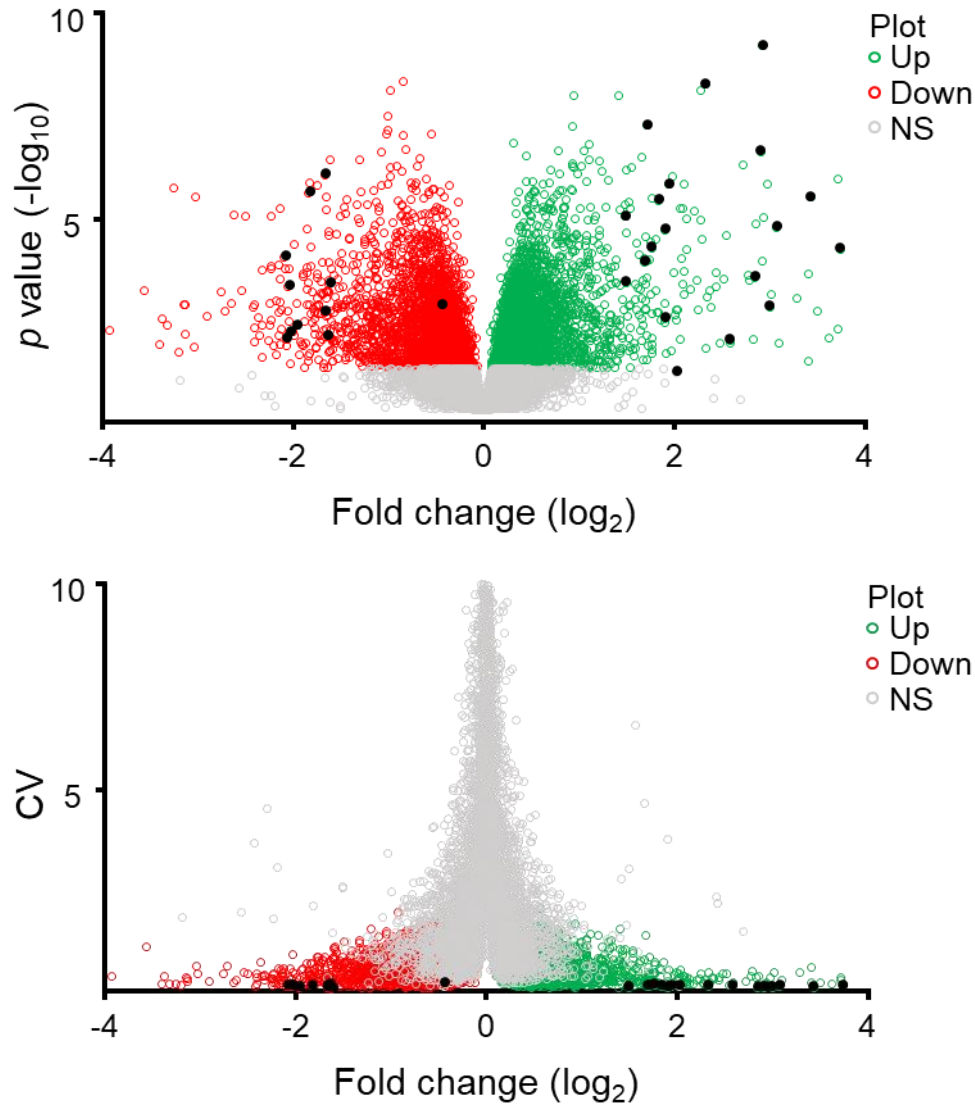


Figure 8 Gene expression analysis by *real-time* RT-PCR and RNA-seq.

2-7 Functional analysis of novel estrogen-responsive genes

To further analyze the entire gene set obtained by RNA-seq, we classified the genes based on $p < 0.05$ and created a Volcano plot (Figure 9) [49]. The results showed that the 30 genes selected had



Up, Down: $p < 0.05$, NS: $p > 0.05$,.

Black circle: 30 genes selected from genes in the entire genome

CV: Coefficient of Variation

Figure 9 Volcano plots of all genes based on RNA-seq data.

high expression variability among all the analyzed genes and were also very low with respect to CV, a measure of stability. Furthermore, for functional analysis of the genes, out of the 13704 genes with

confirmed expression variation, we selected 3030 up-regulated and 2690 down-regulated genes based on $p < 0.05$ and performed enrichment analysis for GO and KEGG using WebGestalt [49] (Figure 10 and Figure 11) [24]. The analysis results were then ordered in ascending order of FDR < 0.05 , and their functions were classified. First, GO found that the group of genes with increased expression contained more genes related to RNA synthesis and function and cell division. Then, the genes with decreased expression were found to contain many genes mainly related to chemical reactions that occur within the cell (Figure 10). Furthermore, KEGG was concentrated in pathways related to the cell cycle, protein synthesis and degradation, or RNA synthesis in the up-regulated genes, while pathways related to various cancers and those related to PI3K and ERBB were clustered in the down-regulated genes (Figure 11). The results of this analysis suggest that statistically significant ERGs clusters are concentrated in transcription, translation, and cell proliferation that occur within the cell.

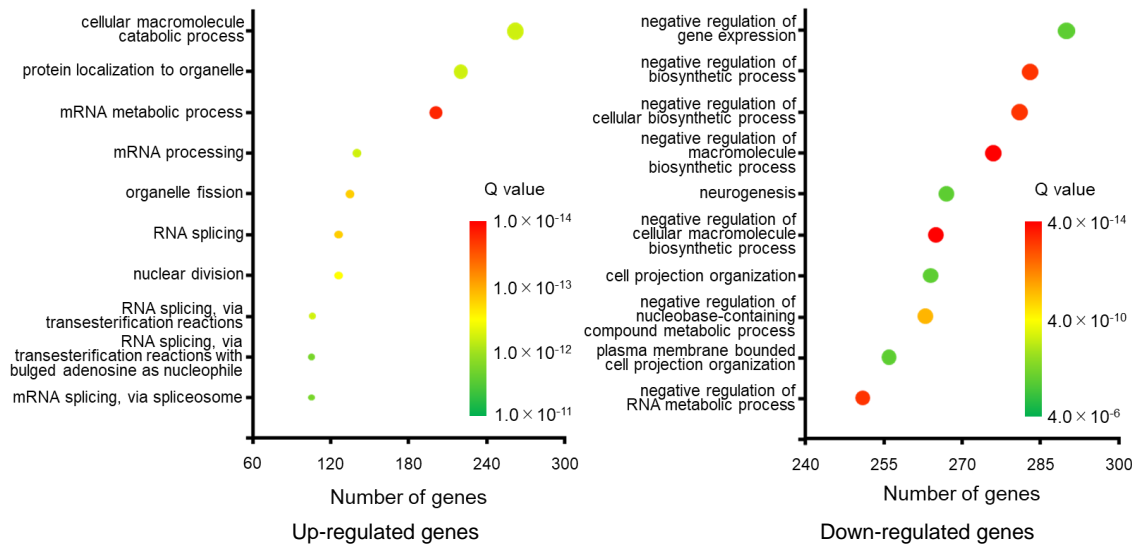


Figure 10 GO of estrogen-responsive genes.

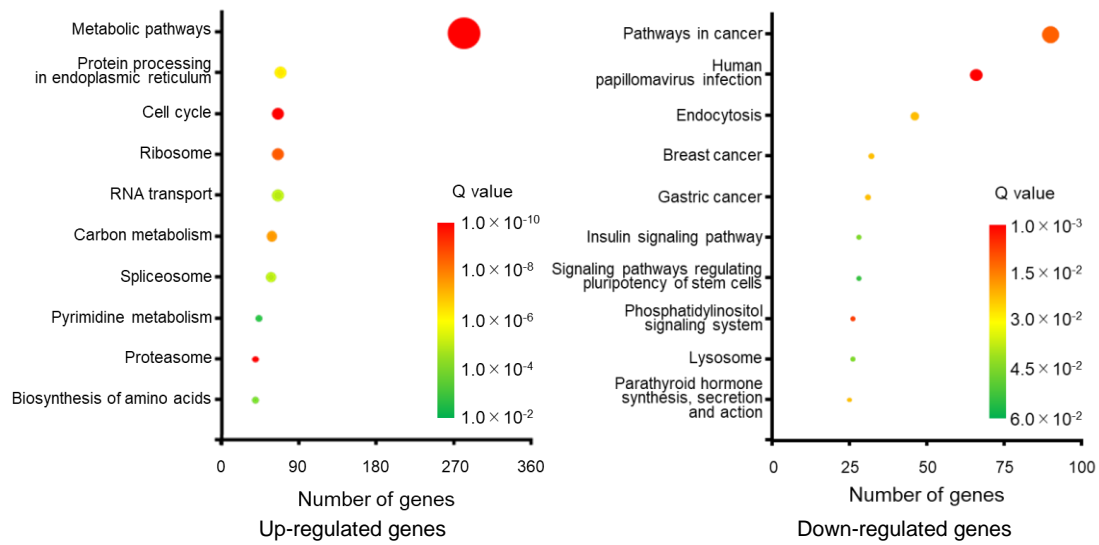


Figure 11 KEGG of estrogen-responsive genes.

2-8 Characteristics of 30 novel estrogen-responsive genes and classification of ERs

Through this research, we were able to select 30 ERGs that are expressed most stably. The characteristics of the 30 genes were then investigated from the literature [24].

EGR3 is a transcription regulator in a gene already recognized as an estrogen response gene [51]. It belongs to the EGR family of zinc finger proteins and plays important roles in various biological processes such as muscle development [52], the immune system [53], and endothelial cell growth and migration [54]. *ACOX2* is an enzyme belonging to the acyl-CoA oxidase family [55]. *ACOX2* plays a role in β -oxidation in peroxisomes as a branched-chain acyl-CoA oxidase [56]. *GATA4* is a transcription factor and the protein binds to the GATA motif present in many promoter regions. *GATA4* is thought to regulate genes involved in embryogenesis and cardiac myocyte differentiation and function, and is also essential for normal testicular development [57]. It is also associated with bone differentiation through the $ER\alpha$ and $TGF\beta$ pathways [58,59]. *SUSD3* encodes a protein with a Sushi domain on the cell surface and is an ERG whose expression is induced by E_2 . *SUSD3* is involved in breast cancer growth and development through the estrogen receptor pathway [60]. *IL20* encodes a pro-inflammatory cytokine implicated in the development of inflammatory diseases [61].

This gene has been identified as an ERG [62], and in breast cancer cells, ER α , GATA3, FOXA1, and Ell3 form a complex that increases IL20 expression [63]. *ZNF521* is a transcription factor that encodes zinc finger protein 521 [64]. In ER-positive breast cancer cells, ZNF521 forms a heterodimer with ZNF423, an ERG, to regulate transcription, and further affects the promoter of *BRCAl*, thereby activating its expression [65]. *PDLIM3* is highly expressed in skeletal and cardiac muscles, playing a crucial role in the growth and remodeling processes of muscle cells [66]. *IGSF1* encodes a glycoprotein belonging to the immunoglobulin superfamily of cell membrane proteins. Males with IGSF1 deficiency exhibit testicular hypertrophy and delayed development of secondary sexual characteristics [67]. *RAPGEFL1* encodes a guanine nucleotide exchange factor (GEF) protein that activates GTP-binding proteins. In breast cancer cells, RAPGEFL1 functions as an estrogen-regulated gene [68]. *LOXL2* encodes lysyl oxidase or protein-lysine 6-oxidase, which catalyzes the cross-linking of collagen and elastin in the extracellular matrix. Furthermore, LOXL2 has been implicated in breast cancer metastasis and invasion [69,70]. *CTSD* encodes cathepsin D, a protease involved in protein degradation and activation of protein precursors. This gene is an ERG, with its expression regulated by E₂ and ER α and ER β [71, 72]. *TMPRSS3* encodes a transmembrane serine protease and is associated with tumor progression, metastasis, and poor prognosis in breast cancer patients [73]. Furthermore, it has been shown that E₂ stimulation of MCF-7 cells enhances the transcription of *TFF1* through interaction with TMPRSS3 [74]. *FDFTI* is a critical enzyme involved in the initial step of cholesterol biosynthesis in the liver. It is implicated in cancer through both oncogenes and tumor suppressor genes, and is considered a potential diagnostic marker and therapeutic target in various cancers [75]. *PKIB* encodes the cAMP-dependent protein kinase inhibitor beta. When MCF-7 cells are stimulated by E₂, PKIB can directly interact with ER α and AP-1, suggesting its importance in breast cancer cell proliferation [76]. *INSYNI* encodes an inhibitory synaptic protein involved in postsynaptic inhibition [77]. *DOK7* belongs to the docking protein (DOK) family and is involved in

intracellular signaling pathways downstream of receptor tyrosine kinases (*RTK*). Overexpression of *DOK7* inhibits breast cancer cell proliferation, invasion, and migration through the *PI3K/PTEN/AKT* pathway, while its downregulation is thought to contribute to breast cancer malignancy [78]. *SPOCD1* encodes a protein belonging to the TFIIS family of transcription factors and promotes cell proliferation and inhibits apoptosis by regulating VEGF in osteosarcoma [79]. *B4GALT1* is an essential enzyme for galactosylation of N-glycans, encoding beta-1,4-galactosyltransferase [80]. Estrogen directly regulates the expression of *B4GALT1* and has been reported to affect the proliferation of MCF-7 cells [81]. *BARX2*, a homeodomain transcription factor, has been identified as a direct regulator of *ESR1* in MCF-7 cells. Increased expression of *BARX2* leads to upregulation of matrix metalloproteinase 9 (MMP9), which is associated with cancer invasion and metastasis, suggesting a crucial role in breast cancer progression [82]. *SYNE1* encodes nesprin-1, a nuclear membrane protein that links the nucleus to the cytoskeleton. Located near *ESR1* on the genome, polymorphisms in *SYNE1* have been associated with estrogen-related ovarian cancer [83, 84]. *RAB26* encodes a small GTPase of the RAB family. Activation of *RAB26* inhibits adhesion, migration, and invasion of breast cancer cells through the autophagy pathway [85]. *RAP1GAP* encodes a GTPase-activating protein (GAP) that downregulates the activity of the RAS-related *RAP1* protein. *GPER1* regulates *RAP1GAP* and is involved in the activation of the *PI3K-AKT* signaling pathway [86]. *CRISP3* encodes a cysteine-rich secreted protein and has been reported as an androgen-responsive gene regulated by androgens in prostate cancer cells [87, 88]. *MATN2*, expressed in the extracellular matrix, encodes a protein composed of two von Willebrand factor A domains, ten EGF-like domains, and a coiled-coil domain [89]. Its expression is regulated by IGF-1R, *GPER*, and *DDR1*, and has been shown to affect tumor progression [90]. *CYP11A1* encodes cytochrome P450 11A1 and is involved in the metabolism of estradiol to 2-hydroxyestrone [91]. *CCDC68*, initially reported as a tumor suppressor gene in colorectal adenocarcinoma [92], encodes a

secreted protein containing a coiled-coil domain and is associated with tumor migration, invasion, and metastasis [93]. *SRGAP3* encodes Slit-robo GTPase-activating protein 3, a protein involved in synapse formation through Rac1 [94] and is considered a tumor suppressor gene in breast cancer [95]. *CSTA* encodes cystatin A, a cysteine protease inhibitor belonging to the cystatin superfamily, and its expression is regulated by estrogen via ER α in breast cancer cells [96]. *FRY*, a potential tumor suppressor, inhibits nuclear localization of YAP, a transcriptional coactivator involved in promoting cell proliferation [97]. Furthermore, *FRY* is essential for mammary gland development and may play a role in suppressing the growth and proliferation of breast cancer cells [98].

Based on these characteristics, we classified the genes according to their functions. *EGR3*, *GATA4*, *ZNF521*, *SPOCD1*, and *BARX2* were classified as transcription factors, while *ACOX2*, *RAPGEFL1*, *LOXL2*, *CTSD*, *TMPRSS3*, *FDFT1*, *PKIB*, *B4GALT1*, *RAB26*, *RAP1GAP*, *CRISP3*, *CYP11A1*, *SRGAP3*, and *CSTA* were classified as genes related to enzymes. *SUSD3*, *IL20*, *PDLIM3*, *IGSF1*, *LOXL2*, *CTSD*, *TMPRSS3*, *FDFT1*, *INSYN1*, *DOK7*, *B4GALT1*, *SYNE1*, *CRISP3*, *MATN2*, *CYP11A1*, *CCDC68*, *CSTA*, and *FRY* were classified as genes related to cellular functions and cancer. Additionally, *EGR3*, *SUSD3*, *IL20*, *RAPGEFL1*, *CTSD*, *TMPRSS3*, *PKIB*, *B4GALT1*, *CYP11A1*, and *CSTA* were identified as estrogen-responsive genes. Furthermore, referring to previous studies on estrogen signaling pathways [99], we constructed and analyzed a pathway using ERGs obtained from DNA microarray analysis [20] and the 30 genes identified in this study (Figure 12) [100-133]. The ERGs identified in this study were found to affect pathways such as matrix metalloproteinases, and to influence the PI3K and MAPK pathways through *EGFR*. Additionally, they were found to affect cell cycle regulation and apoptosis through *ESR1*, *BRCA1*, and *TP53*. Furthermore, it was found that all 30 genes directly affected cancer cell invasion. Therefore, pathway analysis suggested that the ERGs identified in this study are related to cell proliferation and signal protein phosphorylation.

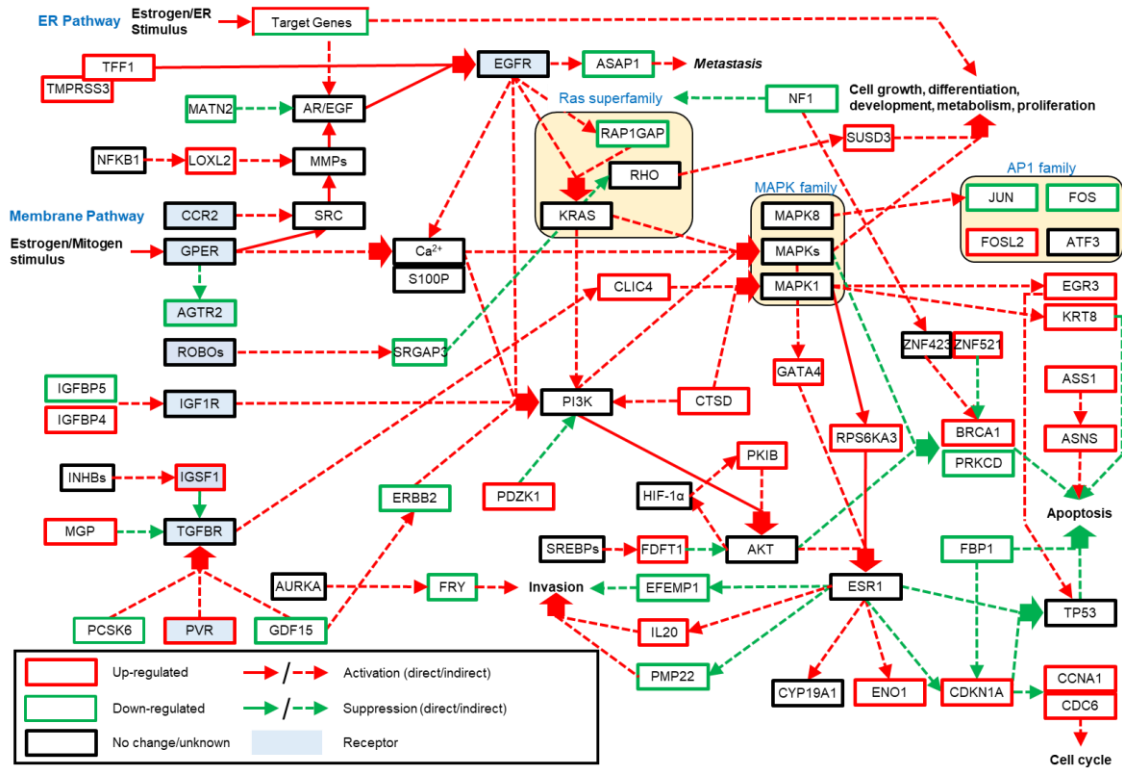


Figure 12 Estrogen Signaling Pathway.

Finally, we obtained ChIP-seq data (GSE117569 [51] and GSE149979 [52]) from the NCBI Gene Expression Omnibus and classified the 30 newly identified estrogen-responsive genes into those associated with ER α , ER β , or both using Chip atlas [50] and the Integrative Genomics Viewer (IGV) (Table 2 and Figure 13). However, since the 20th gene, LINC02593, is a long intergenic non-protein coding RNA, it was excluded from the analysis. Combining the results of the two analyses, 10 genes were associated with ER α only, 2 genes were associated with ER β only, and 14 genes were associated with both ER α and ER β . Furthermore, it was found that 3 genes did not belong to either category (Figure 13). Regarding the three genes that did not belong to either ER α or ER β , we considered the following. Since *ZNF521* is a paralog of *ZNF423*, which has been reported to respond to estrogen, we speculated that *ZNF521* is also an ERG. Next, both *IGSF1* and *CRISP3* are strongly associated with prostate cancer and their expression is regulated by androgen. Given that the androgen receptor and estrogen receptor can interact and affect genes, we hypothesized that when estrogen acti-

vates the estrogen receptor, it may interact with the androgen receptor, leading to stable expression changes in these two genes.

The 30 novel estrogen-responsive genes were characterized, pathway analyzed, and classified as receptors, and once again appear to be reliable genes with stable and highly variable expression upon estrogen action.

Table 2 Interaction of 30 estrogen-responsive genes with ER using ChIP-seq data.

Gene No.	Gene symbol	ER α ^a		ER α binding ^c	ER β ^a		Receptor subtype
		E ₂ -	E ₂ +		E ₂ +	Er β binding ^c	
		Q value ^b (n = 3)	Q value ^b (n = 3)		Average of S/N ratio ^d (n = 2)		
1	<i>EGR3</i>	0	279	+	1.1	+	ER α / β
2	<i>ACOX2</i>	0	0	-	1.4	+	ER β
3	<i>GATA4</i>	133	2133	+	1.2	+	ER α / β
4	<i>SUSD3</i>	449	3026	+	0.7	-	ER α
5	<i>IL20</i>	1307	3091	+	1.1	+	ER α / β
6	<i>ZNF521</i>	0	0	-	0.9	-	-
7	<i>PDLIM3</i>	0	72	+	1.1	+	ER α / β
8	<i>IGSF1</i>	0	0	-	1	-	-
9	<i>RAPGEFL1</i>	764	4529	+	0	-	ER α
10	<i>LOXL2</i>	0	0	-	8.2	+	ER β
11	<i>CTSD</i>	234	1683	+	4.4	+	ER α / β
12	<i>TMPRSS3</i>	263	2761	+	3.2	+	ER α / β
13	<i>FDFT1</i>	1121	3753	+	1.2	+	ER α / β
14	<i>PKIB</i>	304	1887	+	0.8	-	ER α
15	<i>INSYN1</i>	200	3575	+	1	-	ER α
16	<i>DOK7</i>	676	2677	+	32.7	+	ER α / β
17	<i>SPOCD1</i>	0	31	+	1	-	ER α
18	<i>B4GALT1</i>	145	1105	+	18.9	+	ER α / β
19	<i>BARX2</i>	89	465	+	1	-	ER α
21	<i>SYNE1</i>	0	395	+	1	-	ER α
22	<i>RAB26</i>	118	991	+	4.8	+	ER α / β
23	<i>RAP1GAP</i>	45	133	+	2.1	+	ER α / β
24	<i>CRISP3</i>	0	0	-	0.8	-	-
25	<i>MATN2</i>	0	200	+	2.5	+	ER α / β
26	<i>CYP1A1</i>	1203	2489	+	12.3	+	ER α / β
27	<i>CCDC68</i>	0	1490	+	1.2	+	ER α / β
28	<i>SRGAP3</i>	125	1290	+	0.9	-	ER α
29	<i>CSTA</i>	124	840	+	1	-	ER α
30	<i>FRY</i>	0	117	+	0.7	-	ER α

^a Data from NCBI's Gene Expression Omnibus accession numbers GSE117569 [51] and GSE149979 [52] were used.

^b Q values were analyzed within ± 10 kb of the Transcription Start Site (TSS) of each gene using the ChIP-Atlas database (<https://chip-atlas.org/>) [50].

^c ER α binding was set to "+" when the value of E₂+ is greater than E₂-.

^d The Integrative genomics viewer (IGV) was used to display the ChIP-seq results and each gene was analyzed by the presence or absence of a peak within ± 10 kb from the TSS. The S/N ratio was then calculated from E₂+ (ER β ChIP-seq rep 1 or 2) (S)/ E₂+ input (N).

^e ER β binding was determined to be+ if the S/N ratio is greater than 1.1.

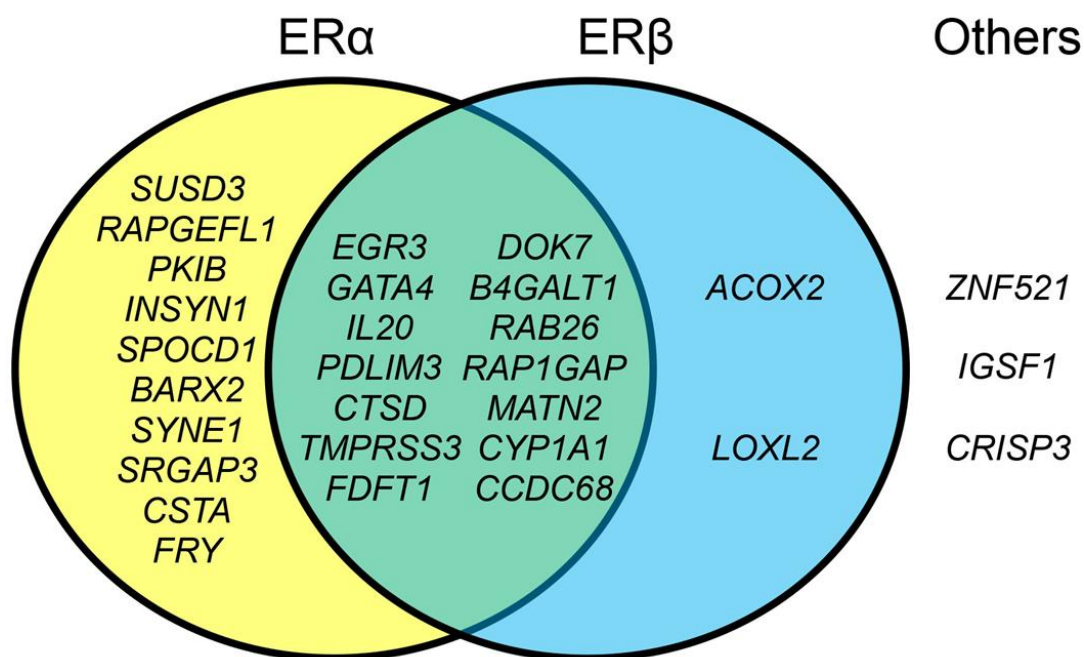


Figure 13 Association of estrogen-responsive genes with ER.

2-9 Conclusion

In this study, we were identified novel estrogen-responsive genes. Among the newly identified ERGs, we selected 30 genes for further analysis using *real-time* PCR, functional analysis, and analysis of their association with each ER. Based on the results of these analyses, we concluded that these 30 genes are highly reliable ERGs and can be expected to be useful for various estrogen activity assessments.

Chapter 3: Estrogenic Activity of Fermented Soymilk Extracts and Soy Compounds

3-1 Introduction

Soybeans have been cultivated in Japan for a long time and are widely used in cooking and food products. Soymilk, obtained as a byproduct of tofu production, has been consumed by many people as a health drink. Soybeans and soymilk contain isoflavones, such as genistein and daidzein (aglycones) and their glycosides, genistin and daidzin (glycones), respectively (Figure 14), which exhibit estrogen-like effects. Soy isoflavones have been reported to have preventive effects on osteoporosis, alleviate menopausal symptoms, reduce the risk of prostate cancer, and prevent atherosclerosis [134-139].

In this study, we produced soymilk using Fukuyutaka (yellow soybean) [140] and Kurodamaru (black soybean) [141], and then fermented the soymilk with lactic acid bacteria (in collaboration with Sansho Pharmaceutical Co., Ltd.) [142]. Soymilk fermentation is generally applied to food processing, including improving the odor, and it also increases the conversion of glycones to aglycones [143-145], thereby enhancing antioxidant, anti-inflammatory [146], and cholesterol-lowering effects [147]. Therefore, in this study, we evaluated the estrogenic activity of extracts of soymilk fermented by lactic acid bacteria and four soy compounds (genistin, genistein, daidzein, and daidzein) to investigate the mechanism of estrogenic activity on MCF-7 cells [142]. Specifically, estrogenic activity was first evaluated by assessing cell proliferation activity, phosphorylation activity of signal proteins, and gene expression analysis with RNA-seq and *real-time* RT-PCR. Furthermore, the data obtained by RNA-seq was used for gene function analysis to examine the mechanism. Although there are many reports on assays using fermented soymilk, there are few reports on estrogenic activity evaluation and gene function analysis as in this experiment. Therefore, we also aimed to obtain new knowledge by novel using new estrogen-responsive genes (ERGs) selected in the previous chapter.

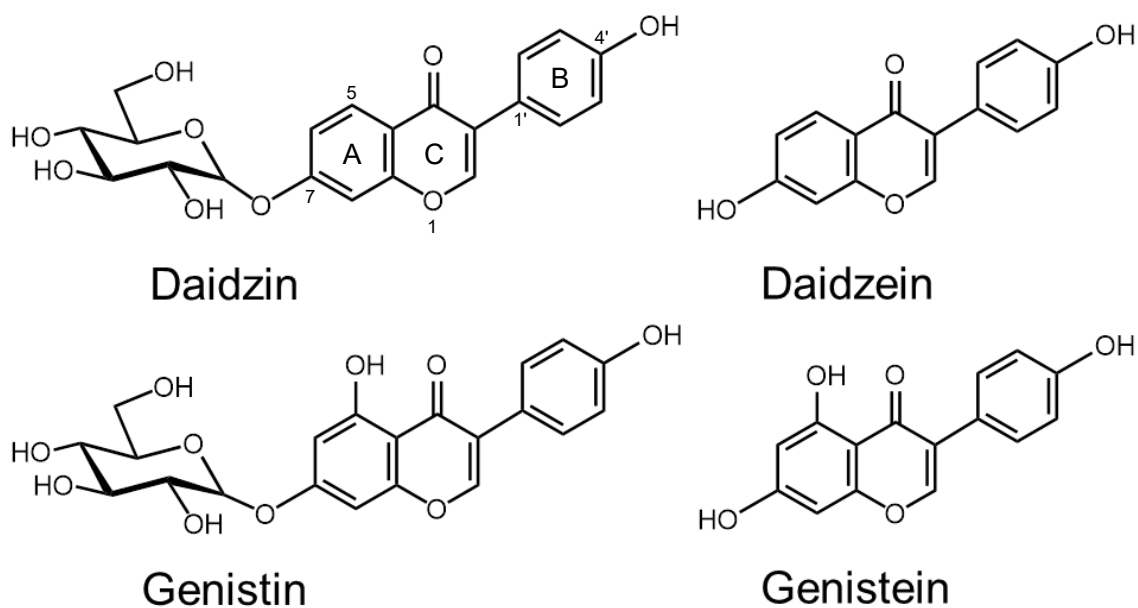


Figure 14 Soy compounds.

3-2 Materials and methods

3-2-1 Materials

The MCF-7 cells were used as in Chapter 2, and the culture conditions were the same as in 2-2-1 [24,124]. The same antibodies also used for Western blotting. Genistin, genistein, daidzin and daidzein were purchased from Fujifilm Wako Pure Chemical.

3-2-2 Fermentation method for soymilk

Soymilk extract were performed by Sansho Pharmaceutical Co., Ltd. Soymilk was made from Fukuyutaka (yellow soybean) [139] and Kurodamaru (black soybean) [140], and fermentation was performed with *Lactobacillus delbrueckii* NBRC3534 (Biological Resource Center, National Institute of Technology and Evaluation, Chiba, Japan) [142]. First, Soymilk was soaked in 4 times the volume of water relative to soybeans and boiled at 110° C for 3 min, followed by centrifugation (CR22G, Hitachi) at 2500 rpm (5°C) for 60 min to collect the supernatant. Then, after filtration through a 1 µm filter (Zeta plus, 3M), the liquid was prepared by passing it through a 0.45 µm filter

(MilliporeSigma) under pressure with nitrogen gas. The soymilk was then sterilized at 130°C (2 atm) for 10 min. Fermentation was inoculated with 2% *L. delbrueckii* relative to the volume of soymilk to be fermented and fermented at 40°C for 24 h while mixing. Fermentation was then confirmed by measuring pH = 4.5. The fermented liquid was passed through a membrane filter, and the resulting Fermented soymilk extract was freeze-dried (Neocool Freeze-Dryer, Yamato Scientific) for 24 hours before being stored at -20°C (Figure 15). The unfermented soymilk extract was adjusted to pH 4.5 with lactic acid and then freeze-dried (Figure 15).

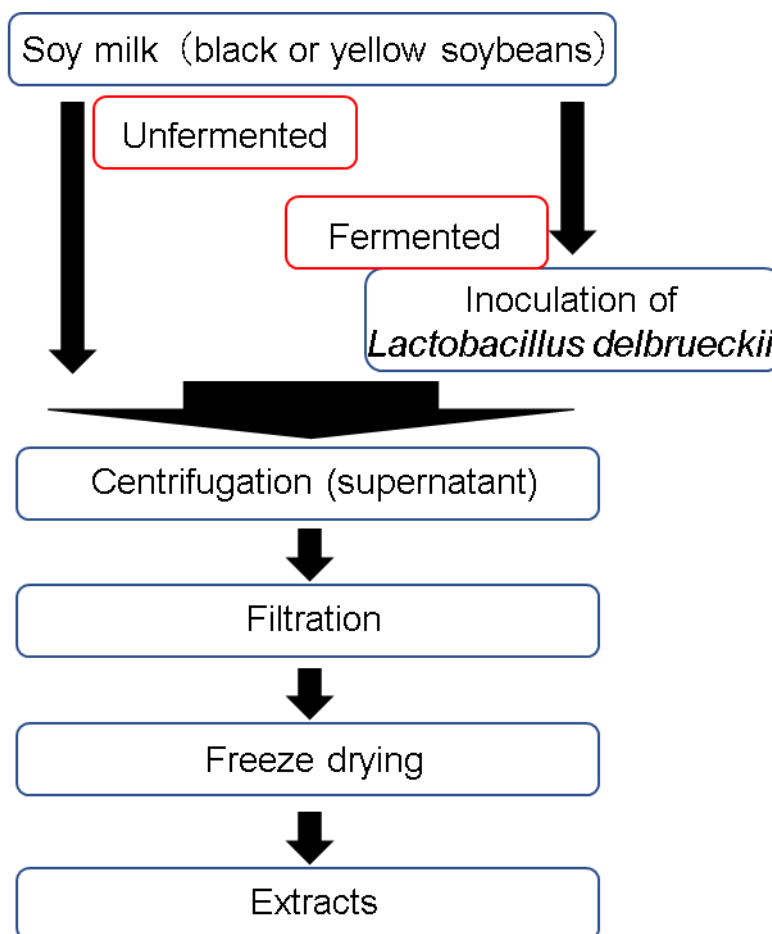


Figure 15 Scheme of soymilk extract preparation.

3-2-3 Sulforhodamine B (SRB) assay

The main experiment was performed as described in 2-2-2 [24,40,41,142]. MCF-7 cells were seeded at a density of 1.5×10^4 cells/well in 24-well plates and cultured in RPMI 1640 supplemented with 10% (v/v) DCC-FBS for 3 days. Subsequently, the cells were incubated with 10 nM E₂, 1 μ M ICI, soymilk extracts (1, 10, or 100 μ g/ml; yellow and black soybeans), soy compounds (genistin, genistein, daidzin or daidzein; 10 nM, 100 nM, 1 μ M, 10 μ M, or 100 μ M), or 0.1% DMSO (vehicle; Cont) in serum-free RPMI 1640 for an additional 3 days on further. After the culture period, the cells were fixed, stained for protein, and subjected to protein melting and absorbance measurement, following the protocol outlined in section 2-2-2. Furthermore, data were analyzed using the same statistical methods described previously.

3-2-4 Western blotting

The main experimental procedures for cell stimulation, sample preparation, and Western blotting were conducted as described in 2-2-3 [24, 40, 41, 142]. After culturing MCF-7 cells in RPMI 1640 containing 10% (v/v) DCC-FBS, the medium was replaced with serum-free RPMI 1640 one day before stimulation. For inhibition experiments using 1 μ M ICI, cells were pretreated for 1 hour. For cell stimulation, cells were treated with 10 nM E₂, 1 μ M ICI, soymilk extracts (1, 10, or 100 μ g/ml; yellow and black soybeans), or soy compounds (genistin, genistein, daidzin, and daidzein) at 10 μ M or vehicle (0.1% DMSO) for 5, 15, 30, or 60 min at 37°C with 5% CO₂. After stimulation, cell lysates were collected, and SDS-PAGE, Western blotting, antigen-antibody reactions, chemiluminescence detection, and subsequent statistical analysis were performed according to the procedures described in 2-2-3.

3-2-5 RNA-seq analysis

MCF-7 cells were prepared as described in 2-2-4 [24, 40, 41, 142]. After culturing MCF-7 cells in RPMI 1640 containing 10% (v/v) DCC-FBS, the medium was replaced with serum-free RPMI 1640

containing 10 nM E₂, 10 µg/ml soymilk extract (yellow or black soybean), 10 µM soy compound (genistin, genistein, daidzin, and daidzein) or 0.1% DMSO (vehicle; control) and cultured for an additional 3 days. Total RNA was extracted with the RNeasy Mini-kit (QIAGEN). RNA-seq analysis was performed by GeneBay Inc. (Yokohama, Japan). Sequencing, genomic mapping, FPKM value calculation, and gene expression fold change were performed as described in 2-2-4. RNA-seq was performed three times with E₂ and twice with soymilk extracts and soy compounds. For the 30 ERGs described in Chapter 2 [24], FPKM/vehicle values and log₂ were calculated with the RNA-seq data of E₂, soymilk extract, and soy compounds. The average (Avg.) and standard deviation (SD) were calculated and were utilized for graph and correlation analysis of the expression fold change of the 30 genes for E₂, soymilk extracts and soy compounds. For correlation analysis, *R* values and *p*-values were calculated with SPSS 12.0 J (SPSS Japan), and statistical analysis was performed with the *t*-test. The RNA-seq data was uploaded to the NCBI Gene Expression Omnibus database, and the accession number is GSE226627.

3-2-6 *Real-time* RT-PCR

MCF-7 cells were prepared as described in 2-2-5 [24, 40, 41, 142]. MCF-7 cells were stimulated with 10 nM E₂, 10 µg/ml soymilk extracts (yellow or black soybean), 10 µM soy compound (genistin, genistein, daidzin, and daidzein), or 0.1% DMSO (vehicle; control). The conditions for *real-time* RT-PCR and the primers were used the same as those described in 2-2-5. The experiment was performed independently three times, and statistical analysis was performed using the *t*-test.

3-2-7 Data analysis for gene expression

Using the FPKM values of all genes in the whole genome obtained from the RNA-seq data in 3-2-5, log₂ gene expression fold change was calculated, and *p*-values were calculated. Then, 3000 genes with increased or decreased gene expression based on *p* < 0.05 were extracted, and GO and KEGG analyses were performed with the WebGestalt software [49]. The analysis conditions were the same

as those described in 2-2-6, and the top 10 categories were summarized based on $FDR < 0.05$ from the analyzed categories. Furthermore, hierarchical cluster analysis was performed with Heatmapper (<http://www.heatmapper.ca/expression/>) for 30 genes among the analyzed genes for each extract and compound.

3-3 Evaluation of cell proliferation activity by soymilk extracts and soy compounds

Unfermented or fermented soymilk extracts (yellow and black soybeans) and soy compounds (genistin, genistein, daidzin, and daidzein) were evaluated for estrogenic activity by SRB assay (Figure 16 and Figure 17) [142]. Cell proliferation activity increased with higher concentrations of all soymilk extracts, whether unfermented or fermented (Figure 16). Furthermore, inhibition experiments with ICI demonstrated that cell proliferation was suppressed at all concentrations of the soymilk extracts (Figure 16). In addition, all soy compounds exhibited the highest cell proliferation activity at a concentration of 10 μ M (Figure 17). Furthermore, inhibition experiments with ICI demonstrated that cell proliferation was suppressed at all concentrations (Figure 17). Thus, it can be inferred that unfermented and fermented soymilk extracts (from yellow and black soybeans) and soy compounds (genistin, genistein, daidzin, and daidzein) contribute to cell proliferation via estrogen receptors, suggesting their estrogenic activity. Furthermore, the cell proliferation activity of the soymilk extracts was higher when fermented. This can be attributed to the reduction in the relative content of glycans or aglycans in the unfermented and fermented soymilk extracts (from yellow and black soybeans). Specifically, the glycan (genistin and daidzin) decreased from 100% to 94.7% in yellow soybeans and from 100% to 96.6% in black soybeans after fermentation (Table 3; data provided by Sansho Pharmaceutical Co., Ltd.). However, aglycans (genistein and daidzein) increased from 0% to 5.2% in yellow soybeans and from 0% to 3.4% in black soybeans, which is assumed to contribute to the observed increase in cell proliferation activity.

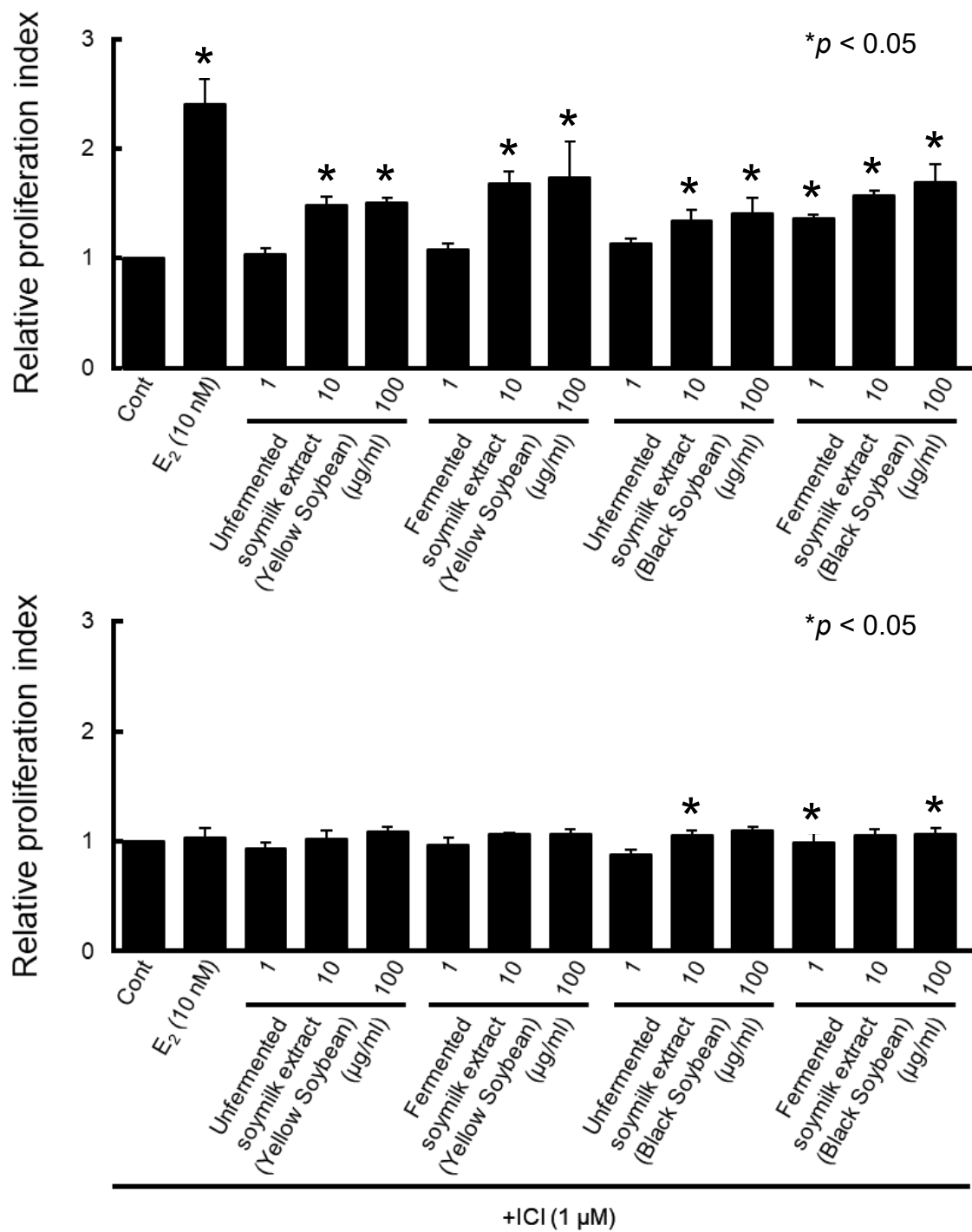


Figure 16 Evaluation of cell proliferative activity of soymilk extracts (yellow and black soybeans).

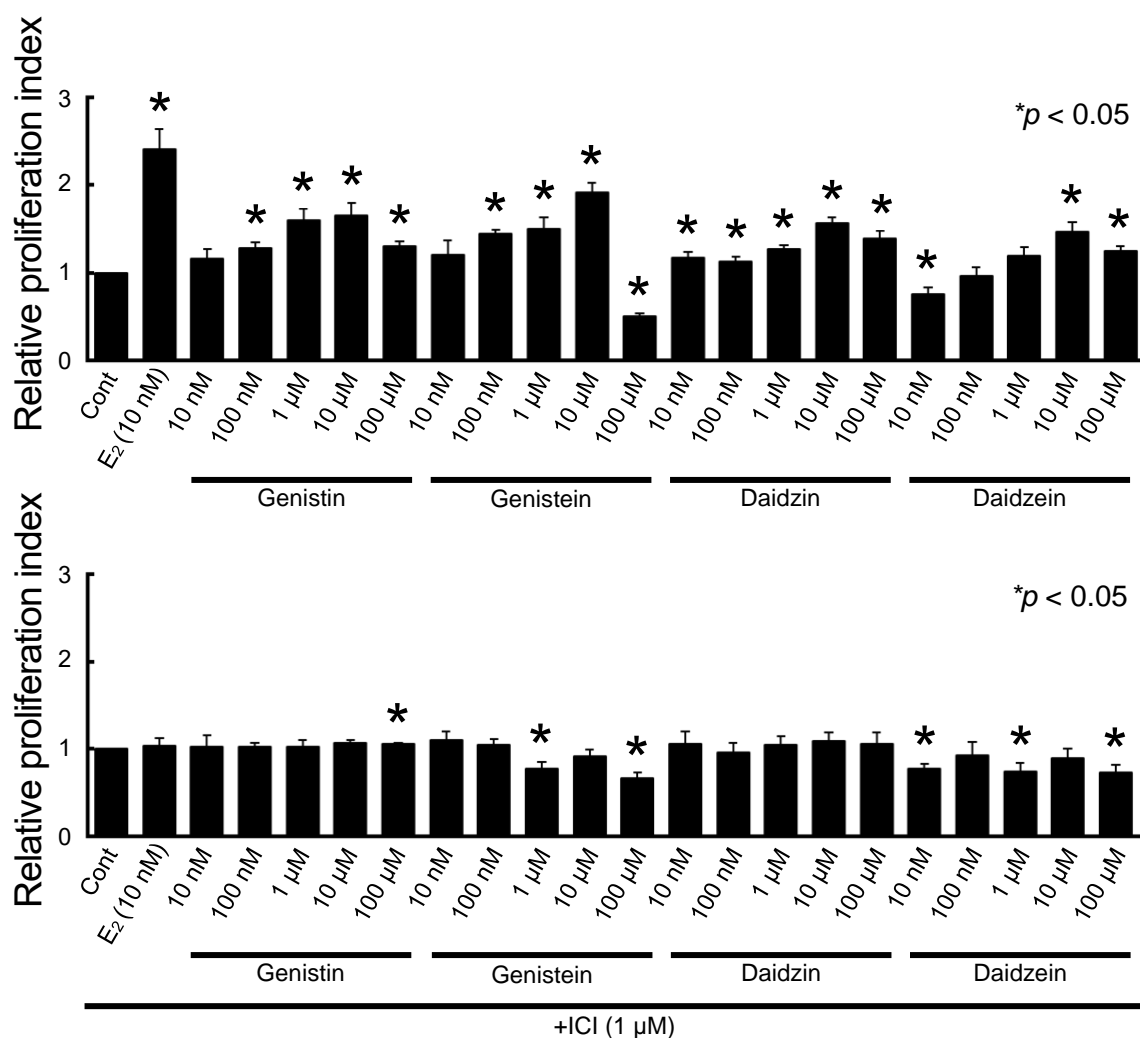


Figure 17 Evaluation of cell proliferative activity of soy compounds.

Table 3 Compositions of isoflavones in soymilk.

	Isoflavone amount (μg/g)			
	Yellow Soybean		Black Soybean	
	Unfermented (%)	Fermented (%)	Unfermented (%)	Fermented (%)
Genistin	311.1 (26.9)	1533.3 (60.0)	1473.7 (39.9)	1340.3 (47.3)
Genistein	ND (0)	51.1 (1.9)	ND (0)	54.5 (1.9)
Daidzin	844.4 (73.1)	1064.4 (38.8)	2215.8 (60.0)	1394.8 (49.3)
Daidzein	ND (0)	93.3 (3.4)	ND (0)	41.9 (1.5)
Isoflavone glycoside	1155.6 (100.0)	2595.6 (94.7)	3694.7 (100.0)	2735.1 (96.6)
Isoflavone aglycon	ND (0)	142.2 (5.2)	ND (0)	96.3 (3.4)
Total isoflavone	1155.6 (100.0)	2740.0 (100.0)	3694.7 (100.0)	2831.4 (100.0)

ND: not detected.

3-4 Evaluation of intracellular signals

Unfermented and fermented soymilk extracts (from yellow and black soybeans) and soy compounds (genistin, genistein, daidzin, and daidzein) were evaluated for their estrogenic activity by detecting cellular signal proteins through Western blotting (Figures 19-28) [142].

Before conducting experiments with soymilk extracts and soy compounds, we stimulated MCF-7 cells with E_2 and examined their phosphorylation activity, obtaining results consistent with Figure 5 in Chapter 2-2-4 (Figure 18). Next, MCF-7 cells were stimulated with low concentrations of unfermented or fermented soymilk extracts (from yellow and black soybeans), which exhibited Erk1/2 phosphorylation activity similar to that induced by E_2 after 5 min (Figures 19-22). At higher concentrations, phosphorylation was observed at both 5 and 15 min (Figures 19-22).

Similarly, Akt phosphorylation was also observed under these conditions (Figures 19-22). All soy compounds induced phosphorylation of Erk1/2 and Akt at 5 to 15 min (Figure 23). Furthermore, inhibition experiments using ICI suppressed the phosphorylation of signal proteins in response to all stimulants (Figures 24-28).

These results suggest that unfermented and fermented soymilk extracts (from yellow and black soybeans) and soy compounds promote phosphorylation via estrogen-like signaling, indicating their estrogenic activity.

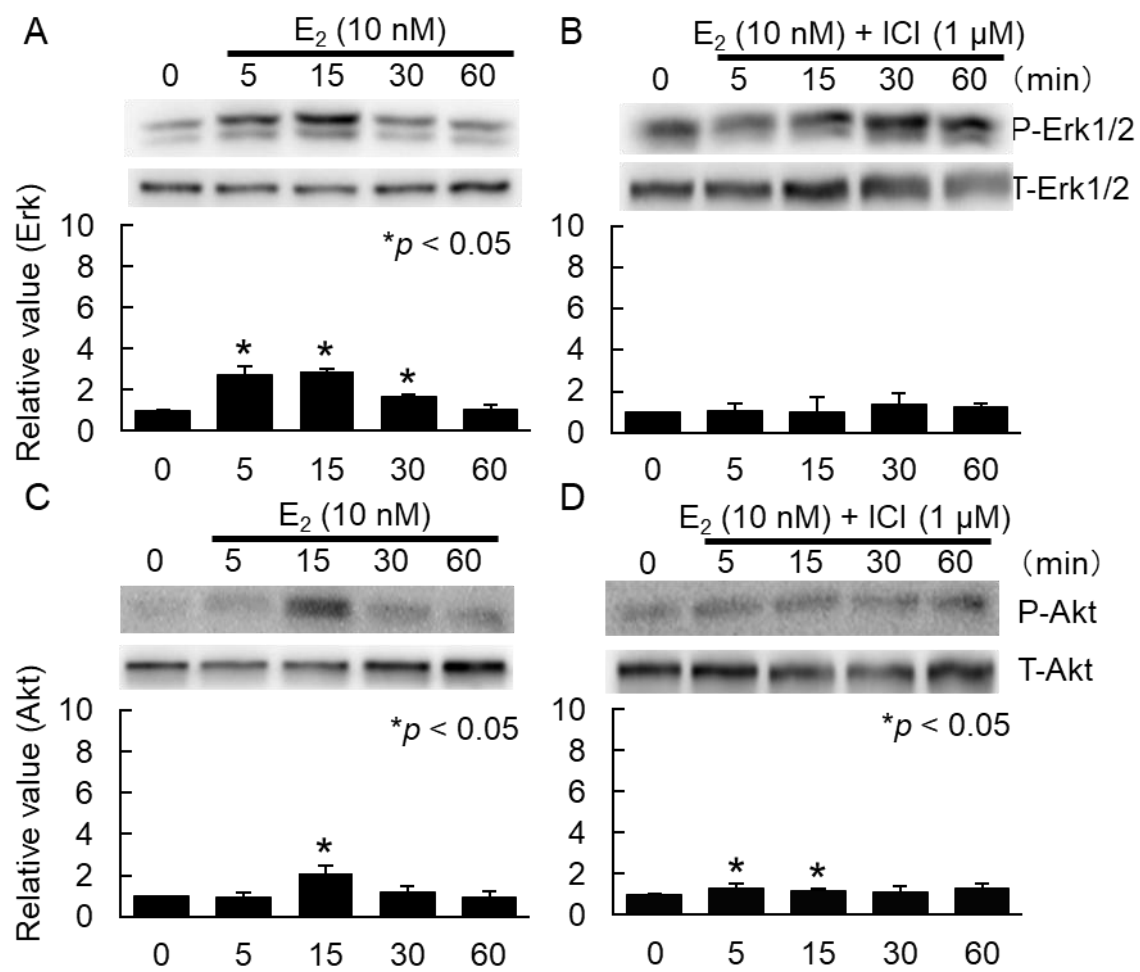


Figure 18 Evaluation of phosphorylation activity of E₂.

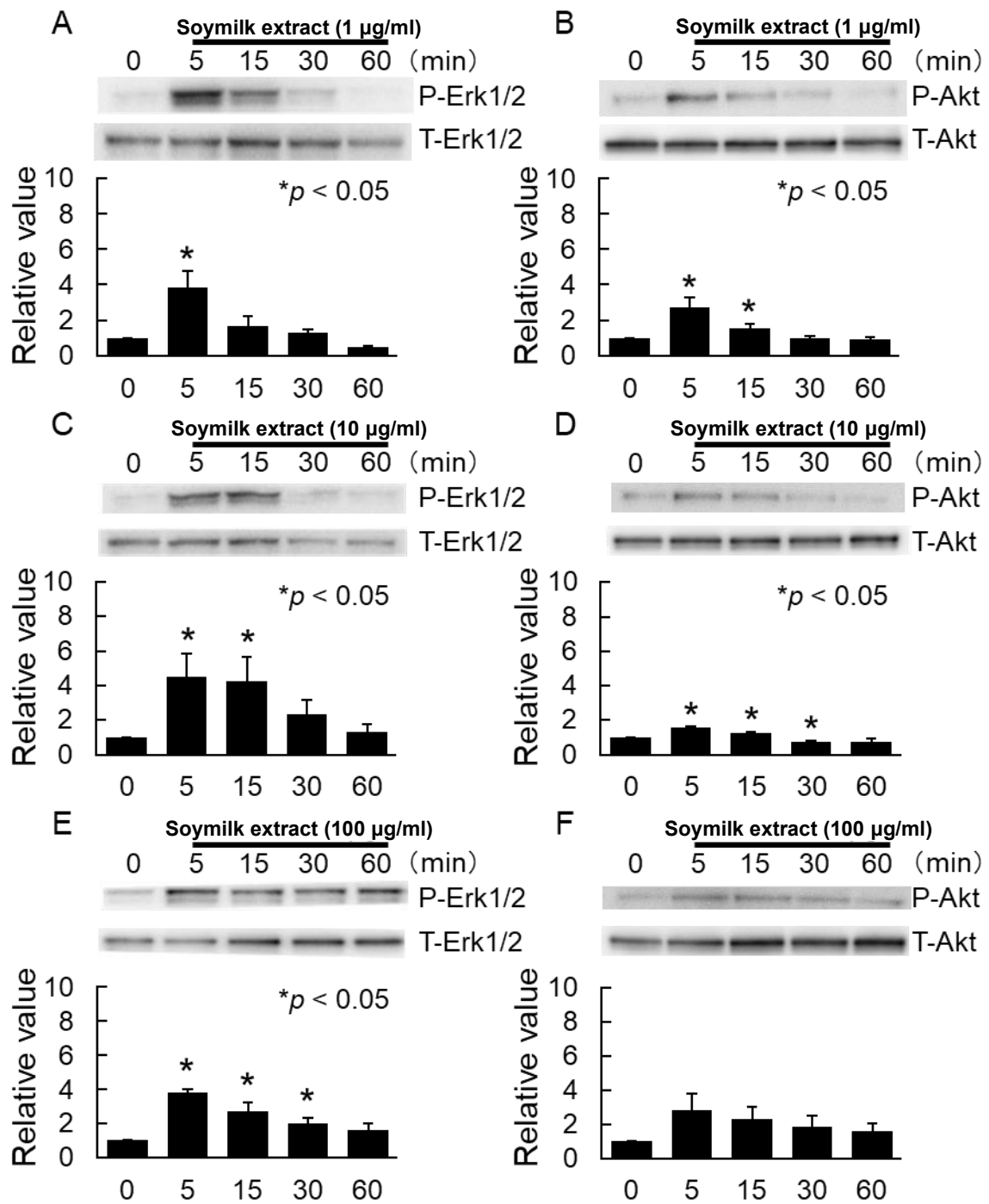


Figure 19 Evaluation of phosphorylation activity of unfermented soymilk extract (yellow soybeans).

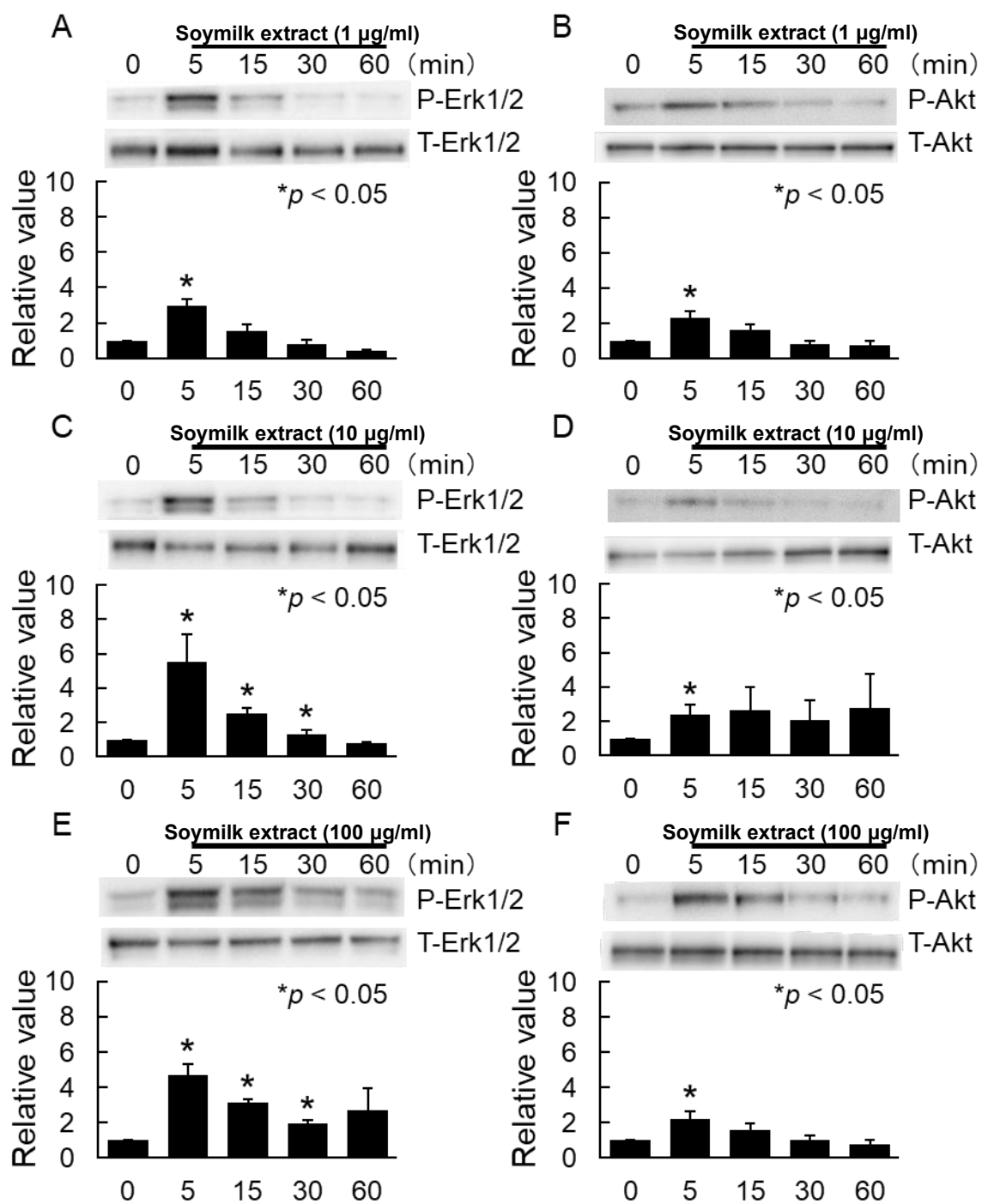


Figure 20 Evaluation of phosphorylation activity of fermented soymilk extract (yellow soybeans).

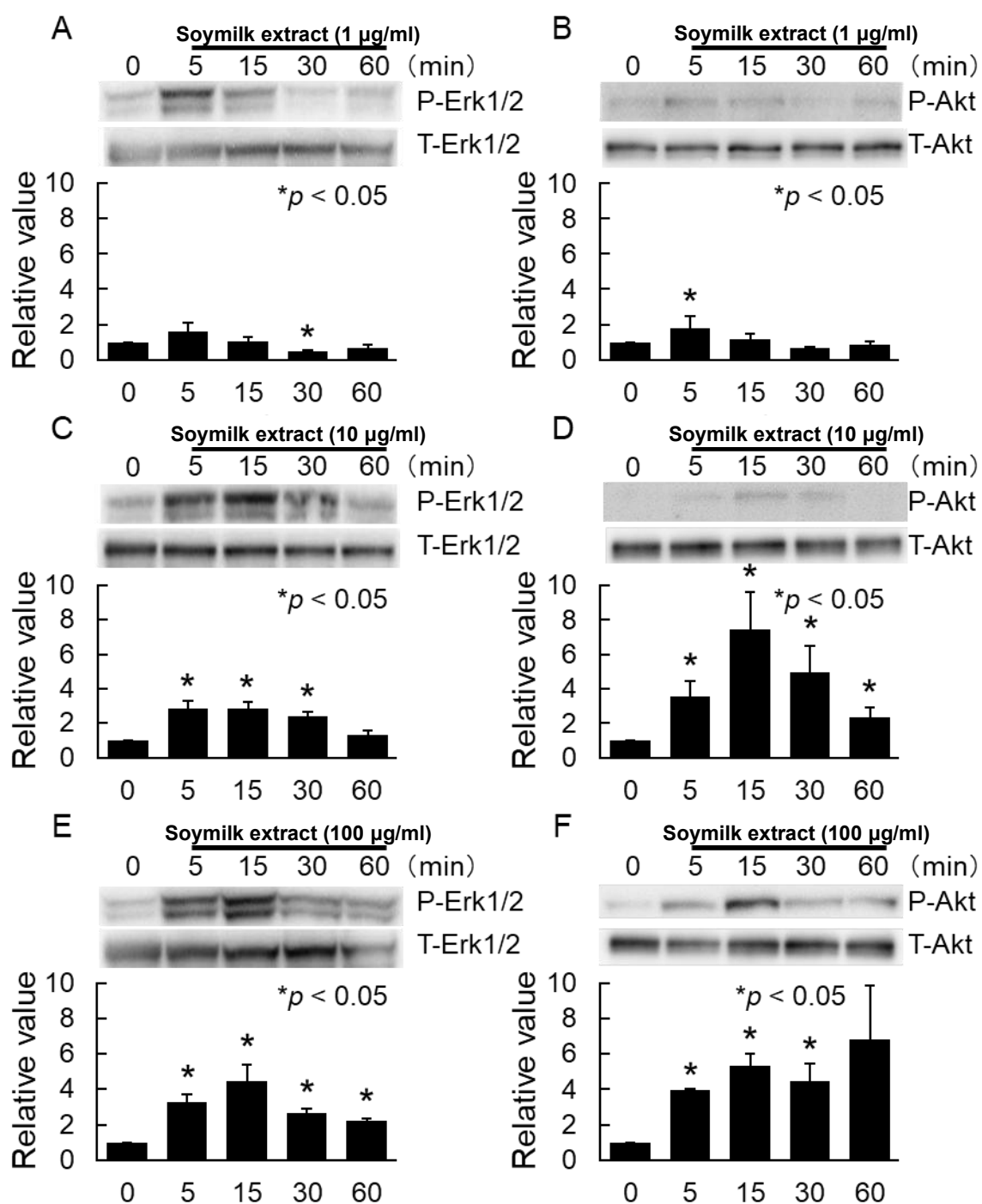


Figure 21 Evaluation of phosphorylation activity of unfermented soymilk extract (black soybeans).

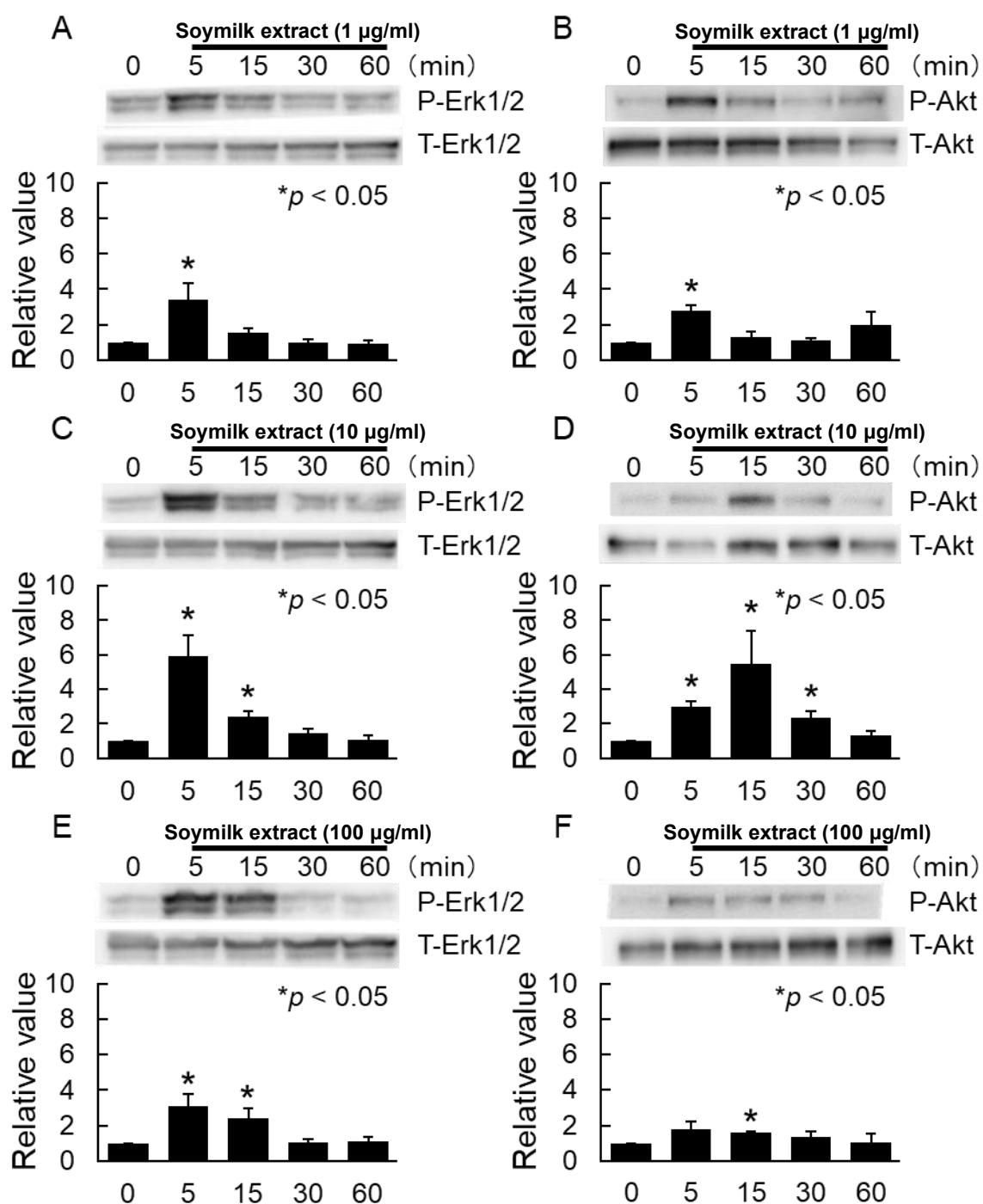


Figure 22 Evaluation of phosphorylation activity of fermented soymilk extract (black soybeans).

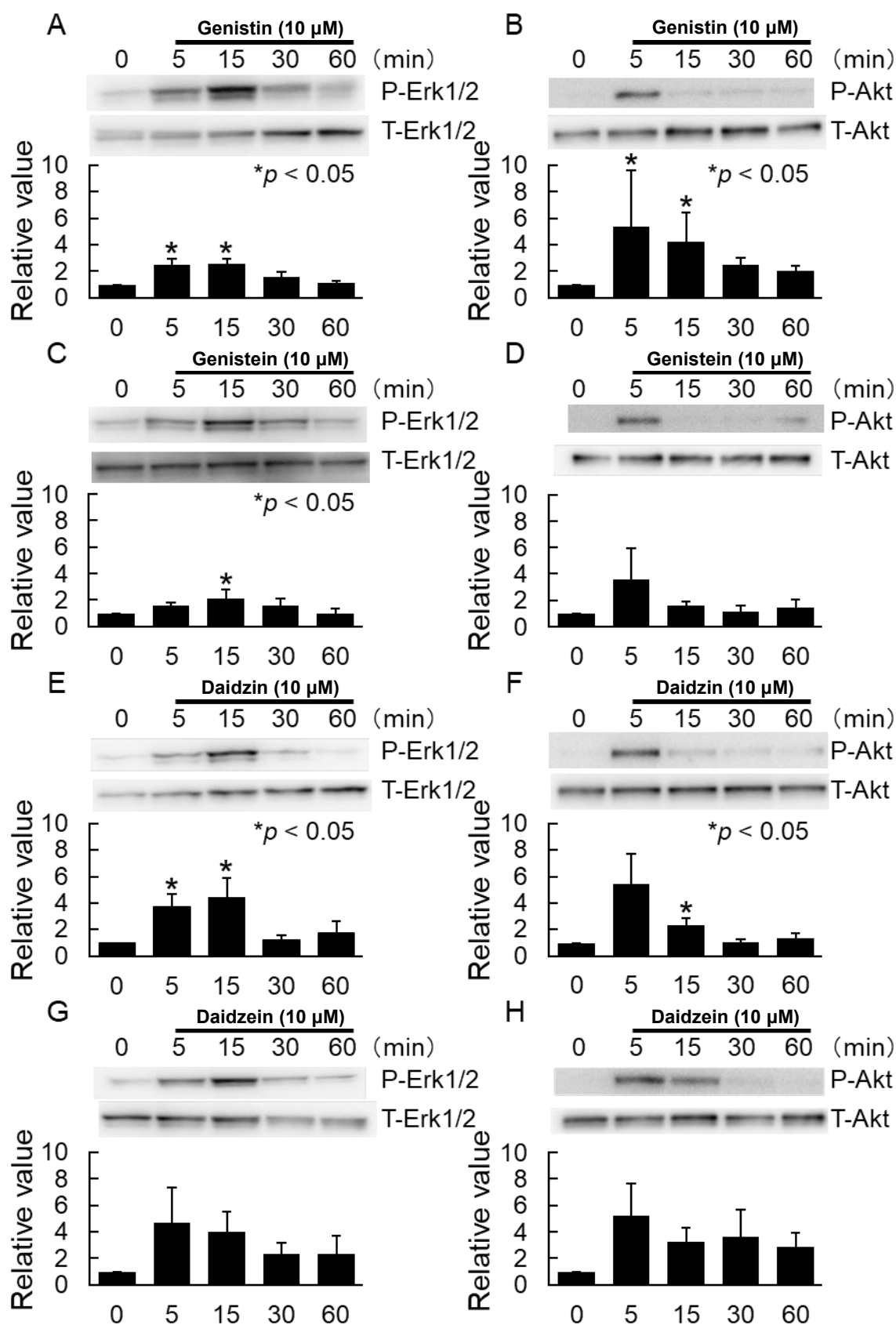


Figure 23 Evaluation of phosphorylation activity of soy compounds.

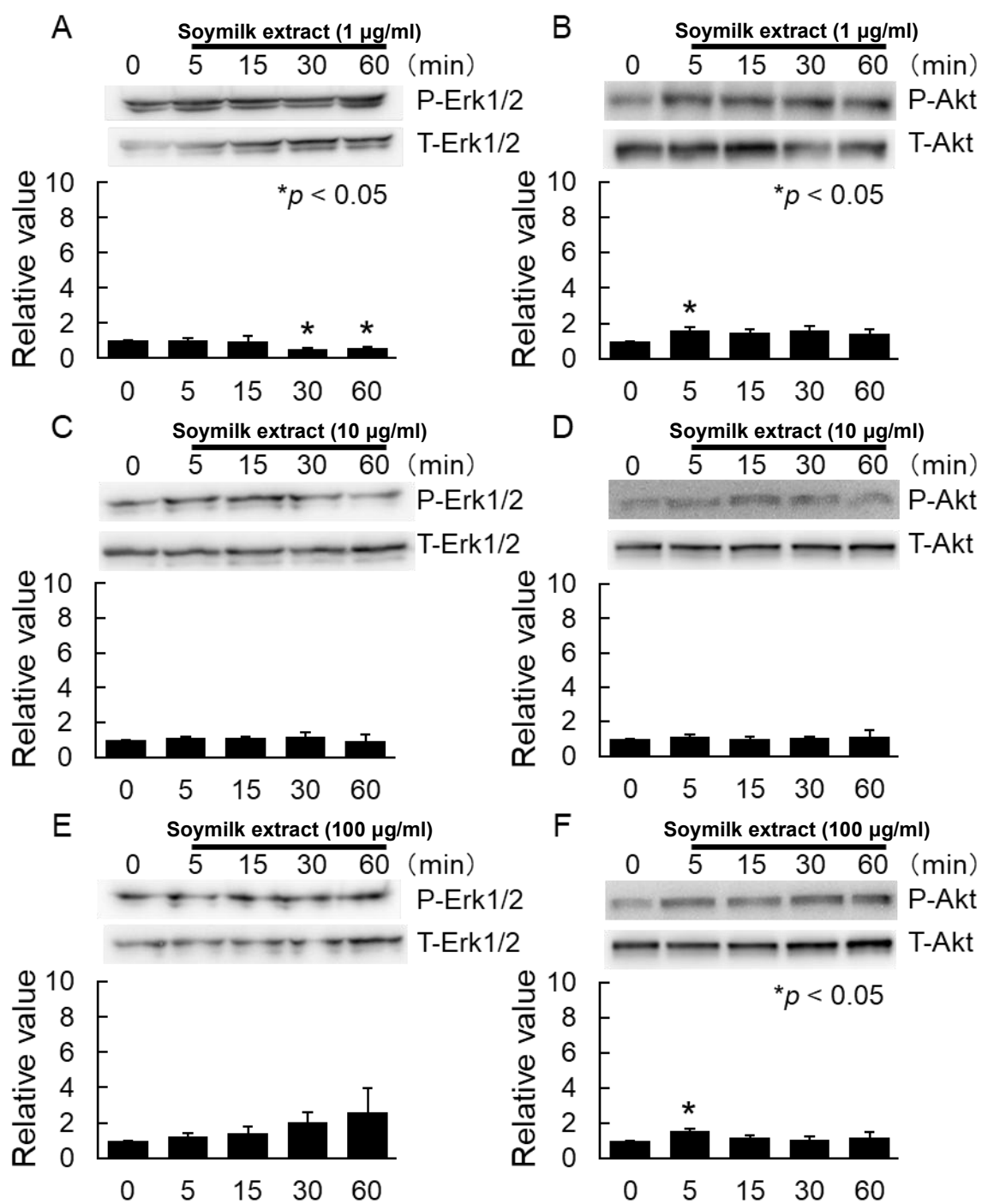


Figure 24 Evaluation of phosphorylation activity of unfermented soymilk extract (yellow soybeans) by ICI.

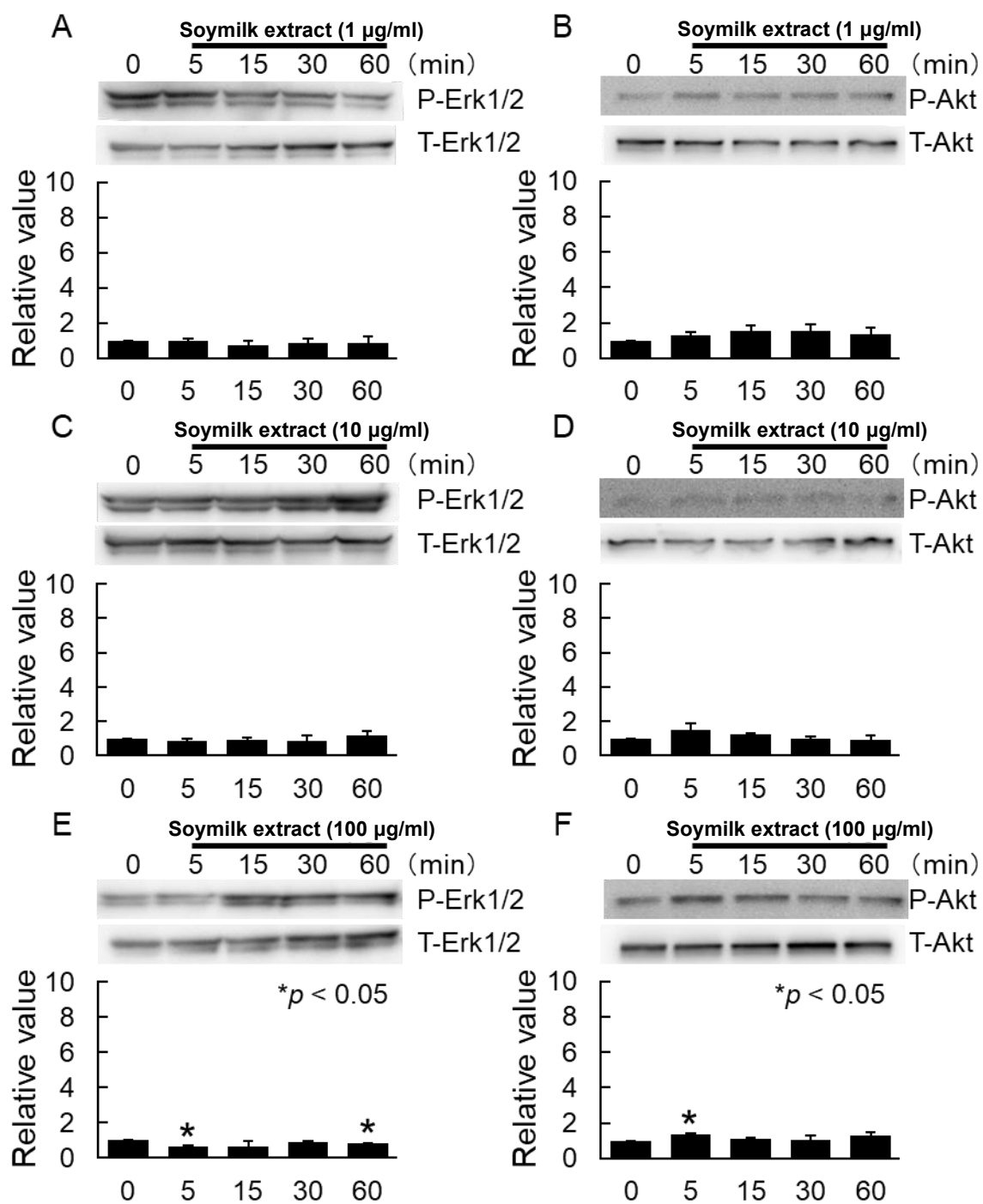


Figure 25 Evaluation of phosphorylation activity of fermented soymilk extracts (yellow soybeans) by ICI.

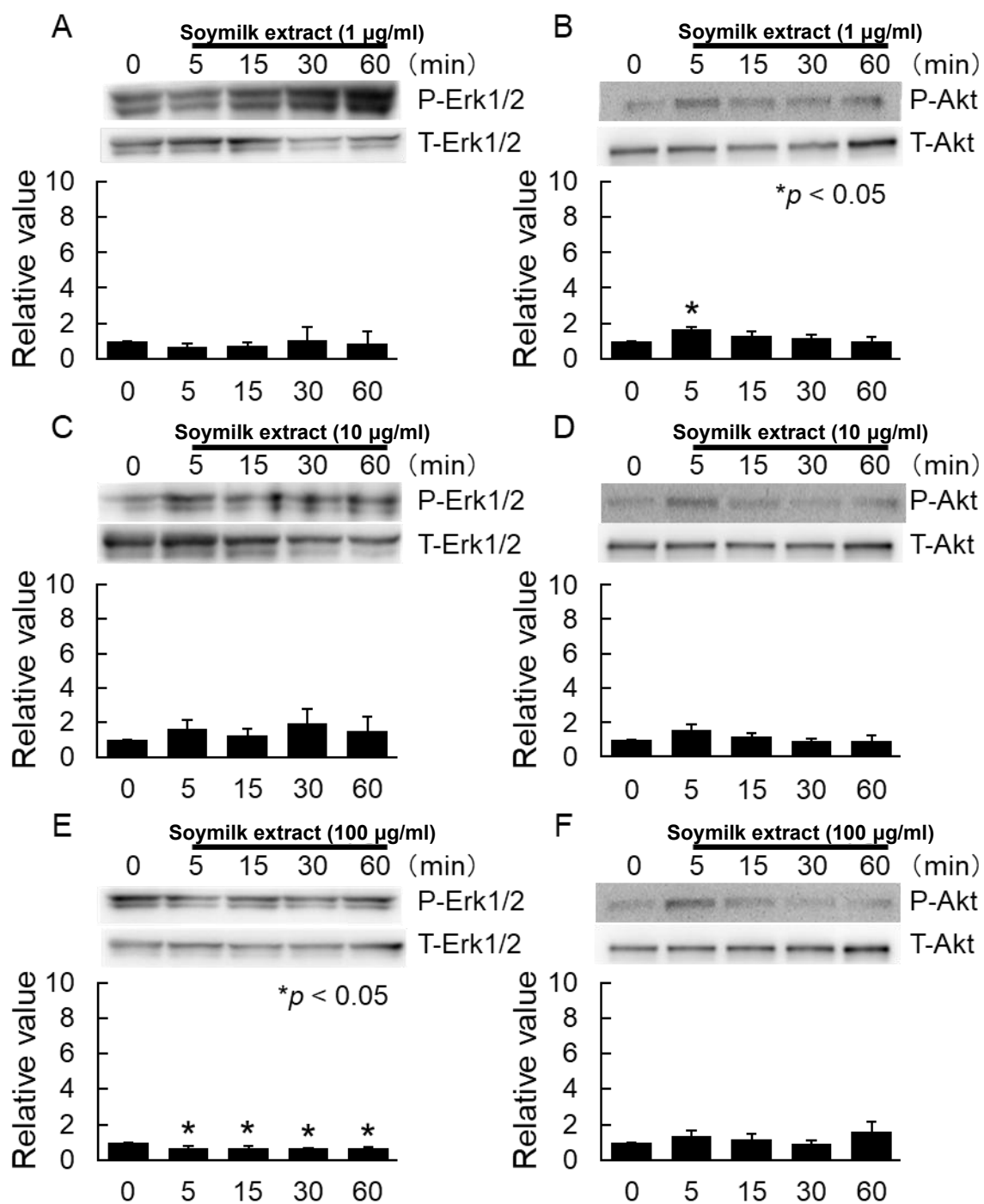


Figure 26 Evaluation of phosphorylation activity of unfermented soymilk extract (black soybeans) by ICI.

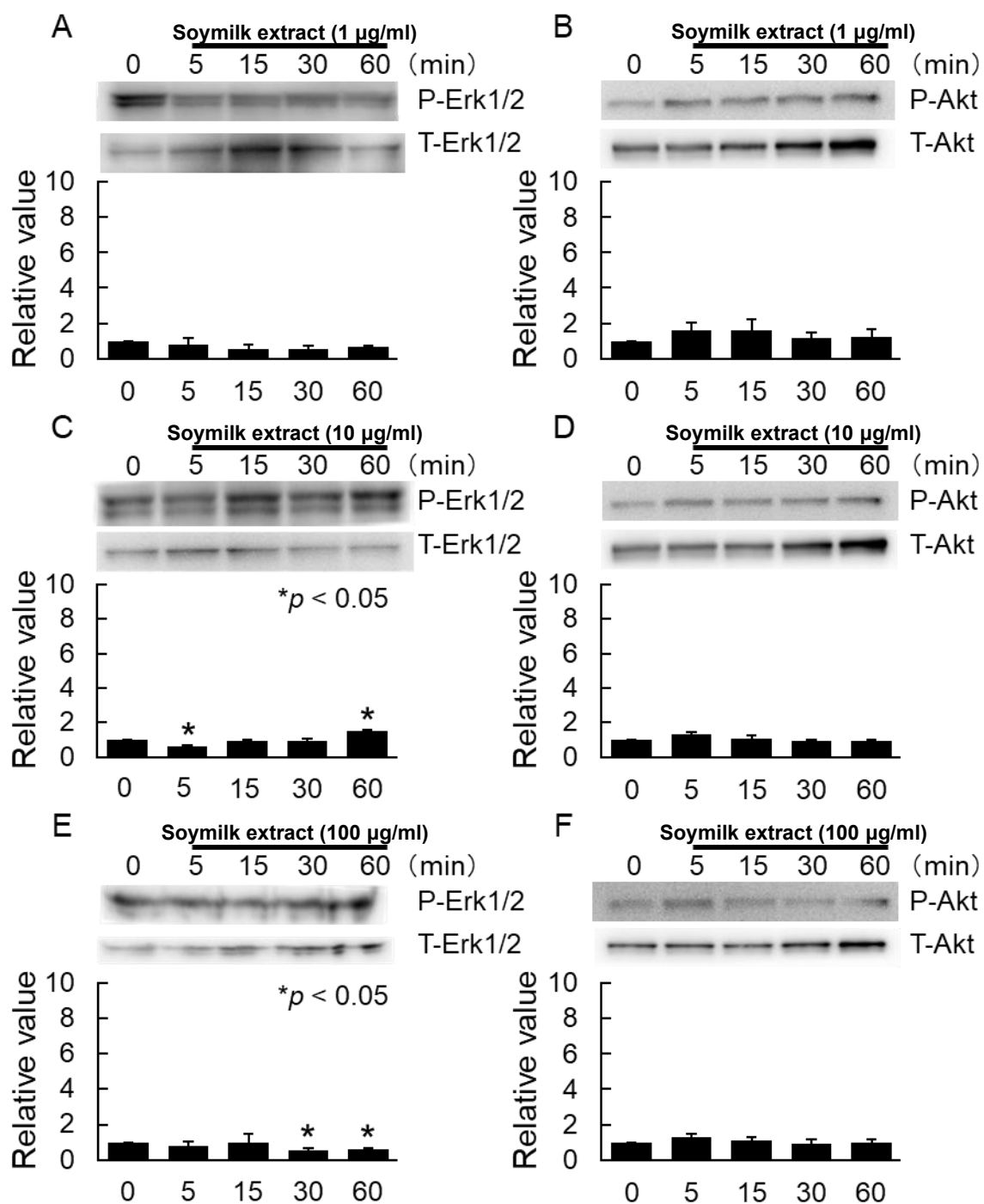


Figure 27 Evaluation of phosphorylation activity of fermented soymilk extract (black soybeans) by ICI.

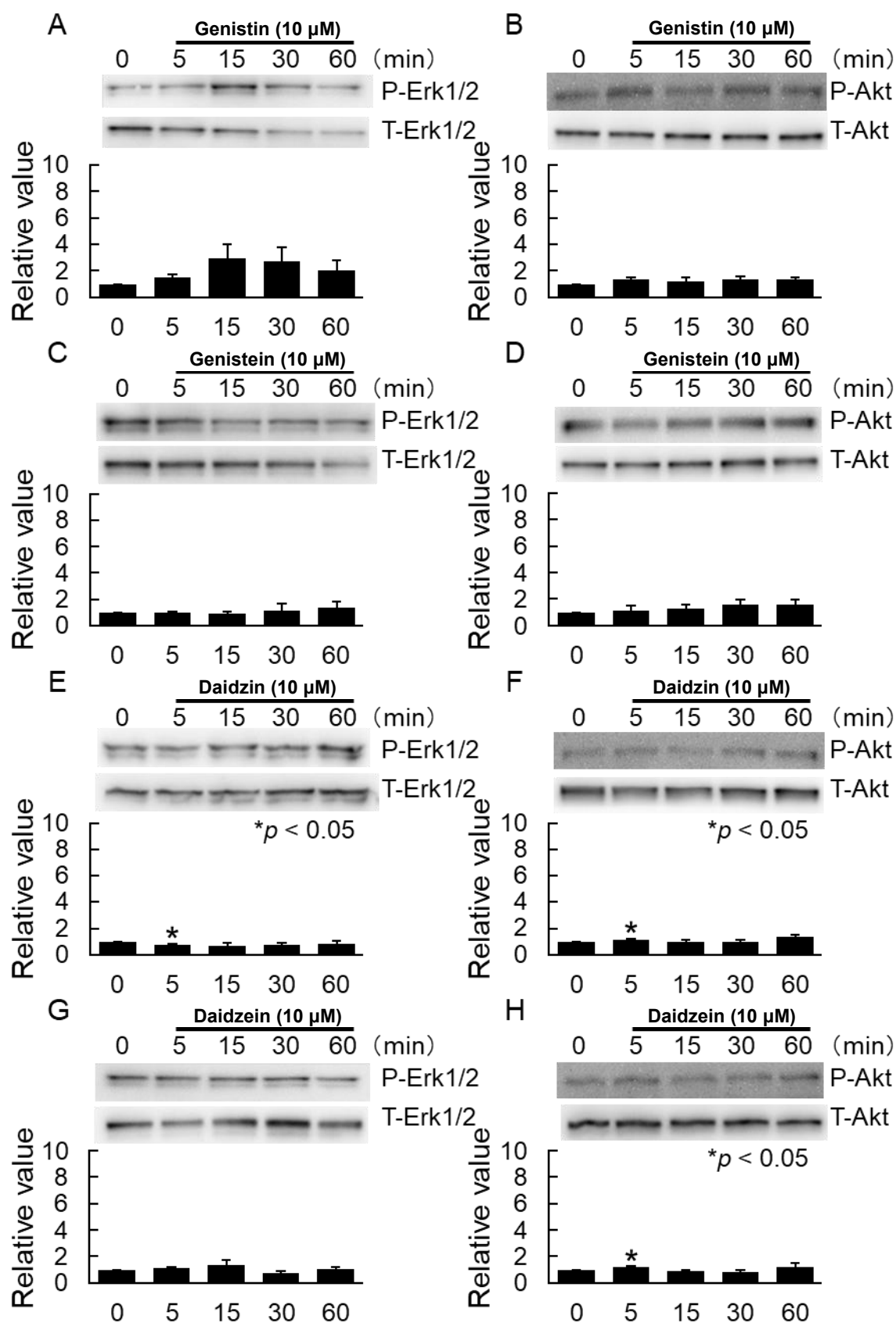


Figure 28 Evaluation of phosphorylation activity of soy compounds by ICI.

3-5 Gene expression analysis by RNA-seq

Utilizing the RNA-seq, gene expression variation was statistically examined for 30 ERGs [24] (Figures 29-37) [142].

In this experiment, stimulation with E₂ (n = 3), soymilk extracts (n = 2), and soy compounds (n = 2) was performed over 3 days. The expression pattern induced by E₂ was similar to that in Figure 8, showing an increase in the expression of *EGR3* to *BARX2* and a decrease in *LINC02593* to *FRY* (Figure 29).

Thus, the 30 ERGs identified in the previous chapter were confirmed to be stable and consistently responsive to 3 days of stimulation. Conversely, the expression patterns induced by unfermented and fermented soymilk extracts differed from those of E₂ (Figure 29). However, the soy compounds exhibited gene expression patterns similar to E₂, with the exception of daidzin (Figure 30).

To further clarify whether they exhibit estrogenic activity, correlation analysis was performed for all combinations using gene expression profiles for E₂ (n = 3), soymilk extracts (n = 2), and soy compounds (n = 2) (Figures 31–36).

First, the correlation for E₂ showed a high value of $R = 0.96$ across all combinations (Figure 31). Using this E₂ data as a reference, we compared the soymilk extracts and soy compounds. The unfermented and fermented soymilk extracts exhibited moderate correlations, with R values ranging from 0.33 to 0.61 (A to D in Figure 32). In contrast, the soy compounds showed high correlations, with R values ranging from 0.84 to 0.97 (E to H in Figure 32). Then, the soymilk extract data alone showed a high correlation, with R values ranging from 0.78 to 0.97, while the soy compounds alone showed an even higher correlation, with R values ranging from 0.87 to 0.99 (Figures 33 and 34).

Furthermore, a comparison between soymilk extracts and soy compounds showed correlations with R values ranging from 0.41 to 0.82 (Figures 35 and 36). These findings suggest that both soymilk extracts and soy compounds exhibit estrogenic activity, even at the gene expression level. It

is also speculated that soymilk extracts and soy compounds share significant similarities in the signaling pathways that activate the 30 ERGs.

Furthermore, cluster analysis using RNA-seq data distinguished soy compounds from soymilk extracts, with the exception of daidzin (Figure 37). This result aligns with the findings of the correlation analysis between soymilk extracts and soy compounds (Figures 35 and 36), where only daidzin showed a higher correlation value with soymilk extracts than with the other compounds.

In terms of the structural features of estrogens, the hydroxyl groups at position 3 of the A ring and position 17 of the D ring are particularly critical for activity, as well as the hydrophobicity of the B and C rings [148]. Previous studies [148,149] have already described the significance of the number and position of hydroxyl groups in determining estrogenic activity. In the gene expression analysis conducted in this section, the unique activity of daidzin compared to the other soy compounds is likely due to differences in the number of hydroxyl groups. Excluding the hydroxyl groups in the sugar moiety, the soy compounds had the following configurations: genistein with three hydroxyl groups (position 7 of the A ring, 5 of the A ring, and 4' of the B ring); genistin and daidzein with two hydroxyl groups (position 7 of the A ring and 4' of the B ring); and daidzin with only one hydroxyl group (position 4' of the B ring) (Figure 14). This suggests that daidzin's lower number of hydroxyl groups may contribute to its lower correlation value compared to the other soy compounds and E₂. Furthermore, the structural difference between genistin and daidzin, which are otherwise nearly identical, is the presence or absence of a hydroxyl group at position 5 of the A ring. This structural difference is assumed to influence gene expression, as evidenced by the comparison of gene expression analysis and compound structures [150,151].

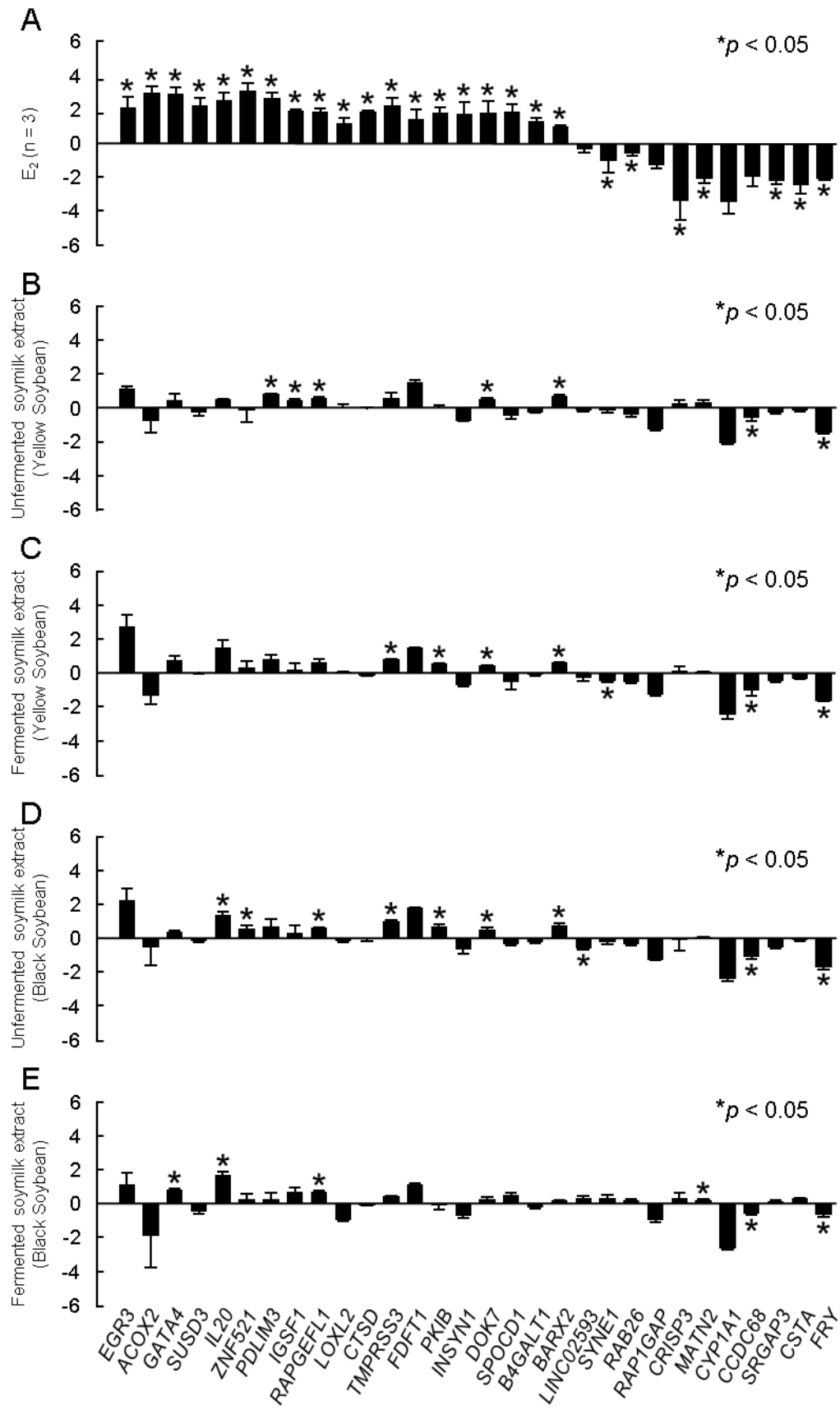


Figure 29 Expression profiles of E_2 and soy milk extracts by RNA-seq.

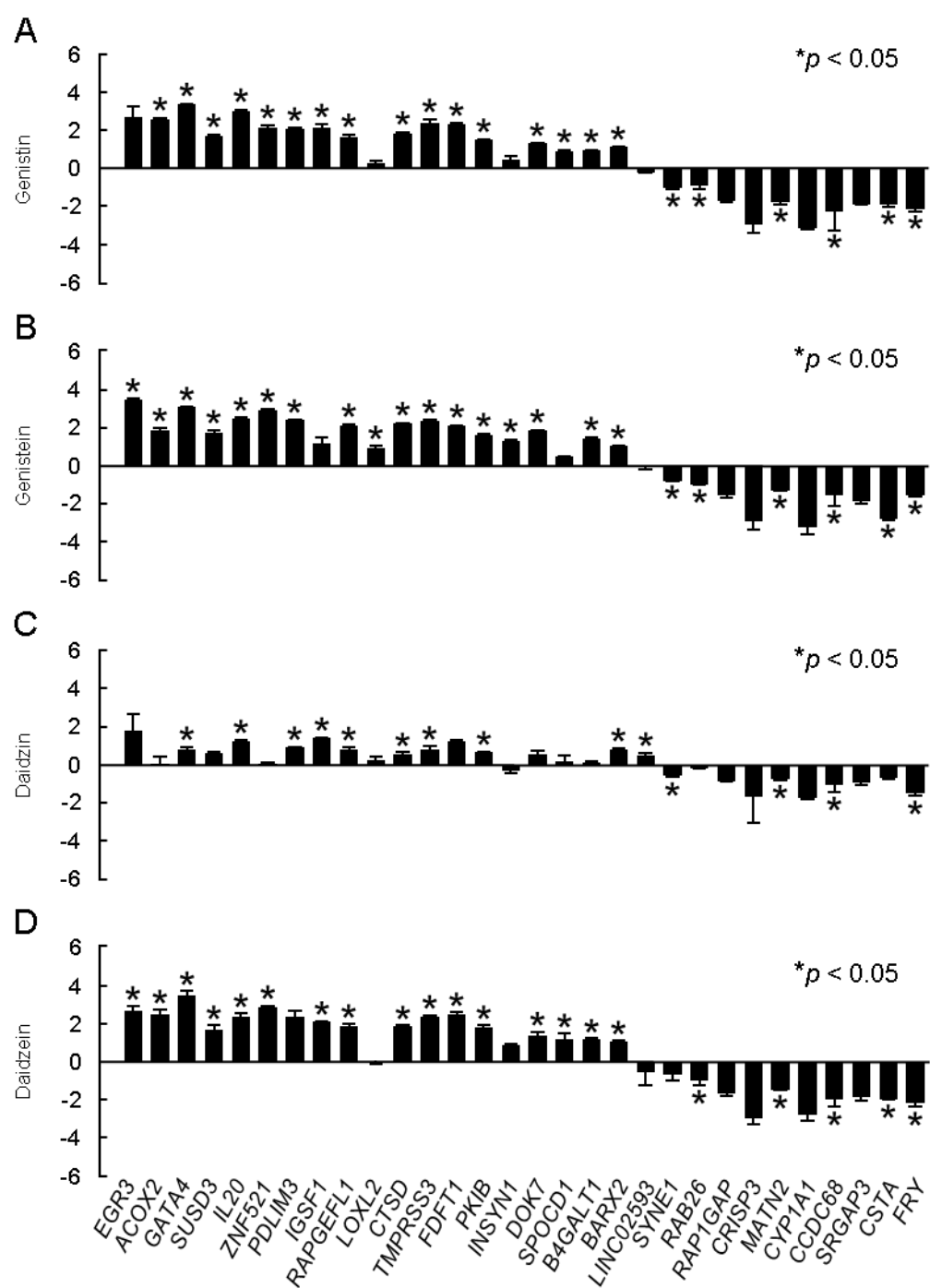


Figure 30 Expression profiles of soy compounds by RNA-seq.

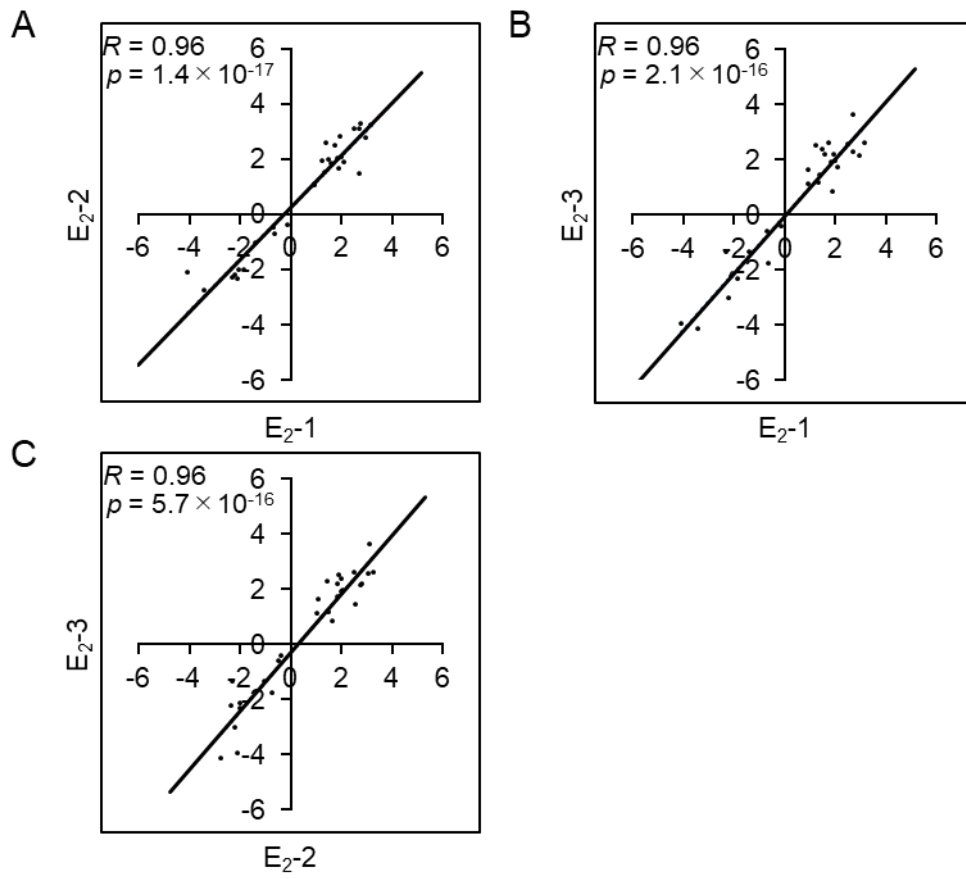


Figure 31 E_2 correlation analysis using ERGs.

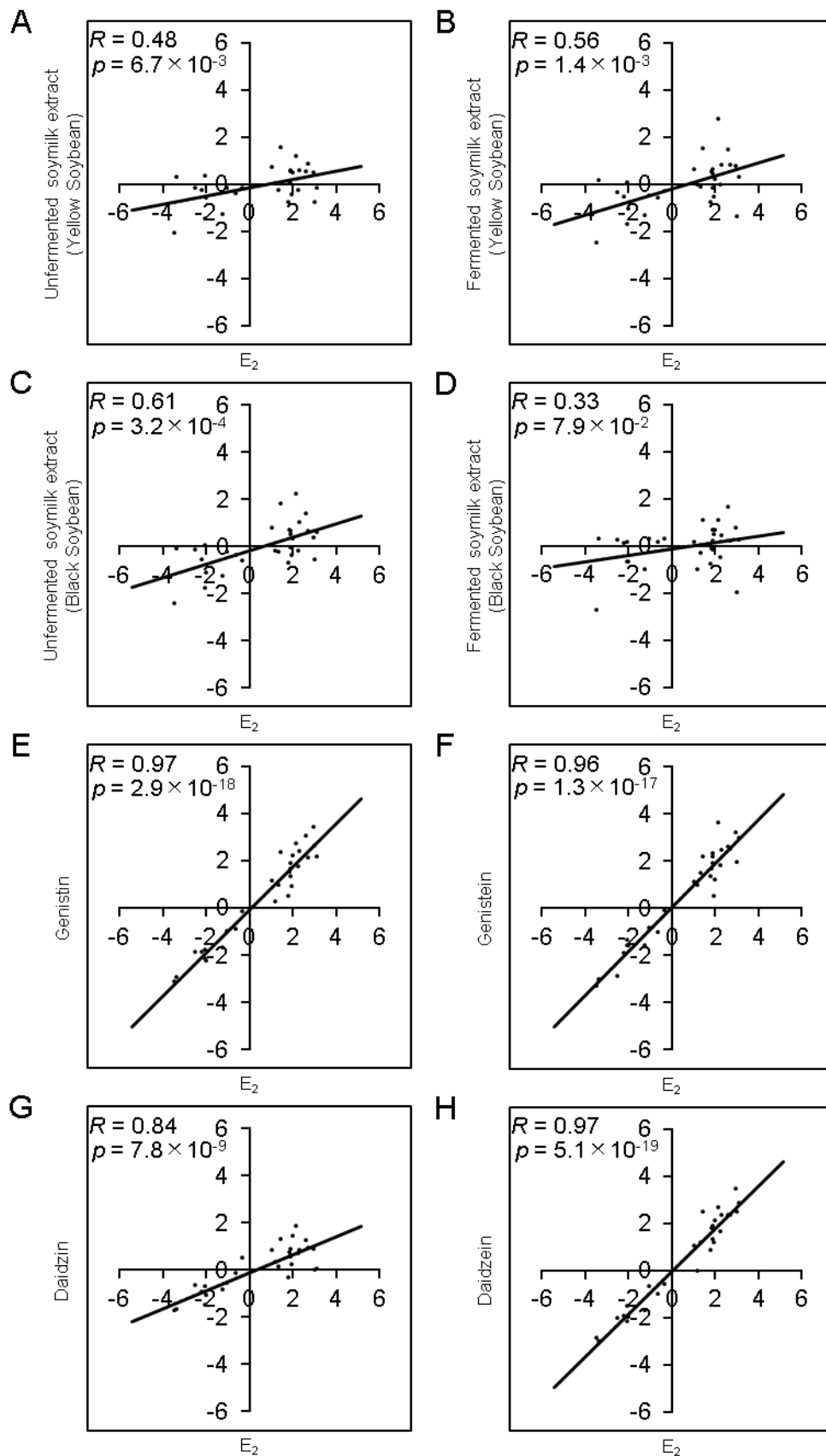


Figure 32 Correlation analysis of E_2 and soymilk extracts or soy compounds using ERGs.

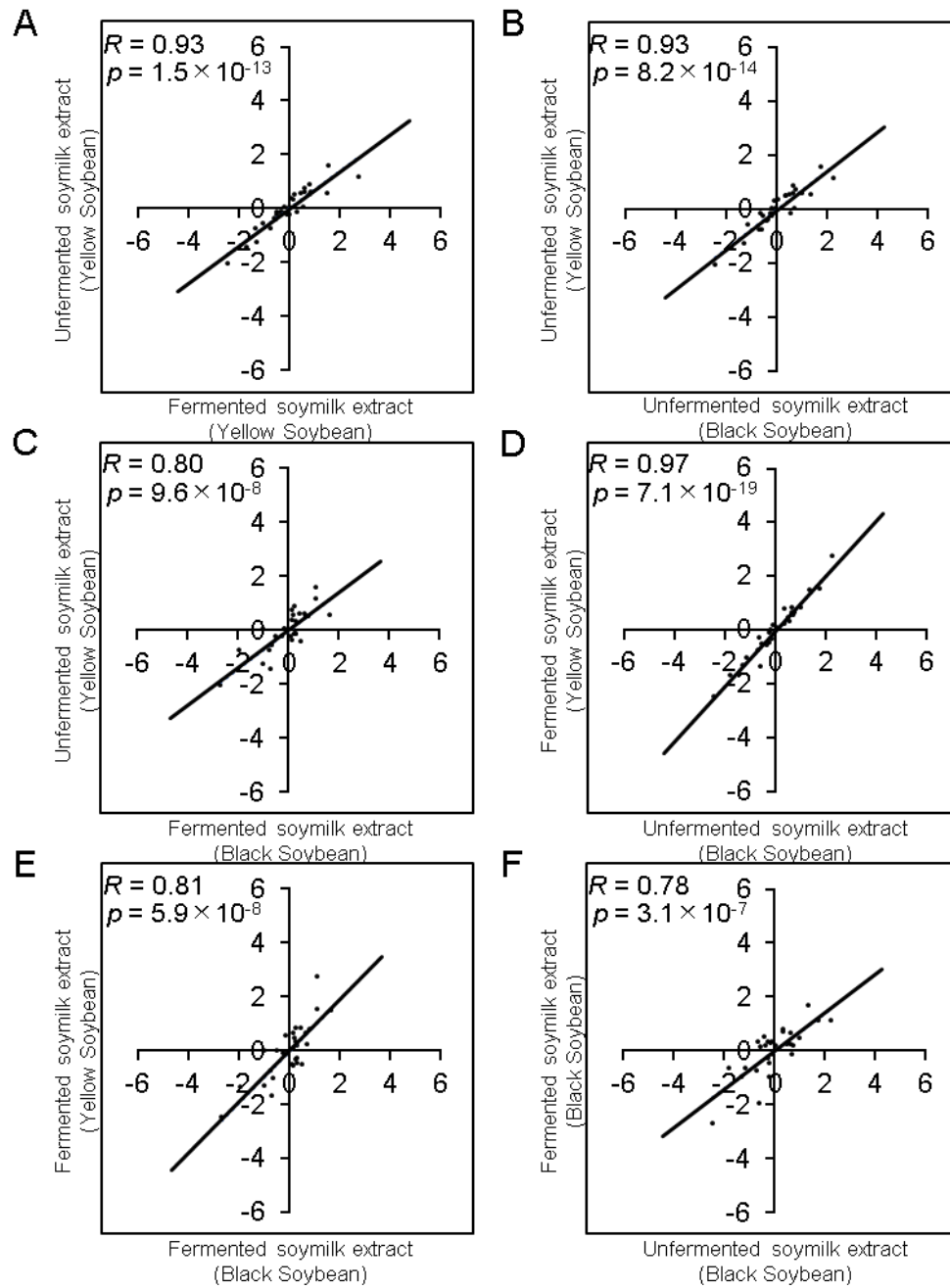


Figure 33 Correlation analysis of soy milk extracts with ERGs.

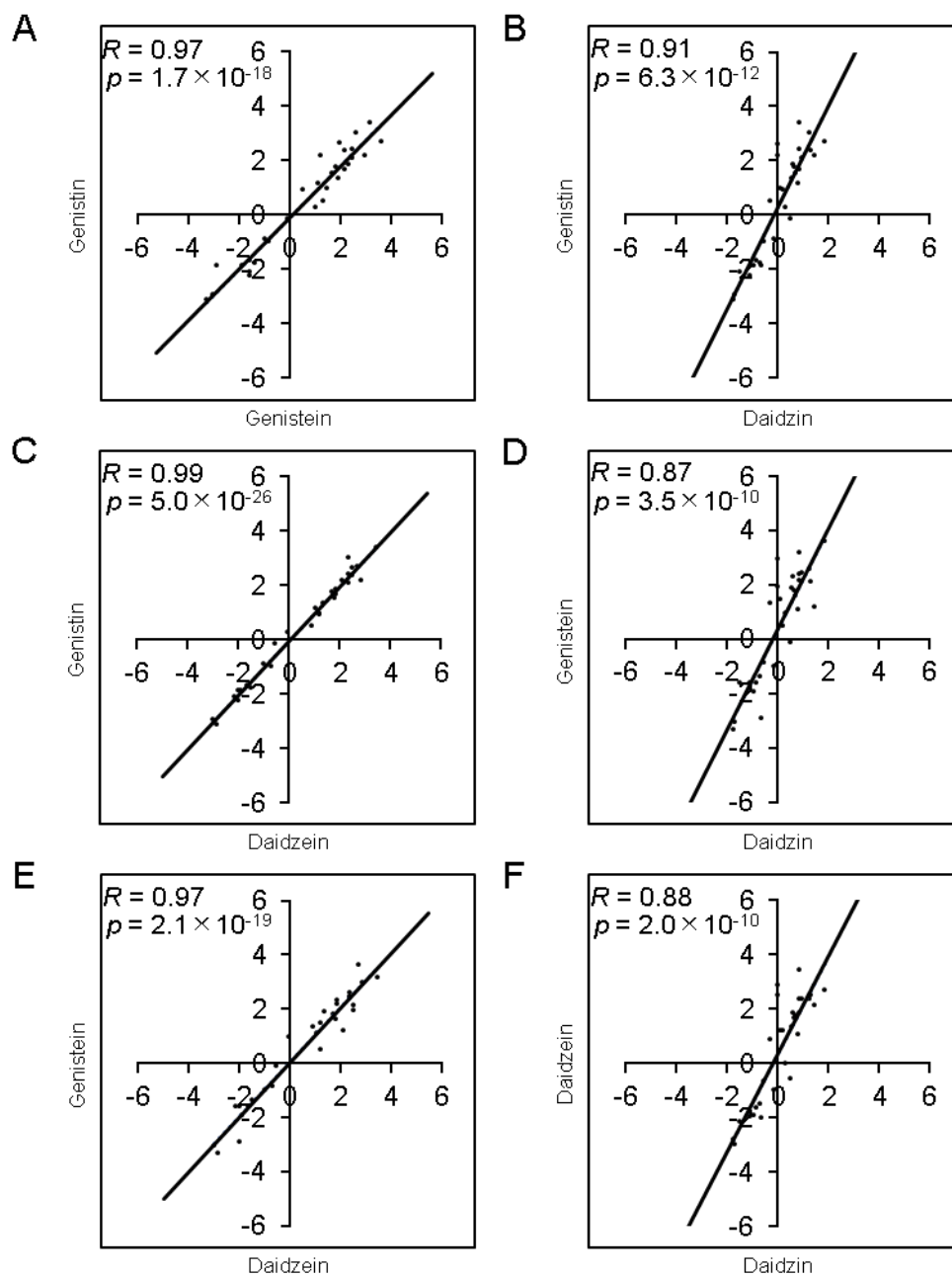


Figure 34 Correlation analysis of soy compounds using ERGs.

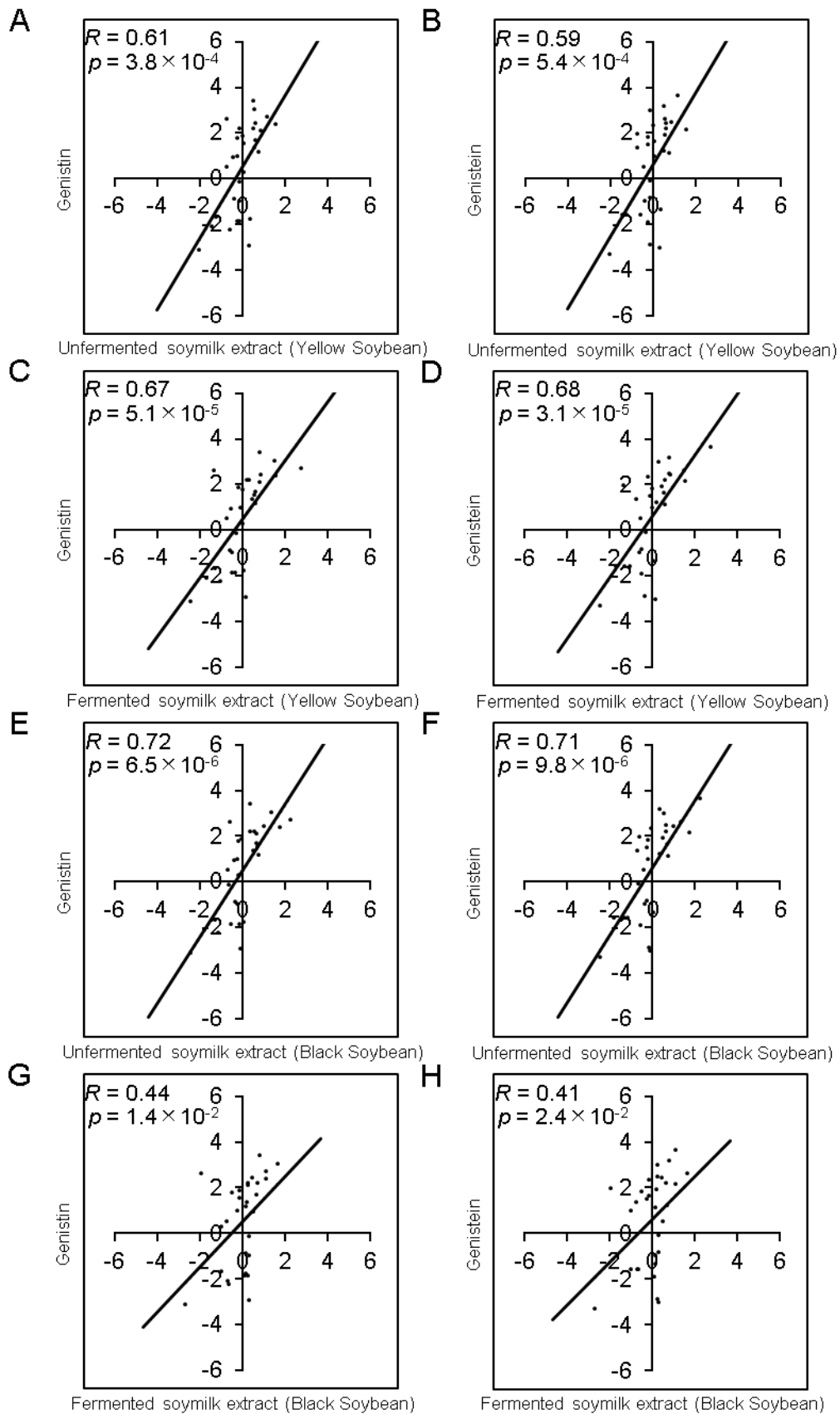


Figure 35 Correlation analysis of soymilk extract and soy compounds using ERGs (1).

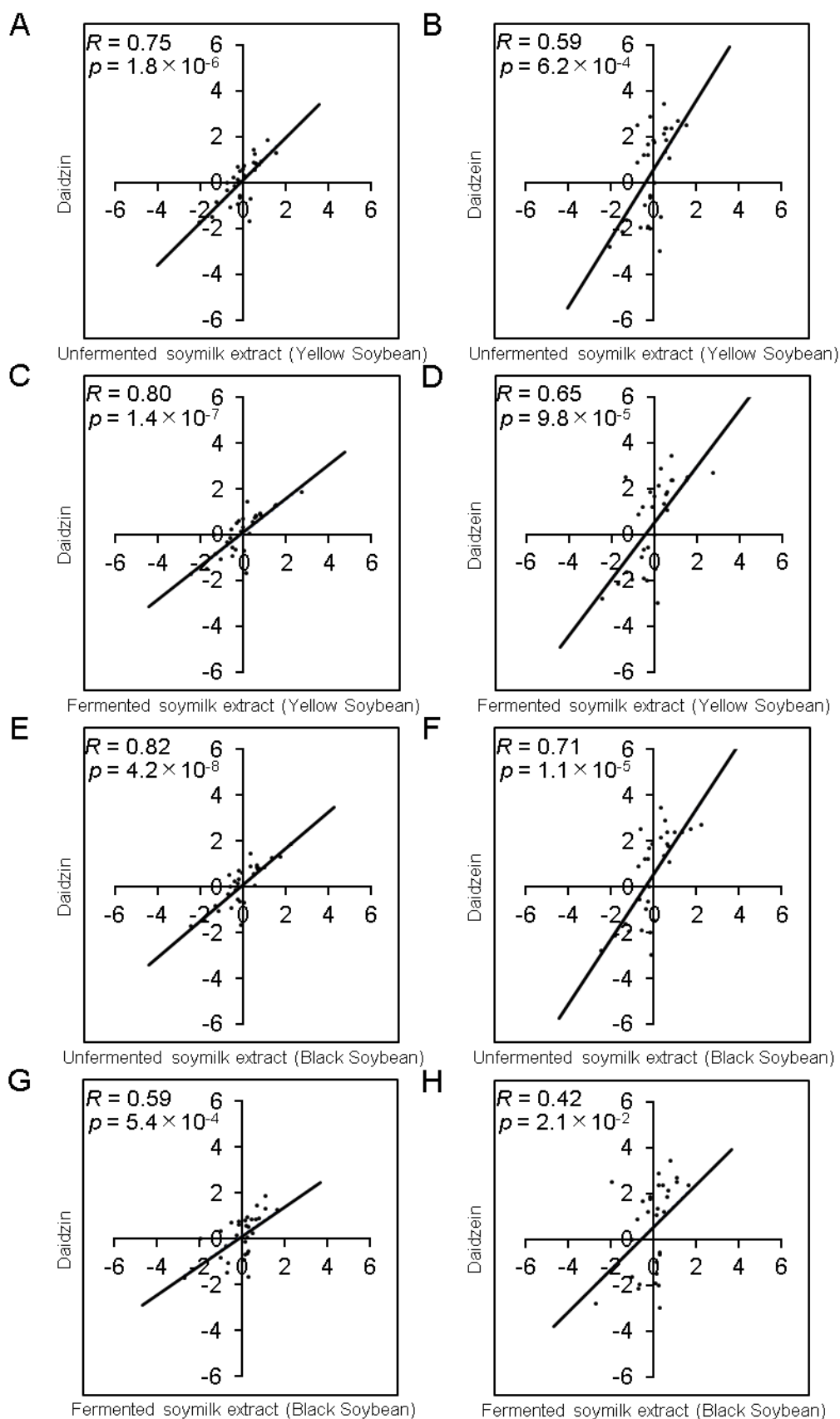


Figure 36 Correlation analysis of soymilk extract and soy compounds using ERGs (2).

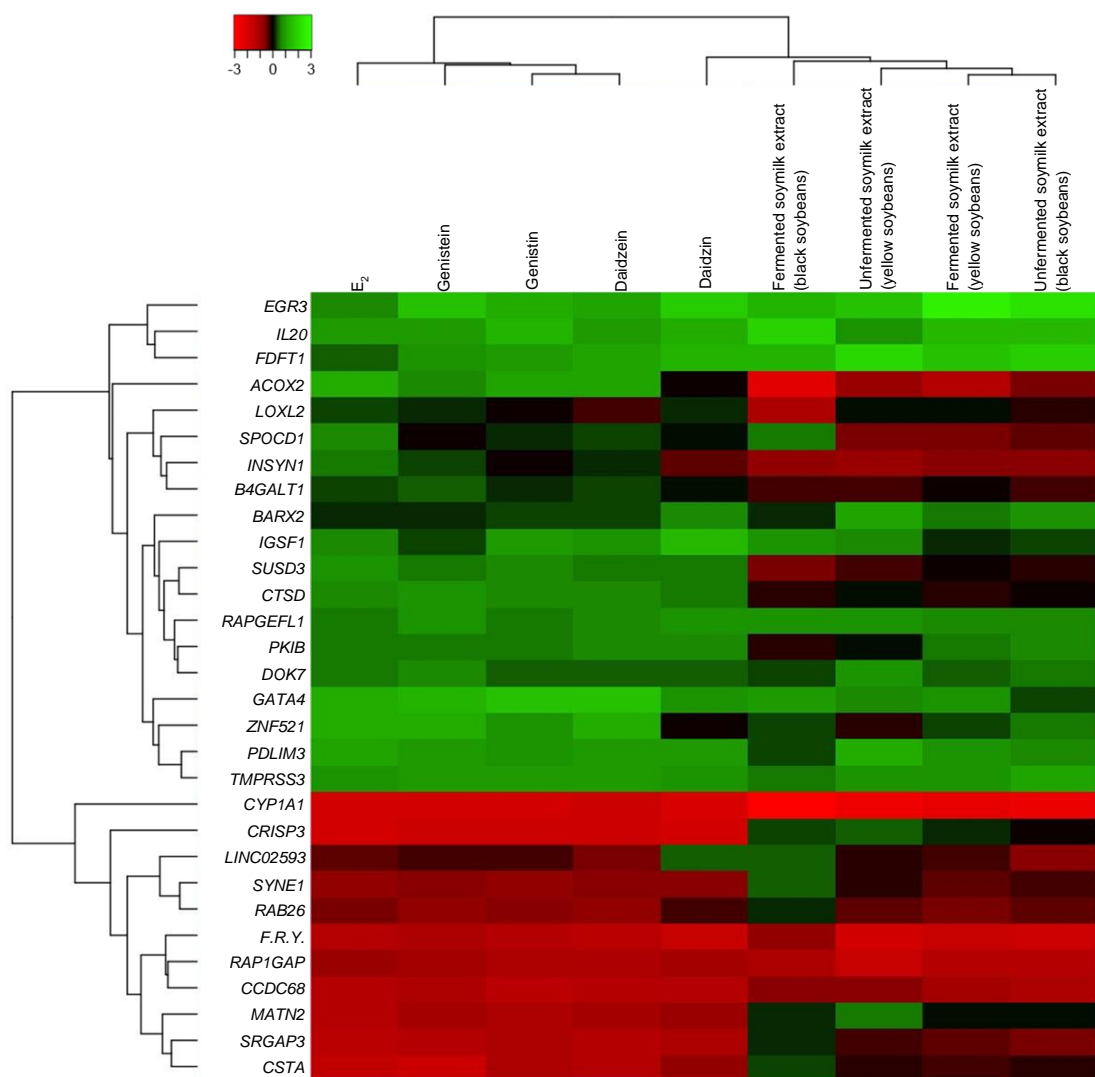


Figure 37 Cluster analysis of soymilk extracts and soy compounds using RNA-seq data.

3-6 Gene expression analysis by *Real-time* RT-PCR

Gene expression variation was statistically examined for 30 ERGs [24] using *real-time* RT-PCR (Figures 38 and 40) [142]. Stimulation with E₂ (n = 3), soymilk extracts (n = 3), and soy compounds (n = 3) was performed at similar concentrations for 3 days. The results for E₂ showed an increase in expression variation for *EGR3* to *BARX2* and a decrease for *LINC02593* to *FRY*, consistent with the RNA-seq data (Figure 38).

Next, the results for each soymilk extracts showed a low expression profiles, as observed in the RNA-seq data (Figure 29). In contrast, the results for each soy compound displayed a pattern consistent with both the RNA-seq data and the E₂ pattern (Figure 30). To further analyze this expression pattern, a correlation analysis was performed between E₂ and soymilk extracts, as well as between E₂ and soy compounds (Figure 40). The analysis revealed a correlation of 0.20 to 0.55 between E₂ and soymilk extracts, and a higher correlation of 0.56 to 0.94 between E₂ and soy compounds.

Thus, the 30 ERGs identified in Chapter 2 suggest that gene expression analysis can effectively assess estrogenic activity using the simple and cost-effective *real-time* RT-PCR method.

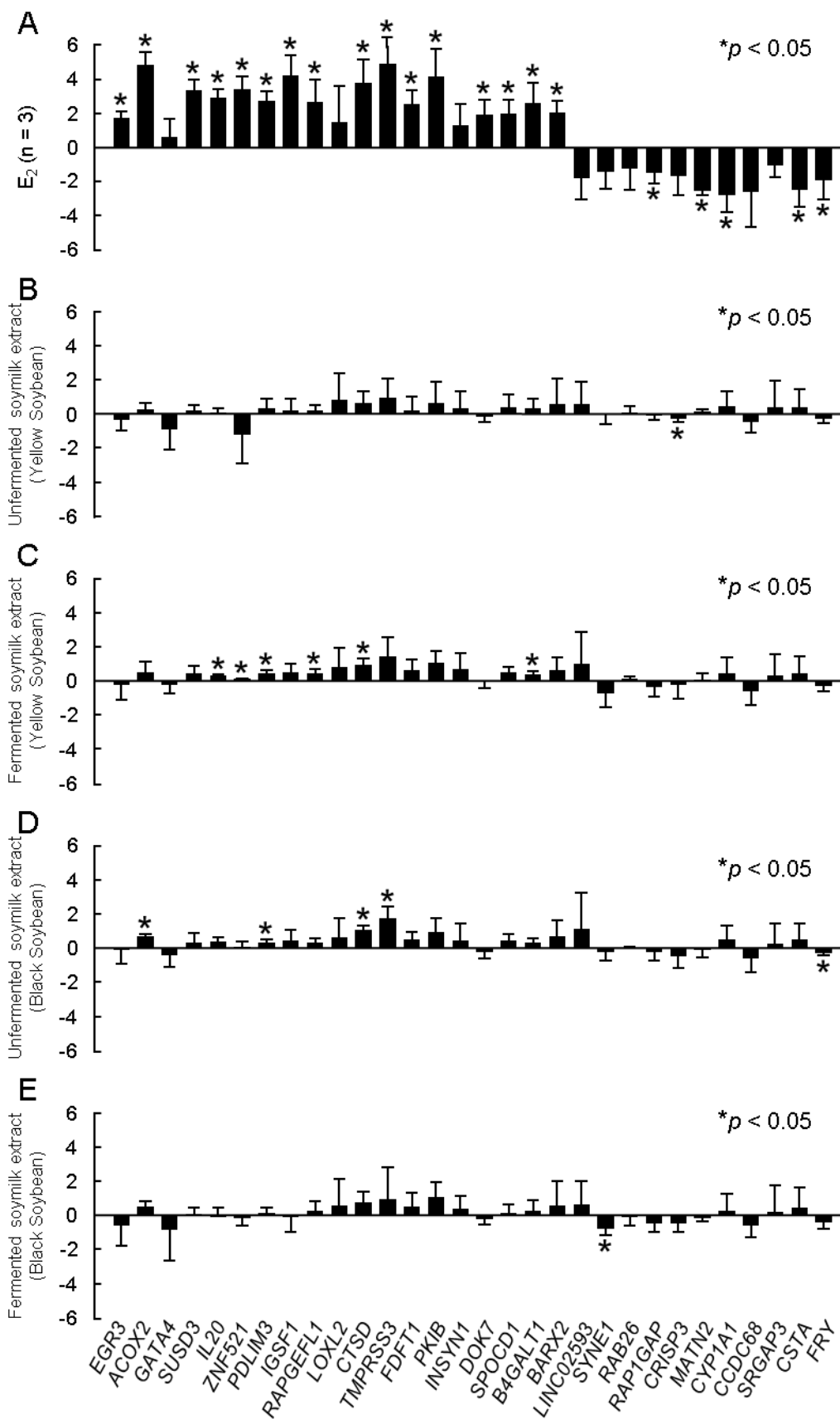


Figure 38 Expression profiles of soy milk extract with ERGs by *real-time* RT-PCR.

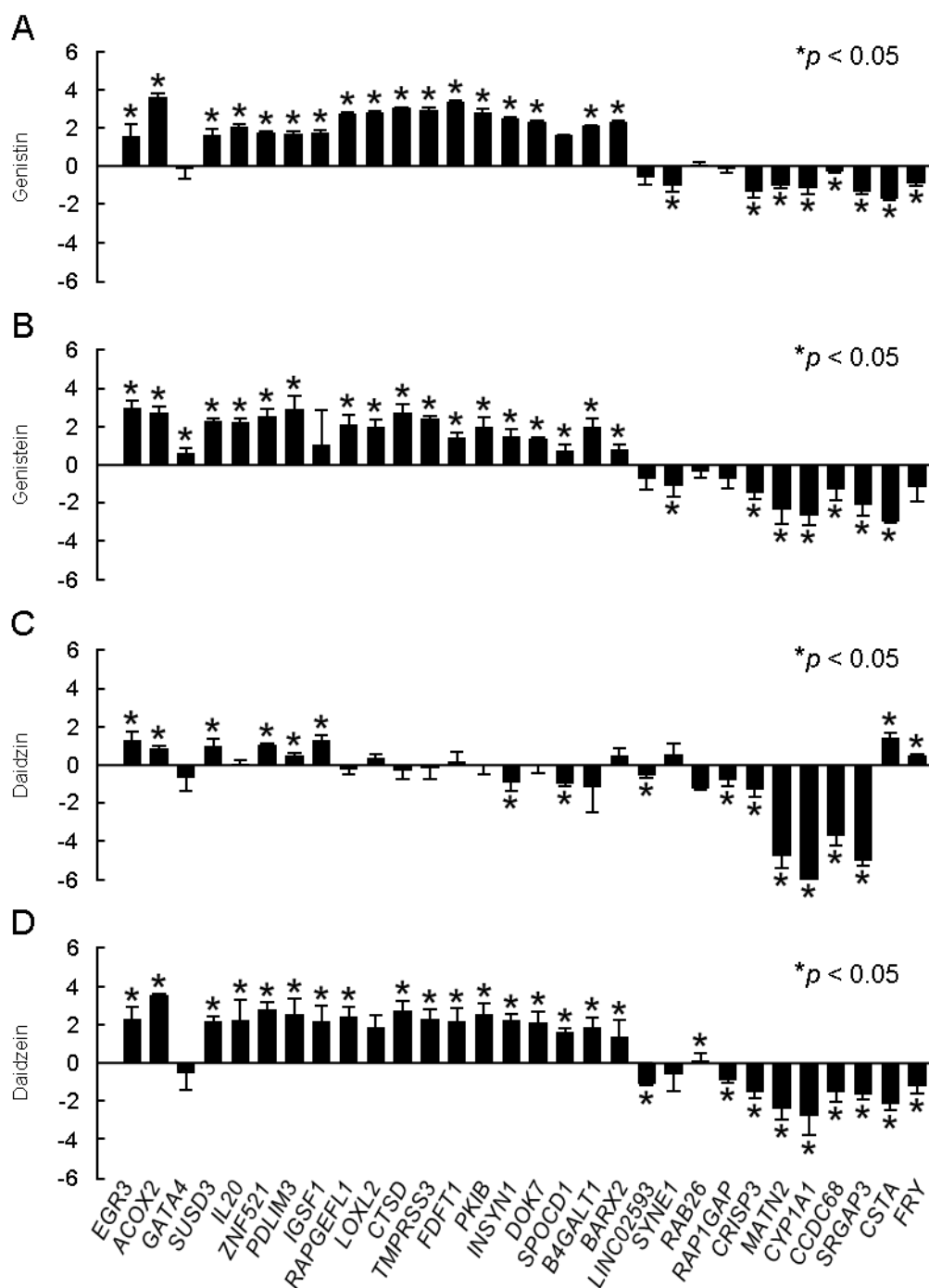


Figure 39 Expression profiles of soy compounds using ERGs by *real-time* RT-PCR.

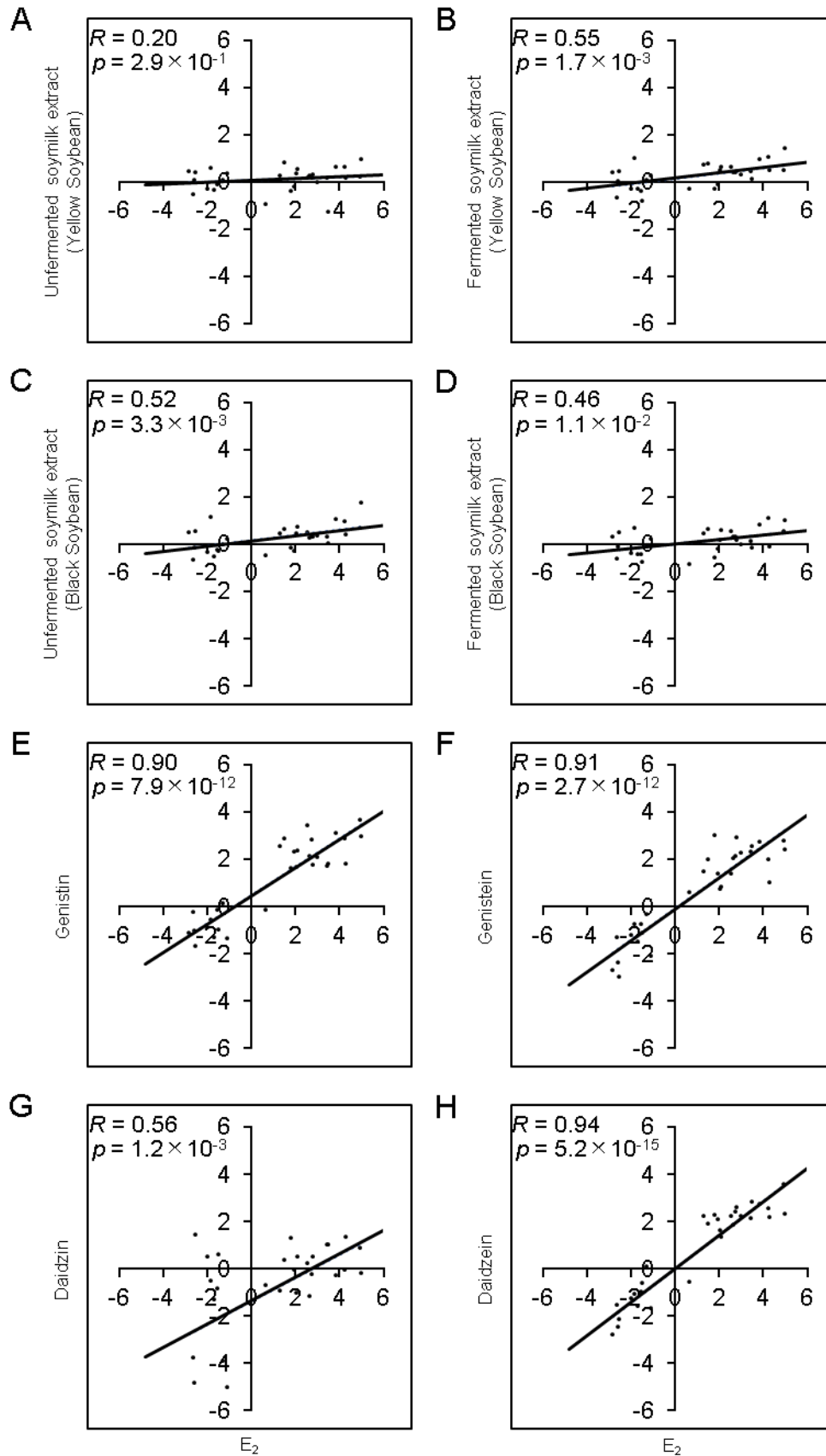


Figure 40 Correlation analysis of E_2 with soymilk extracts and soy compounds by *real-time* RT-PCR.

3-7 Enrichment analysis using RNA-seq data

For the soymilk extracts and soy compounds data obtained with RNA-seq, 3,000 genes with significant up- or down-regulated expression variation and $p < 0.05$ were selected from all genes in the whole genome and examined for Gene Ontology and KEGG pathway analysis (Tables 4 and 5) [142]. Gene Ontology analysis revealed that the up-regulated gene set included genes related to the cell cycle and RNA biosynthesis (Table 4). On the other hand, the down-regulated gene set mainly contained hydrolytic enzymes, such as GTPases, and genes associated with autophagy (Table 4). KEGG pathway analysis found that the up-regulated gene set included genes related to the cell cycle and DNA replication, which was consistent with the Gene Ontology results (Table 5). In contrast, the down-regulated gene set was found to include pathways such as the phosphatidylinositol signaling pathway and autophagy, which are involved in cell proliferation, intracellular material transport, and cytoskeletal regulation, as well as the ErbB signaling pathway (Table 5). Thus, the significant gene groups regulated by soymilk extracts and soy compounds, many of which are related to cell functions, suggest that these soymilk extracts and soy compounds affected cell proliferation and the phosphorylation of Erk and Akt proteins.

Table 4 Gene Ontology using RNA-seq data of soymilk extracts and soy compounds.

Up-regulation			Down-regulation		
Rank	Count	Description	Rank	Count	Description
1	8	cellular response to DNA damage stimulus	1	6	cell morphogenesis
1	8	DNA metabolic process	1	6	positive regulation of GTPase activity
1	8	mitotic cell cycle	1	6	regulation of GTPase activity
1	8	mitotic cell cycle process	4	5	cell part morphogenesis
1	8	regulation of cell cycle process	4	5	neuron projection development
1	8	regulation of mitotic cell cycle	4	5	regulation of catabolic process
7	7	cell division	4	5	small GTPase mediated signal transduction
7	7	RNA processing	8	4	autophagy
9	5	amide biosynthetic process	8	4	process utilizing autophagic mechanism
9	5	mRNA metabolic process	8	4	regulation of cell projection organization

Table 5 KEGG pathway using RNA-seq data for soymilk extracts and soy compounds.

Up-regulation			Down-regulation		
Rank	Count	Description	Rank	Count	Description
1	8	Base excision repair	1	8	Inositol phosphate metabolism
1	8	Cell cycle	1	8	Insulin resistance
1	8	DNA replication	1	8	Phosphatidylinositol signaling system
1	8	Mismatch repair	4	7	Autophagy
1	8	Nucleotide excision repair	4	7	AGE-RAGE signaling pathway in diabetic complications
1	8	Oocyte meiosis	6	6	FoxO signaling pathway
1	8	Pyrimidine metabolism	6	6	MicroRNAs in cancer
1	8	Spliceosome	8	5	ErbB signaling pathway
9	7	Carbon metabolism	8	5	Lysosome
9	7	Pathogenic Escherichia coli infection	8	5	Mitophagy

3-8 Conclusion

In this study, the estrogenic activity of soymilk extract before and after fermentation was examined by examining cell, protein, and gene expression. The results of each experiment suggest that the soymilk extract has estrogenic activity, and furthermore, that the estrogenic activity is enhanced by fermentation. In addition, when using the 30 ERGs selected in the previous chapter, soy compounds showed the same gene expression pattern as E₂ and a high correlation by correlation analysis. These findings suggest that both RNA-seq and *real-time* RT-PCR can be used to evaluate estrogenic activity.

Therefore, it is expected that the *real-time* RT-PCR method using 30 novel ERGs can be used for inexpensive screening investigation of estrogenic activity of other compounds.

Chapter 4: Estrogenic prenylated flavonoids in *sophora flavescens*

4-1 Introduction

Kurara (*Sophora flavescens*: *S. flavescens*) is a perennial herb belonging to the genus *Sophora* (Fabaceae) and is widely distributed across Asia, Oceania, and the Pacific Islands. In Japan, it grows naturally in the mountains and fields of Honshu, Shikoku, and Kyushu. Traditionally, the root of *S. flavescens* has been used as a herbal medicine and is commonly employed in China to treat conditions such as bloody stool, jaundice, oliguria, eczema, ulcers, and scabies [152]. The primary phytoconstituents of *S. flavescens* include flavonoids and alkaloids, with matrine and oxymatrine being the major components [153]. Its pharmacological effects include promoting apoptosis, modulating the cell cycle, and inhibiting cancer metastasis and invasion [154].

In addition to these compounds, *S. flavescens* contains prenylated flavanones. Prenylated flavanones are characterized by a prenyl group and a labanduryl group attached to the carbon at position 8 of the A-ring in the flavanone skeleton (Figure 41). Prenylation has been reported to increase lipophilicity, thereby enhancing affinity for cell membranes and contributing to antibacterial, anti-inflammatory, and enhanced estrogenic activities [155].

In the present study, the estrogenic activity of several prenylated flavonoids in *S. flavescens* were evaluated, specifically kurarinone, kushenol A and I, and sophoraflavanone G (Figure 41) [156-158]. While kurarinone and sophoraflavanone G have been reported to possess biological activities [158,159], their estrogenic activity was examined in this study. On the other hand, although kushenol A and I have been studied to some extent, no prior research has focused on their estrogenic activity. Thus, this study represents the first evaluation of their potential estrogenic effects.

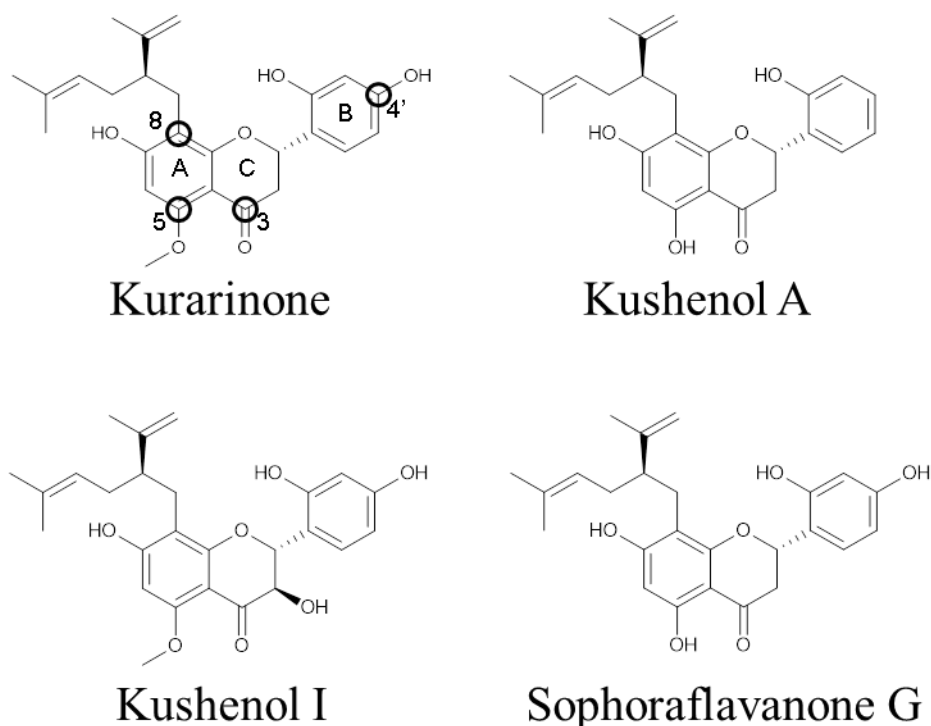


Figure 41 Structure of compounds in *S. flavescens*.

4-2 Materials and methods

4-2-1 Materials

MCF-7 cells were used as described in Chapter 2, and the culture conditions were identical to those in Section 2-2-1. Antibodies used for Western blotting were the same as previously described. Kurarinone was purchased from Sigma-Aldrich, kushenol A from BioBioPha (Kunming, China), and kushenol I and sophoraflavanone G from MedChemExpress (Monmouth Junction, NJ, USA)..

4-2-2 Sulforhodamine B (SRB) assay

MCF-7 cells were routinely cultured and seeded in 24-well plates at a density of 1.5×10^4 cells/well, following the protocol described in Section 2-2-2 [24,40,41]. The cells were maintained in RPMI 1640 medium supplemented with 10% (v/v) DCC-FBS for three days [24,40,41]. After the incubation, the medium was replaced with RPMI 1640 containing 10 nM E₂, 1 μ M ICI, or varying concentrations (10 nM, 100 nM, 1 μ M, and 10 μ M) of the compounds isolated from *S. flavescens*

(kurarinone, kushenol A, kushenol I, and sophoraflavanone G), or 0.1% DMSO as the vehicle control (Cont). The cells were incubated for an additional three days. Subsequently, cells were fixed with TCA as described in Section 2-2-2, total protein was stained with sulforhodamine B, and the dye was solubilized using 10 mM Tris buffer. Absorbance at 490 nm was measured, and the relative ratios of compound-treated cells to the control were calculated. Graphing and statistical analyses were performed as described in Section 2-2-2.

4-2-3 Western blotting

MCF-7 cell lysates were prepared following the protocol in Section 2-2-3. One day prior to stimulation, the cells were switched to RPMI 1640 without serum and maintained under these conditions. For inhibition experiments, cells were pretreated with 1 μ M ICI for 1 hour, followed by stimulation with 10 nM E₂, 1 μ M ICI, or compounds from *S. flavescens* (kurarinone, kushenol A, kushenol I, and sophoraflavanone G) at concentrations of 10 nM and 100 nM, or 0.1% DMSO as the vehicle control. Stimulations were carried out for 5, 15, 30, and 60 min at 37°C in a 5% CO₂ atmosphere. Lysate collection, SDS-PAGE, Western blotting, antigen-antibody reactions, and luminescence detection were performed as described in Section 2-2-3 [24,40,41].

4-2-4 Real-time RT-PCR

MCF-7 cells were stimulated with 10 nM E₂, or with compounds from *S. flavescens* (kurarinone, kushenol A, kushenol I, and sophoraflavanone G) at concentrations of 100 nM and 1 μ M, or with 0.1% DMSO (vehicle control). RNA samples were extracted, and *real-time* RT-PCR was performed under the same conditions as described in Section 2-2-5 [24]. Each experiment was independently repeated three times. Except for *GATA4*, primers were the same as listed in Table 1. The redesigned primer sequences for *GATA4* are as follows: forward primer:

5'-TCCAAACCAGAAAACGGAAG-3', reverse primer: 5'-CTGTGTGCCCGTAGTGATGA-3'.

4-2-5 Cluster analysis using *real-time* RT-PCR data

Hierarchical cluster analysis was performed using the Heatmapper soft (<http://www.heatmapper.ca/expression/>) based on expression profiles of 30 estrogen-responsive genes obtained from *real-time* RT-PCR.

4-3 Evaluation of cell proliferation activity by prenylated flavonoids

Four compounds in *S. flavescens* (kurarinone, kushenol A, kushenol I, and sophoraflavanone G) were evaluated for their effects on cell proliferative activity in MCF-7 cells (Figure 42). Consistent with previous experiments, stimulation with E₂ resulted in approximately a 2.3-fold increase in proliferative activity. Kurarinone, kushenol I, and sophoraflavanone G exhibited maximal proliferative activity at a concentration of 100 nM, while kushenol A showed maximal activity at 10 nM. At higher concentrations, the proliferation of MCF-7 cells was either comparable to or reduced relative to the control. Additionally, when inhibition experiments were conducted using ICI (Figure 42), the proliferative effects of all four compounds were suppressed at all concentrations. These results suggest that the four compounds in *S. flavescens* influence the proliferation of MCF-7 cells via estrogen receptor (ER)-mediated mechanisms, similar to E₂.

4-4 Evaluation of intracellular signals

We examined whether the four compounds in *S. flavescens* (kurarinone, kushenol A, kushenol I, and sophoraflavanone G) phosphorylate the signaling proteins Erk1/2 and Akt in MCF-7 cells (Figures 43–46). First, as a control, MCF-7 cells were stimulated with E₂, yielding results consistent with previous findings (Figure 43). When MCF-7 cells were subsequently stimulated with the four compounds, phosphorylation of Erk1/2 was observed within 5 min. For Akt, phosphorylation was observed at 15 min for kurarinone and within 5 min for the other compounds (Figure 44). Furthermore,

the phosphorylation was inhibited for all compounds (Figure 45). These results suggest that four compounds also act via estrogen receptors (ER) in signaling pathways. Although E₂-induced phosphorylation of Akt was observed at 15 min in previous studies, the reaction occurred within 5 min for some compounds in this study (Figure 44). We hypothesized that this discrepancy might be due to the concentration of the compounds. To test this, we diluted the compounds tenfold and repeated the Western blotting analysis (Figure 46). The results showed that Erk1/2 was still phosphorylated at 5 min and Akt phosphorylation shifted to 15 min reaction for all compounds. Thus, it can be concluded that all compounds exhibit phosphorylation activity comparable to that of E₂.

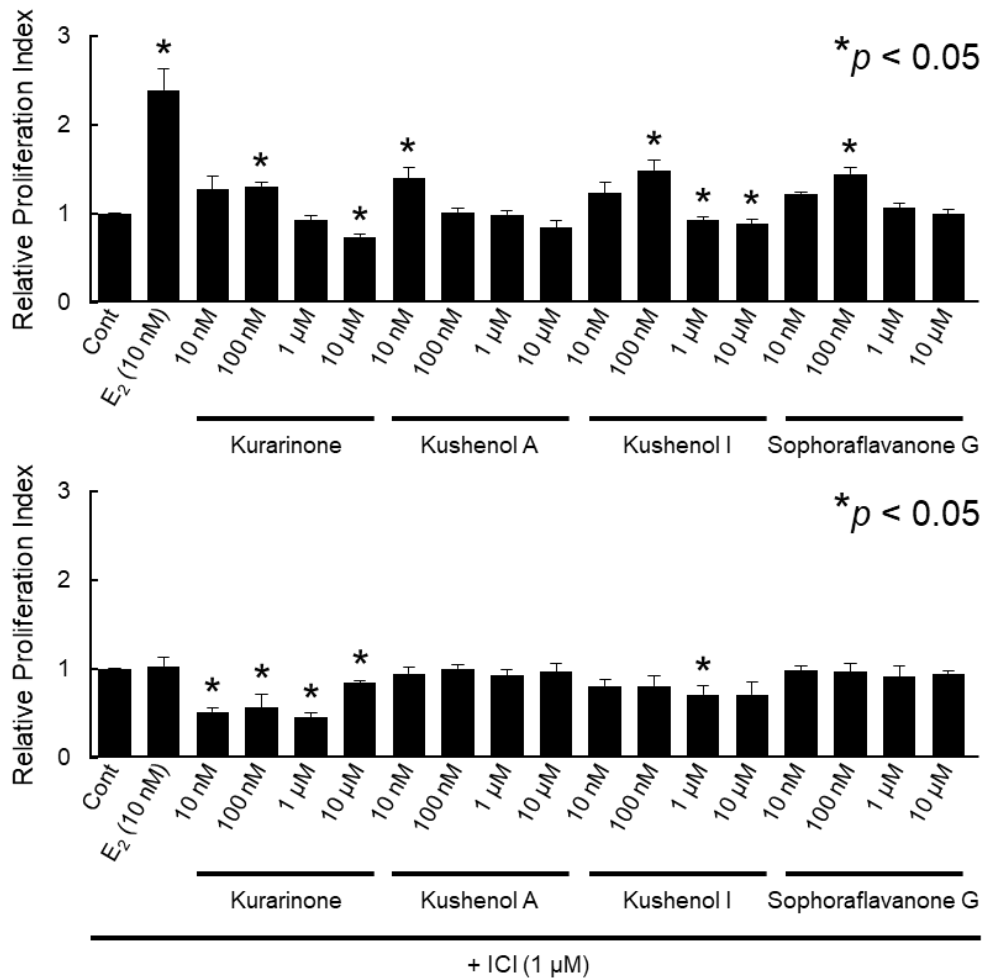


Figure 42 Evaluation of cell proliferative activity of *S. flavesceus*.

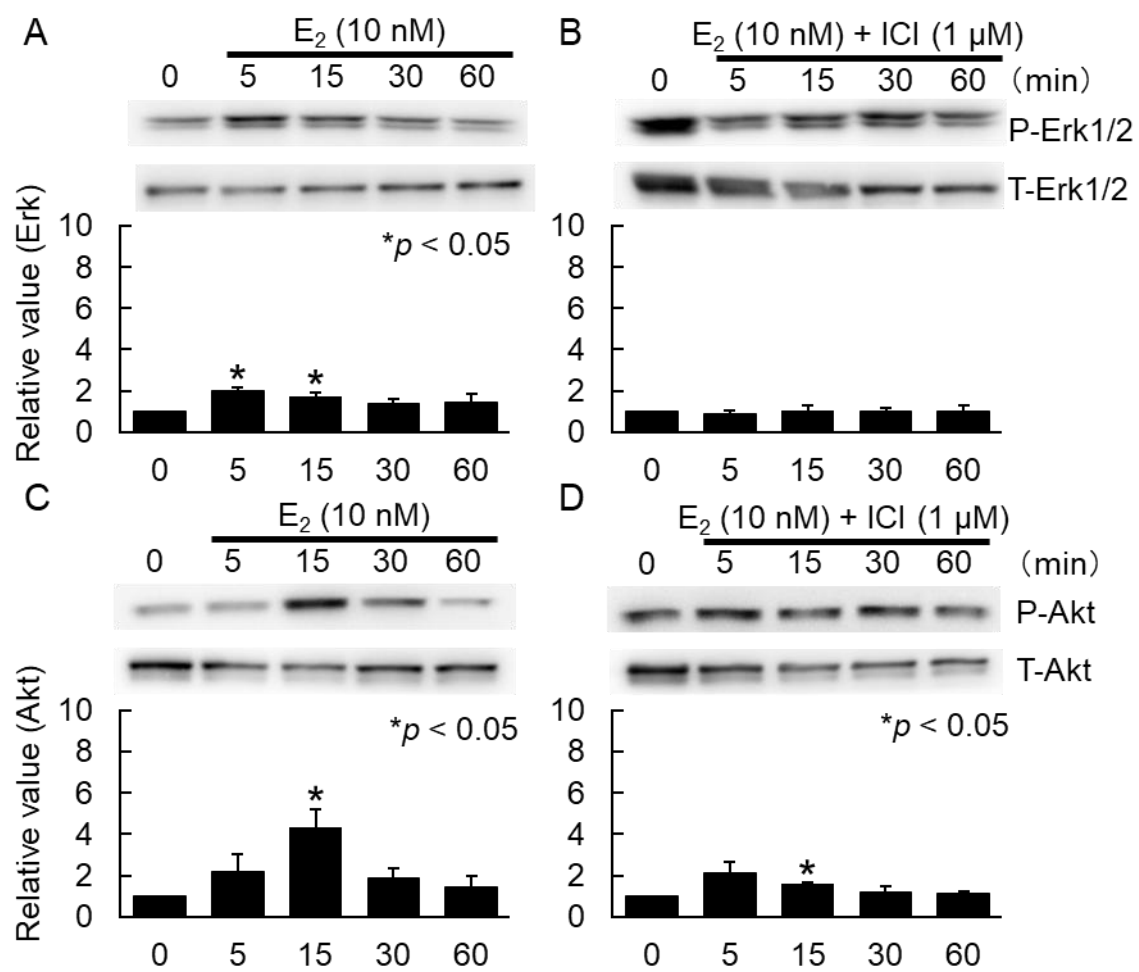


Figure 43 Evaluation of phosphorylation activity of E₂.

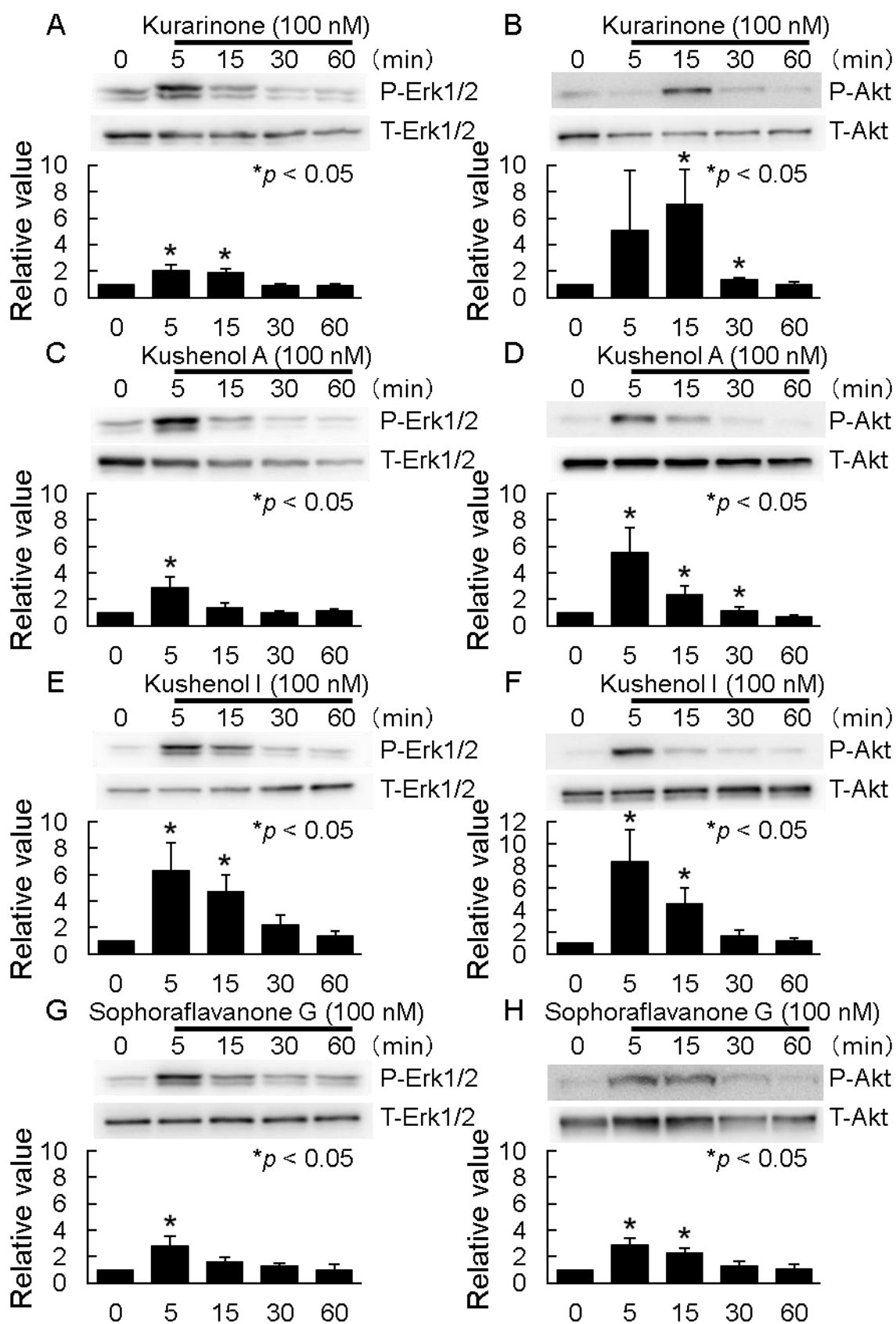


Figure 44 Evaluation of phosphorylation activity of *S. flavescens* (100 nM).

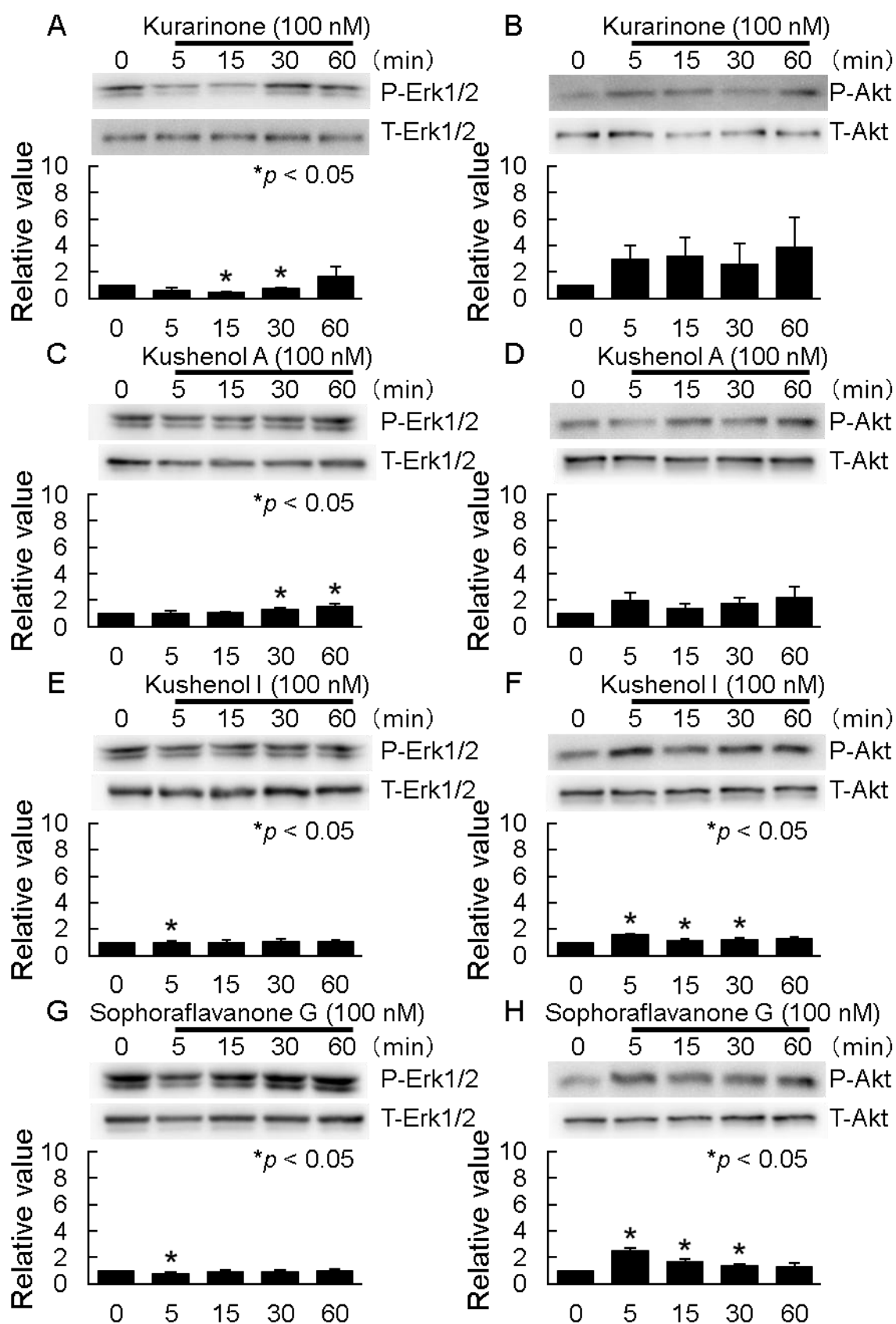


Figure 45 Evaluation of phosphorylation activity of *S. flavescens* (100 nM) by ICI.

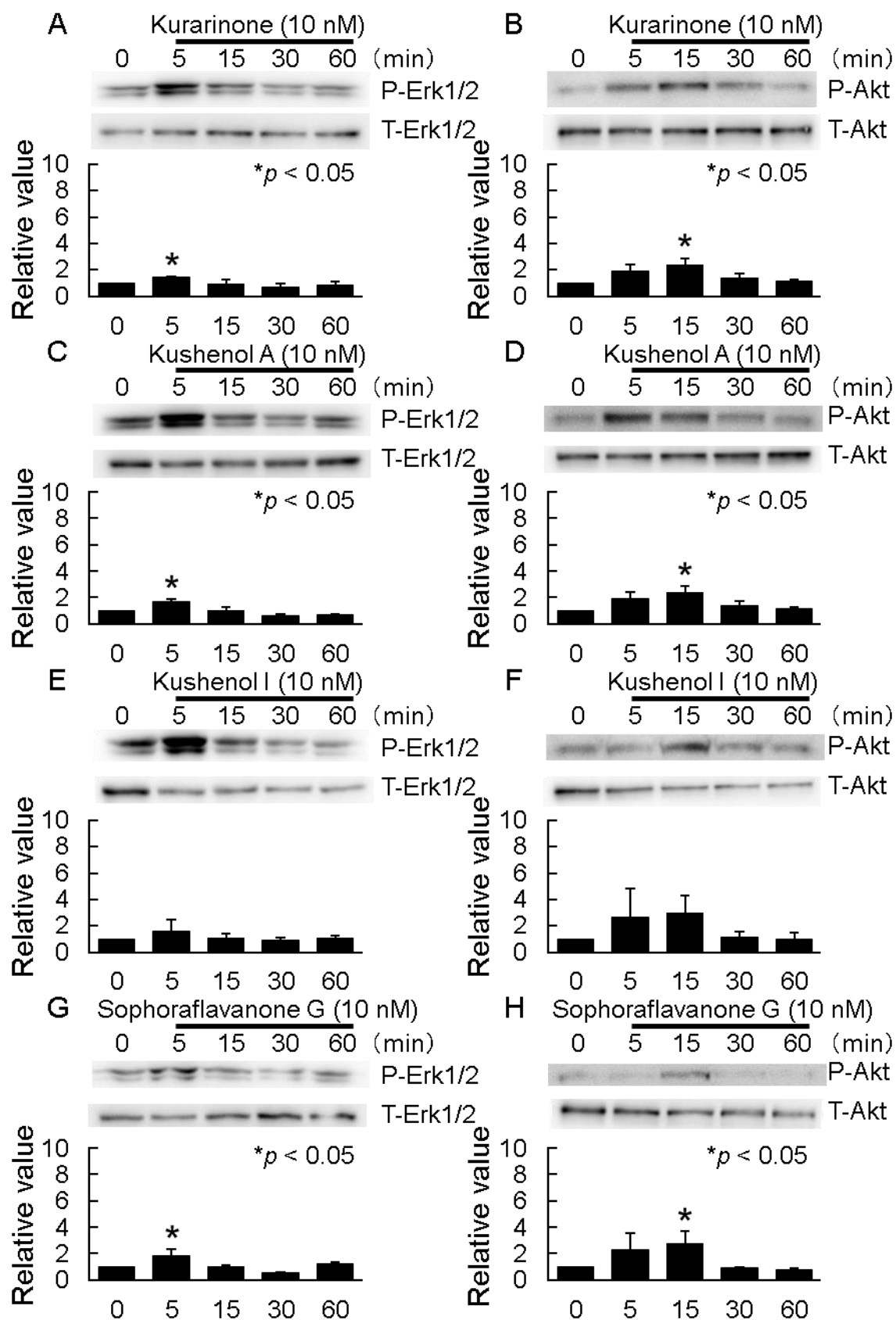


Figure 46 Evaluation of phosphorylation activity of *S. flavescens* (10 nM).

4-5 Gene expression analysis by *Real-time* RT-PCR

MCF-7 cells were stimulated with four compounds in *S. flavescens* (kurarinone, kushenol A, kushenol I, and sophoraflavanone G) and were also analyzed for gene expression (Figures 47 to 52). First, MCF-7 cells were stimulated with E₂, RNA was extracted, and *real-time* RT-PCR was performed for 30 estrogen-responsive genes (ERGs), which showed the same expression pattern as in [24]. For *GATA4*, new primers were designed, but the expression variation was similar to previous results [24]. The stimulation of MCF-7 cells with each compound at a concentration of 100 nM was performed in the same way as with E₂, based on the results of the SRB assay. However, the expression profiles was lower, and no correlation was obtained in the correlation analysis with E₂ (Figures 47 to 49). We considered that the concentration of each compound stimulating the cells was low, so we stimulated MCF-7 cells with each compound at a concentration of 1 μ M and performed *real-time* RT-PCR in the same way. As a result, although the gene expression profiles was still low (Figure 50), correlation analysis with E₂ [20] showed that kurarinone and kushenol I had the highest correlation at 0.50, and sophoraflavanone G at 0.82, while kushenol A showed no correlation (Figure 51). Correlation analysis between compounds showed that the correlation was lower when combined with kushenol A (Figure 52). Further analysis by hierarchical clustering of compounds and E₂ revealed that sophoraflavanone G was considered to have the most similar properties to E₂, followed by kurarinone and kushenol I, with kushenol A being the only compound in a separate group (Figure 53). To better understand these results, we focused on the chemical structure of each compound and speculated that the number and position of hydroxyl groups might be key factors. First, sophoraflavanone G has a total of four hydroxyl groups and is highly correlated with E₂. On the other hand, kushenol I has the same number of hydroxyl groups but a lower correlation with E₂ than sophoraflavanone G. Kurarinone and kushenol A have the same number of hydroxyl groups, but kushenol A shows a lower correlation with E₂. This suggests that the hydroxyl group at the 4' position of ring B

may significantly contribute to estrogenic activity [149]. Furthermore, the fact that kurarinone and kushenol I have the same correlation despite having different numbers of hydroxyl groups indicates that the hydroxyl group at position 3 of ring C may have little effect on gene expression. Therefore, both the number and position of hydroxyl groups may be important factors affecting estrogenic activity.

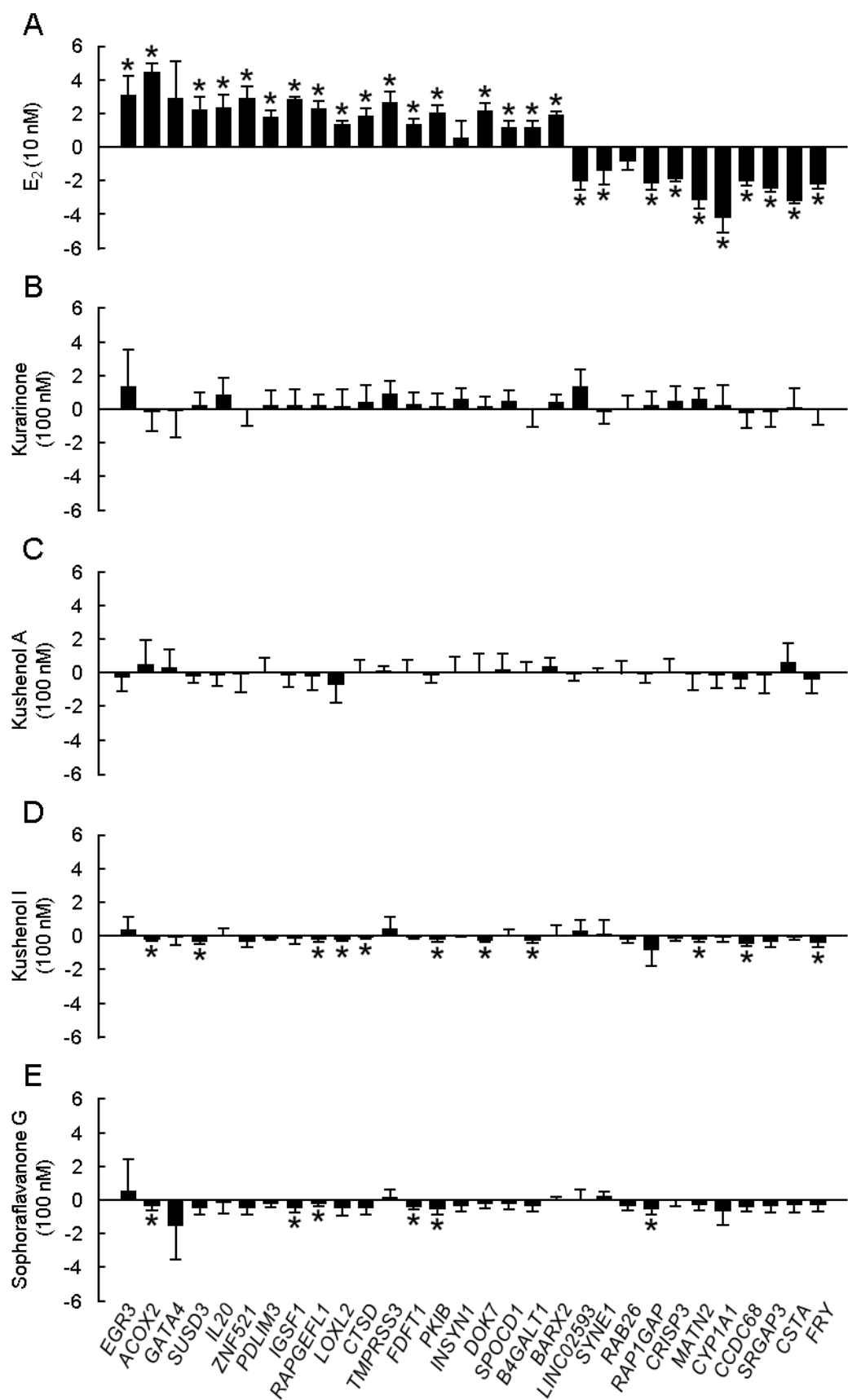


Figure 47 Expression profiles of *S. flavescentis* (100 nM) using ERGs.

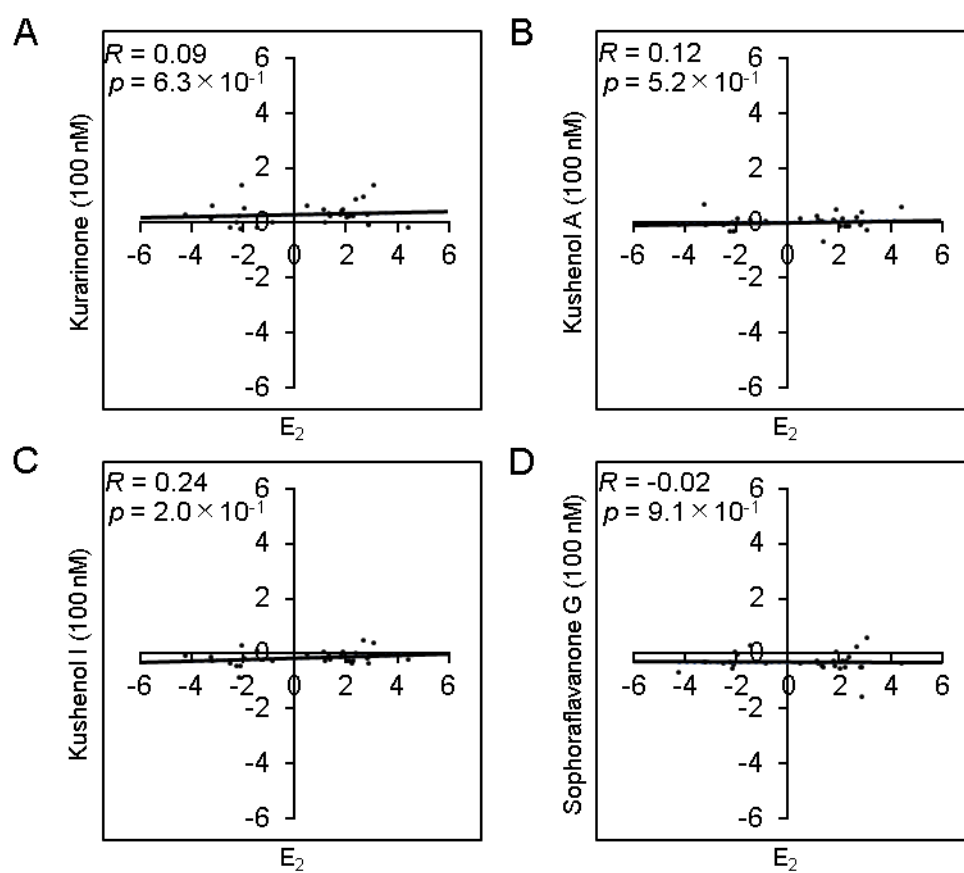


Figure 48 Correlation analysis of E_2 and *S. flavescens* (100 nM) by *real-time* RT-PCR.

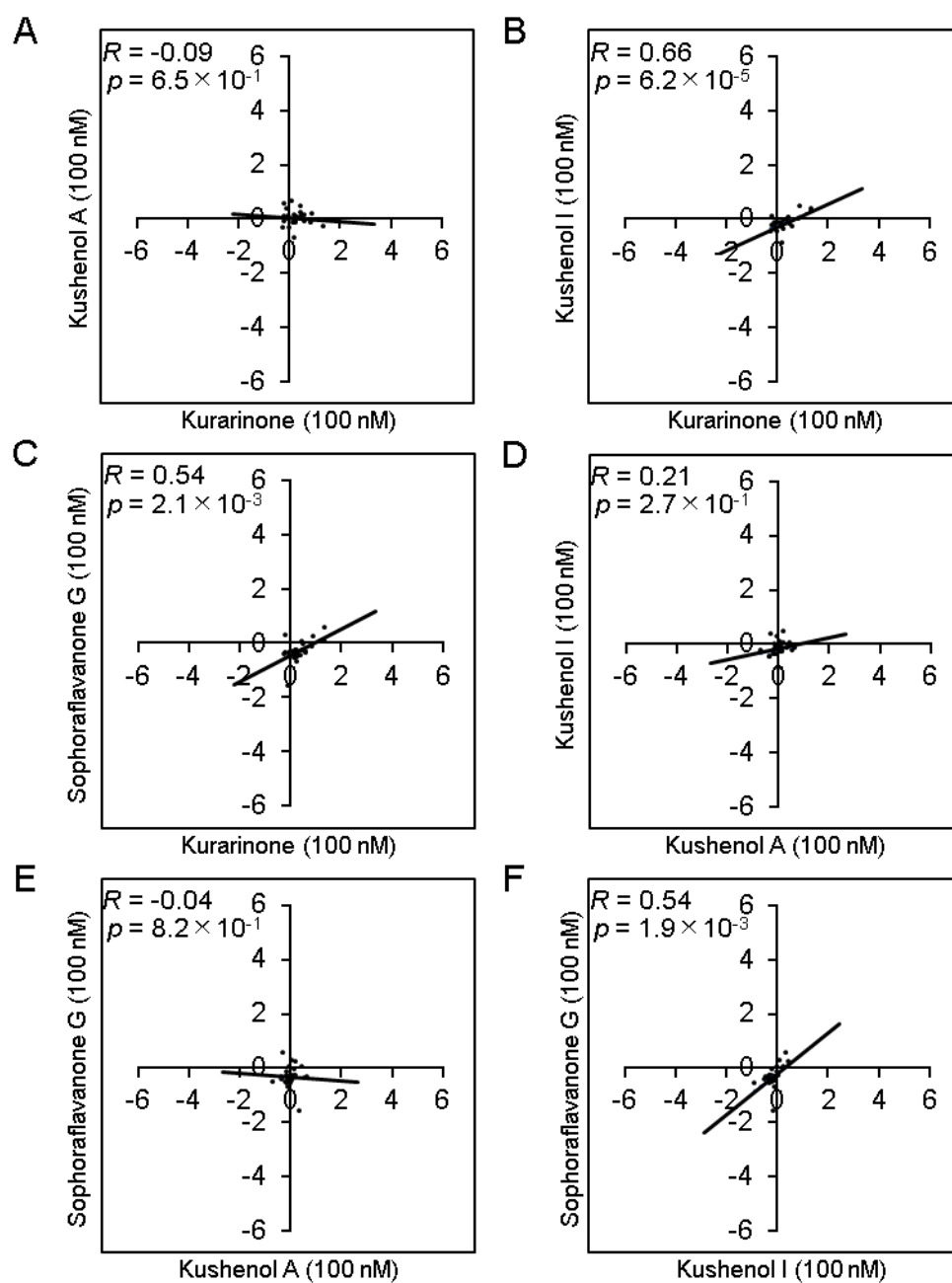


Figure 49 Correlation analysis of *S. flavescens* (100 nM) by *real-time* RT-PCR.

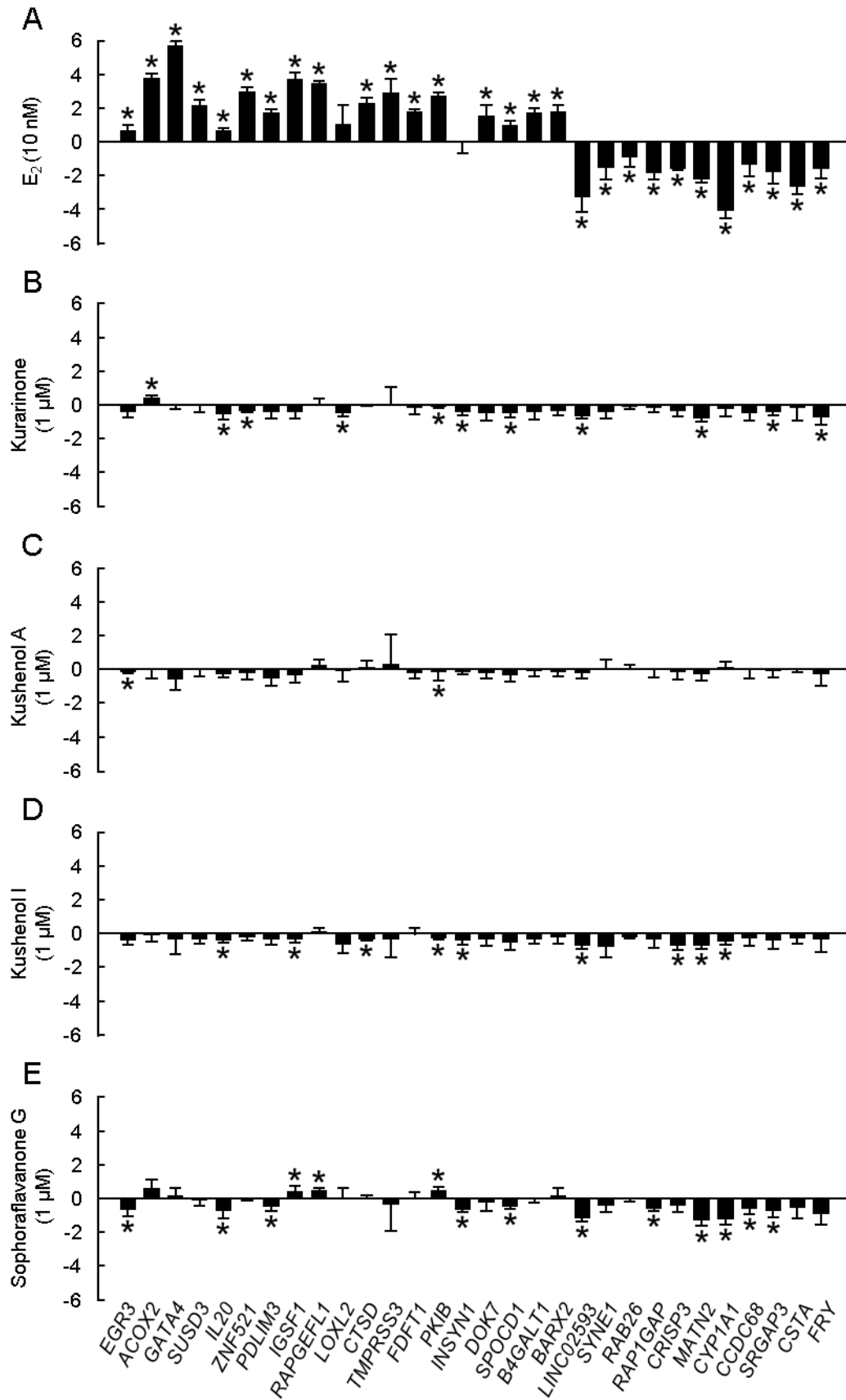


Figure 50 Expression profiles of *S. flavescens* (1 μ M) using ERGs.

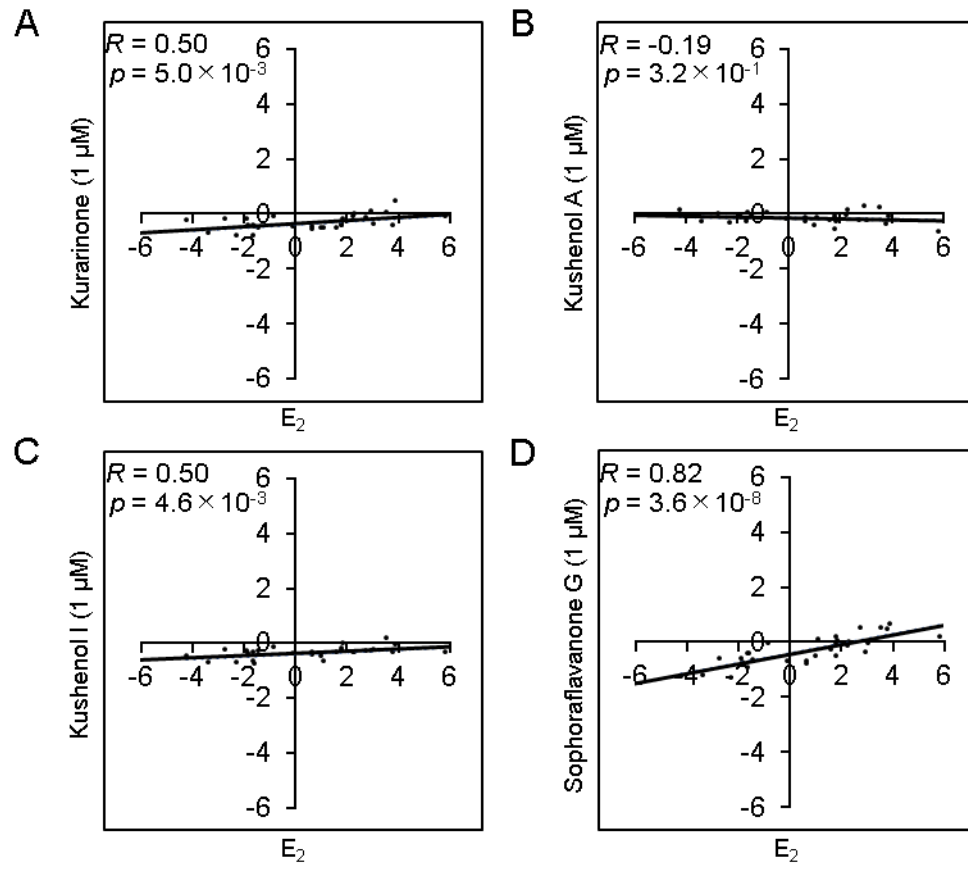


Figure 51 Correlation analysis of E_2 and *S. flavescens* (1 μM) by *real-time* RT-PCR.

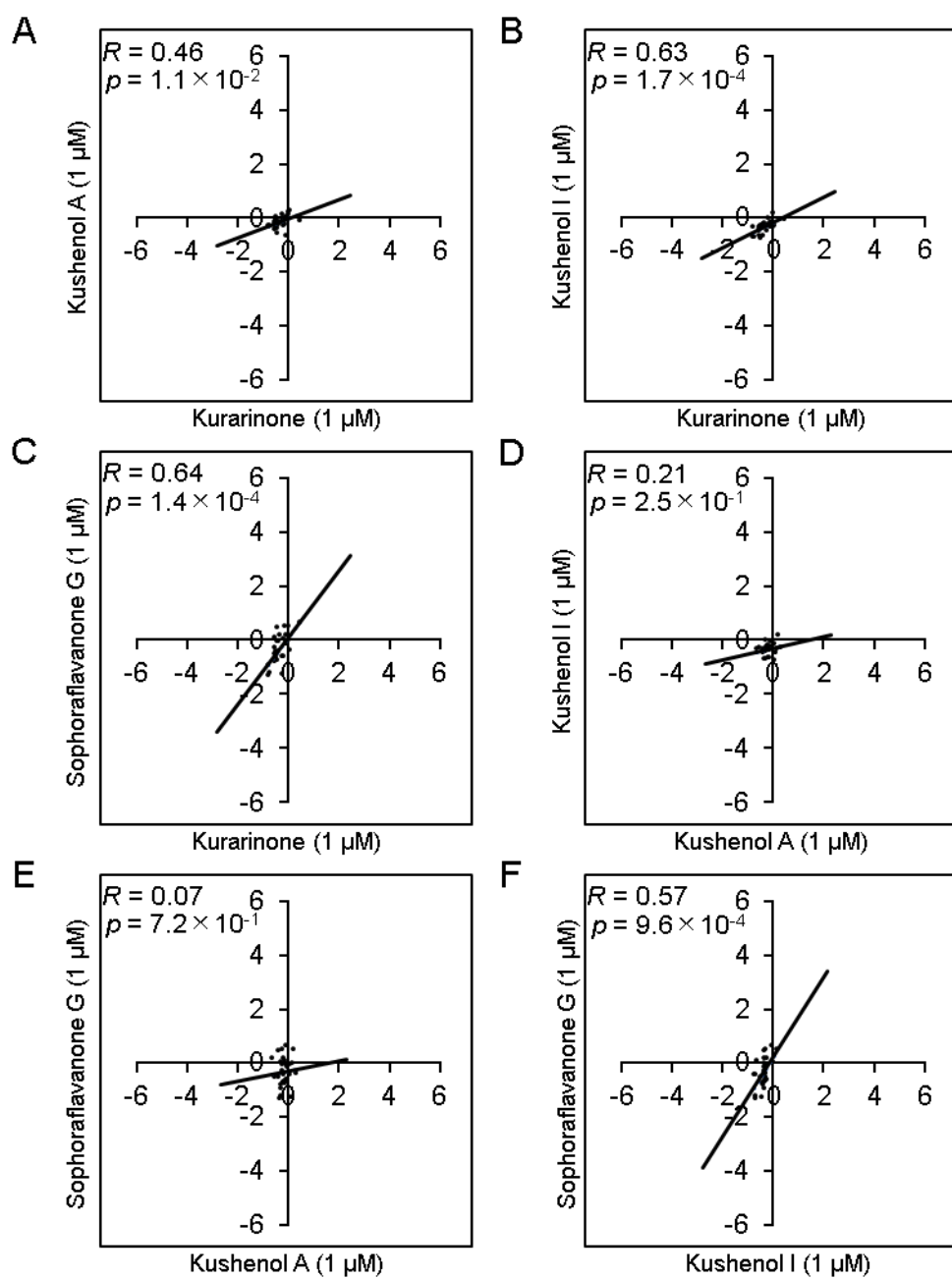


Figure 52 Correlation analysis of *S. flavescens* (1 μ M) by real-time RT-PCR.

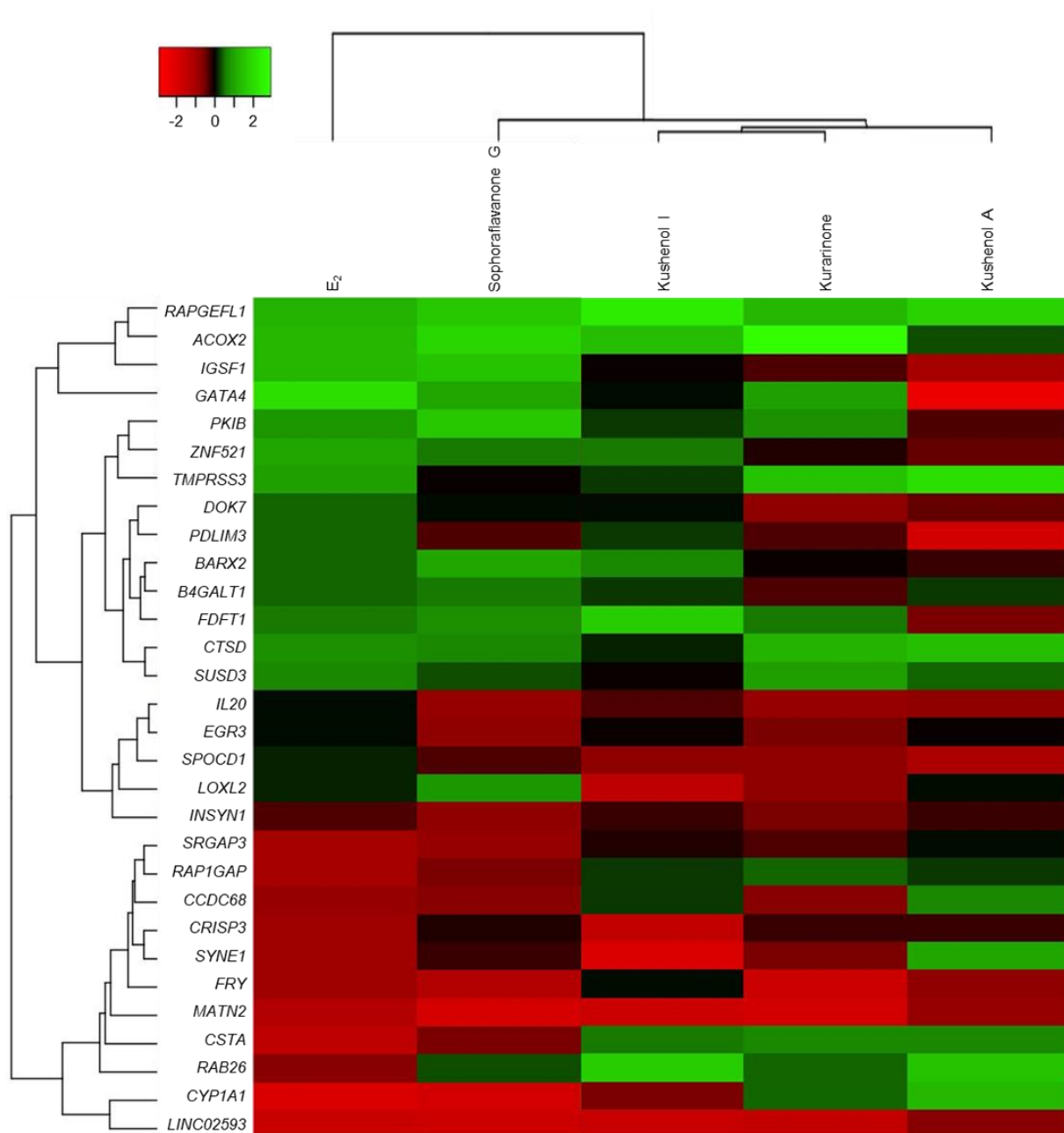


Figure 53 Cluster analysis of E₂ and *S. flavescens* using expression profiles.

4-6 Conclusion

This study is the first to report the estrogenic activity of kushenol A and kushenol I. Gene expression analysis, including cell proliferation, signaling proteins, and estrogen-responsive genes, has elucidated the mechanism of estrogenic activity of the respective compounds in *S. flavescens*. The results of this study also provide insights into the effects of the number and position of hydroxyl groups in the structures of kurarinone, kushenol A and I, and sophoraflavanone G on estrogenic activity. This study will also enable the investigation of the estrogenic activity of unique compounds, such as those in *S. flavescens*, and contribute to the evaluation of estrogenic activity in unknown compounds.

Chapter 5: General conclusion

This study identified novel estrogen-responsive genes and elucidated their mechanisms of action.

In Chapter 1, estrogen-responsive genes were identified using RNA-seq, and 30-novel estrogen-responsive genes with stable expression were selected based on their coefficient of variation. These selected genes were further analyzed using *real-time* RT-PCR, which demonstrated that their expression patterns of up-regulation and down-regulation were consistent with those obtained through RNA-seq analysis. Furthermore, GO and KEGG analyses were performed on approximately 3,000 estrogen-responsive genes, and the relationship between ER α and ER β was clarified for the selected 30 genes. It was revealed that these genes maintain stable expression and can be clearly distinguished functionally.

In Chapter 2, the estrogen activity of soymilk extracts was revealed through cell proliferation activity, signaling proteins, and the 30 novel estrogen-responsive genes. In this study, the expression patterns of these 30 estrogen-responsive genes were also confirmed using RNA-seq, and correlation analyses were conducted to further discuss their estrogen activity. Furthermore, similar to the previous chapter, *real-time* RT-PCR method was performed to compare the expression patterns obtained through RNA-seq. The results showed that, for soy-derived compounds, the expression patterns closely resembled those of E₂, highlighting the utility of these 30 estrogen-responsive genes. It was demonstrated that fermentation not only enhances the estrogen activity of soymilk extracts but also enables their evaluation in a cost-effective manner using estrogen-responsive genes.

In Chapter 3, it was shown that these 30 estrogen-responsive genes could be applied for the analysis of unknown compounds, providing new insights into the mechanisms of estrogen activity. As in the previous chapters, estrogen activity was elucidated through cell proliferation activity and the signaling proteins. In this study, the gene profiles were further investigated using only *real-time* RT-PCR, which revealed the presence or absence of estrogen activity at the genetic level. Addition-

ally, by focusing on these gene profiles and the chemical structures of the compounds, it was demonstrated that the mechanisms of estrogen activity could be explored.

In conclusion, the novel estrogen-responsive genes identified in this study enabled the exploration of useful compounds with estrogen activity and provided further insights into their mechanisms of action. Advancing the profiling of these estrogen-responsive genes is expected to lead to the discovery of alternative compounds that can replace hormone therapies, contributing not only to safer and more reliable treatments but also to a deeper genetic-level understanding of the mechanisms underlying breast cancer. This, in turn, holds great potential for improving breast cancer treatment methods that are determined at the genetic level, making this research highly valuable for future therapeutic advancements.

Acknowledgements

I would like to express my sincere gratitude to Professor Ryoichi Kiyama of the Department of Life Sciences, Faculty of Life Sciences, Kyushu Sangyo University, who provided guidance and support throughout this research. I would also like to thank Professor Shinji Mitsuiki of the Department of Life Sciences, Faculty of Life Sciences, Kyushu Sangyo University, for his advice on the third paper. My heartfelt thanks go to all the students involved, especially Mr. Wenqiang Fu, who was in the same laboratory as I, and to Ms. Sumasu, who was a researcher at the time, as well as to graduate students Ms. Imamura, Mr. Hoashi, and Mr. Hasegawa. I am also deeply grateful to Mr. Iga and Mr. Takemoto of Sansho Pharmaceutical Co., Ltd, who provided soymilk extracts and gave valuable advice on my paper and thesis. I would like to express my sincere gratitude to Professor Yoshiki Katayama and Associate Professor Takeshi Mori of the Department of Applied Chemistry, Graduate School of Engineering, Kyushu University, for their invaluable guidance and support throughout my graduate studies and during the preparation of this doctoral dissertation. I am also very grateful to the faculty, administrative staff, and Kyushu Sangyo University, where I have conducted this research. In particular, I would like to express my deep gratitude to Mr. Hashimoto of Support Office at Kyushu Sangyo University for his efforts in handling the administrative procedures for my research, and also to Professor Shin-ichiro Isobe of the Faculty of Life Sciences at Kyushu Sangyo University, as well as to Mr. Yohei Matsuoka and Mr. Yan Hui, who were researchers at Kyushu Sangyo University at the time, for their support in my research activities. Finally, I would like to express my deepest gratitude to my family.

References

1. Tatsuo S and Katsumasa K. Structure, function and materials of the human body. 2nd edition, Tokyo, Japan Medical Journal, 2014, 437, ISBN: 978-4-7849-3179-08
2. Weichselbaum RR, Hellman S, Piro AJ, Nove JJ, Little JB. Proliferation kinetics of a human breast cancer line in vitro following treatment with 17 β -estradiol and 1- β -D-arabinofuranosyl-cytosine. *Cancer Res.* 1978 Aug;38(8):2339-42.
3. Jakesz R, Smith CA, Aitken S, Huff K, Schuette W, Shackney S, Lippman M. Influence of cell proliferation and cell cycle phase on expression of estrogen receptor in MCF-7 breast cancer cells. *Cancer Res.* 1984 Feb;44(2):619-25.
4. Reiner GC, Katzenellenbogen BS, Bindal RD, Katzenellenbogen JA. Biological activity and receptor binding of a strongly interacting estrogen in human breast cancer cells. *Cancer Res.* 1984 Jun;44(6):2302-8.
5. Zivadinovic D, Watson CS. Membrane estrogen receptor- α levels predict estrogen-induced ERK1/2 activation in MCF-7 cells. *Breast Cancer Res.* 2005;7(1):R130-44. doi: 10.1186/bcr959.
6. Liu Q, Liu Y, Li X, Wang D, Zhang A, Pang J, He J, Chen X, Tang NJ. Perfluoroalkyl substances promote breast cancer progression via ER α and GPER mediated PI3K/Akt and MAPK/Erk signaling pathways. *Ecotoxicol Environ Saf.* 2023 Jun 15;258:114980. doi: 10.1016/j.ecoenv.2023.114980.
7. Filardo EJ, Quinn JA, Frackelton AR Jr, Bland KI. Estrogen action via the G protein-coupled re-ceptor, GPR30: stimulation of adenylyl cyclase and cAMP-mediated attenuation of the epidermal growth factor receptor-to-MAPK signaling axis. *Mol Endocrinol.* 2002 Jan;16(1):70-84. doi: 10.1210/mend.16.1.0758.
8. Almeida M, Laurent MR, Dubois V, Claessens F, O'Brien CA, Bouillon R, Vanderschueren D, Manolagas SC. Estrogens and Androgens in Skeletal Physiology and Pathophysiology. *Physiol Rev.* 2017 Jan;97(1):135-187. doi: 10.1152/physrev.00033.2015.
9. Poschner S, Maier-Salamon A, Zehl M, Wackerlig J, Dobusch D, Pachmann B, Sterlini KL, Jäger W. The Impacts of Genistein and Daidzein on Estrogen Conjugations in Human Breast Cancer Cells: A Targeted Metabolomics Approach. *Front Pharmacol.* 2017 Oct 5;8:699. doi: 10.3389/fphar.2017.00699.
10. Pawlicka MA, Zmorzyński S, Popek-Marciniak S, Filip AA. The Effects of Genistein at Different Concentrations on MCF-7 Breast Cancer Cells and BJ Dermal Fibroblasts. *Int J Mol Sci.* 2022 Oct 15;23(20):12360. doi: 10.3390/ijms232012360.
11. Hsieh CY, Santell RC, Haslam SZ, Helferich WG. Estrogenic effects of genistein on the growth of estrogen receptor-positive human breast cancer (MCF-7) cells in vitro and in vivo. *Cancer Res.* 1998 Sep 1;58(17):3833-8.
12. Tsuji M, Tanaka T, Nagashima R, Sagisaka Y, Tousen Y, Nishide Y, Ishimi Y, Ishimi Y. Effect of daidzein and equol on DNA replication in MCF-7 cells. *J Biochem.* 2018 May 1;163(5):371-380.

doi: 10.1093/jb/mvy006.

13. Kaushik S, Shyam H, Sharma R, Balapure AK. Dietary isoflavone daidzein synergizes cent-chroman action via induction of apoptosis and inhibition of PI3K/Akt pathway in MCF-7/MDA MB-231 human breast cancer cells. *Phytomedicine*. 2018 Feb 1;40:116-124. doi: 10.1016/j.phymed.2018.01.007.
14. Krishnan AV, Stathis P, Permuth SF, Tokes L, Feldman D. Bisphenol-A: an estrogenic substance is released from polycarbonate flasks during autoclaving. *Endocrinology*. 1993 Jun;132(6):2279-86. doi: 10.1210/endo.132.6.8504731.
15. Kiyama R, Furutani Y, Kawaguchi K, Nakanishi T. Genome sequence of the cauliflower mushroom *Sparassis crispa* (Hymenochaetales) and its association with beneficial usage. *Sci Rep*. 2018 Oct 30;8(1):16053. doi: 10.1038/s41598-018-34415-6.
16. Prossnitz ER, Arterburn JB, Sklar LA. GPR30: A G protein-coupled receptor for estrogen. *Mol Cell Endocrinol*. 2007 Feb;265-266:138-42. doi: 10.1016/j.mce.2006.12.010.
17. Xu XL, Huang ZY, Yu K, Li J, Fu XW, Deng SL. Estrogen Biosynthesis and Signal Transduction in Ovarian Disease. *Front Endocrinol (Lausanne)*. 2022 Mar 1;13:827032. doi: 10.3389/fendo.2022.827032.
18. Kuiper GG, Enmark E, Peltö-Huikko M, Nilsson S, Gustafsson JA. Cloning of a novel receptor expressed in rat prostate and ovary. *Proc Natl Acad Sci U S A*. 1996 Jun 11;93(12):5925-30. doi: 10.1073/pnas.93.12.5925.
19. Cowley SM, Hoare S, Mosselman S, Parker MG. Estrogen receptors alpha and beta form heterodimers on DNA. *J Biol Chem*. 1997 Aug 8;272(32):19858-62. doi: 10.1074/jbc.272.32.19858.
20. Kiyama R, Zhu Y. DNA microarray-based gene expression profiling of estrogenic chemicals. *Cell Mol Life Sci*. 2014 Jun;71(11):2065-82. doi: 10.1007/s00018-013-1544-5.
21. Derakhshan F, Reis-Filho JS. Pathogenesis of Triple-Negative Breast Cancer. *Annu Rev Pathol*. 2022 Jan 24;17:181-204. doi: 10.1146/annurev-pathol-042420-093238.
22. Lee AV, Oesterreich S, Davidson NE. MCF-7 cells--changing the course of breast cancer research and care for 45 years. *J Natl Cancer Inst*. 2015 Mar 31;107(7):djv073. doi: 10.1093/jnci/djv073.
23. Watters JJ, Campbell JS, Cunningham MJ, Krebs EG, Dorsa DM. Rapid membrane effects of steroids in neuroblastoma cells: effects of estrogen on mitogen activated protein kinase signalling cascade and c-fos immediate early gene transcription. *Endocrinology*. 1997 Sep;138(9):4030-3. doi: 10.1210/endo.138.9.5489.
24. Nishi K, Fu W, Kiyama R. Novel estrogen-responsive genes (ERGs) for the evaluation of estrogenic activity. *PLoS One*. 2022 Aug 17;17(8):e0273164. doi: 10.1371/journal.pone.0273164. eCollection 2022.
25. Yang M, Lee JH, Zhang Z, De La Rosa R, Bi M, Tan Y, Liao Y, Hong J, Du B, Wu Y, Scheirer J,

- Hong T, Li W, Fei T, Hsieh CL, Liu Z, Li W, Rosenfeld MG, Xu K. Enhancer RNAs Mediate Estrogen-Induced Decommissioning of Selective Enhancers by Recruiting ER α and Its Cofactor. *Cell Rep.* 2020 Jun 23;31(12):107803. doi: 10.1016/j.celrep.2020.107803.
26. Mueller GC, Vonderhaar B, Kim UH, Le Mahieu M. Estrogen action: an inroad to cell biology. *Recent Prog Horm Res.* 1972;28:1-49. doi: 10.1007/BF02558535
27. Mori K, Fujii R, Kida N, Takahashi H, Ohkubo S, Fujino M, Ohta M, Hayashi K. Complete primary structure of the human estrogen-responsive gene (pS2) product. *J Biochem.* 1990 Jan;107(1):73-6. doi: 10.1093/oxfordjournals.jbchem.a123014.
28. Terasaka S, Aita Y, Inoue A, Hayashi S, Nishigaki M, Aoyagi K, Sasaki H, Wada-Kiyama Y, Sa-kuma Y, Akaba S, Tanaka J, Sone H, Yonemoto J, Tanji M, Kiyama R. Using a customized DNA microarray for expression profiling of the estrogen-responsive genes to evaluate estrogen activity among natural estrogens and industrial chemicals. *Environ Health Perspect.* 2004 May;112(7):773-81. doi: 10.1289/ehp.6753.
29. Tang S, Han H, Bajic VB. ERGDB: Estrogen Responsive Genes Database. *Nucleic Acids Res.* 2004 Jan 1;32(Database issue):D533-6. doi: 10.1093/nar/gkh083.
30. Yamaga R, Ikeda K, Horie-Inoue K, Ouchi Y, Suzuki Y, Inoue S. RNA sequencing of MCF-7 breast cancer cells identifies novel estrogen-responsive genes with functional estrogen receptor-binding sites in the vicinity of their transcription start sites. *Horm Cancer.* 2013 Aug;4(4):222-32. doi: 10.1007/s12672-013-0140-3.
31. Ikeda K, Horie-Inoue K, Inoue S. Identification of estrogen-responsive genes based on the DNA binding properties of estrogen receptors using high-throughput sequencing technology. *Acta Phar-macol Sin.* 2015 Jan;36(1):24-31. doi: 10.1038/aps.2014.123.
32. Smid M, Wang Y, Klijn JG, Sieuwerts AM, Zhang Y, Atkins D, Martens JW, Foekens JA. Genes associated with breast cancer metastatic to bone. *J Clin Oncol.* 2006 May 20;24(15):2261-7. doi: 10.1200/JCO.2005.03.8802.
33. May FE. The potential of trefoil proteins as biomarkers in human cancer. *Biomark Med.* 2012 Jun;6(3):301-4. doi: 10.2217/bmm.12.22.
34. Domińska K, Okła P, Kowalska K, Habrowska-Górczyńska DE, Urbanek KA, Ochędalski T, Piastowska-Ciesielska AW. Angiotensin 1-7 modulates molecular and cellular processes central to the pathogenesis of prostate cancer. *Sci Rep.* 2018 Oct 25;8(1):15772. doi: 10.1038/s41598-018-34049-8.
35. Ghosh MG, Thompson DA, Weigel RJ. PDZK1 and GREB1 are estrogen-regulated genes expressed in hormone-responsive breast cancer. *Cancer Res.* 2000 Nov 15;60(22):6367-75.
36. Kim H, Tarhuni A, Abd Elmageed ZY, Boulares AH. Poly(ADP-ribose) polymerase as a novel regulator of 17 β -estradiol-induced cell growth through a control of the estrogen receptor/IGF-1 receptor/PDZK1 axis. *J Transl Med.* 2015 Jul 17;13:233. doi: 10.1186/s12967-015-0589-7.

37. Haines CN, Klingensmith HD, Komara M, Burd CJ. GREB1 regulates PI3K/Akt signaling to control hormone-sensitive breast cancer proliferation. *Carcinogenesis*. 2020 Dec 31;41(12):1660-1670. doi: 10.1093/carcin/bgaa096.
38. Sun L, Wu A, Bean GR, Hagemann IS, Lin CY. Molecular Testing in Breast Cancer: Current Status and Future Directions. *J Mol Diagn*. 2021 Nov;23(11):1422-1432. doi: 10.1016/j.jmoldx.2021.07.026.
39. Terasaka S, Inoue A, Tanji M, Kiyama R. Expression profiling of estrogen-responsive genes in breast cancer cells treated with alkylphenols, chlorinated phenols, parabens, or bis- and benzoylphenols for evaluation of estrogenic activity. *Toxicol Lett*. 2006 May 25;163(2):130-41. doi: 10.1016/j.toxlet.2005.10.005.
40. Dong S, Furutani Y, Kimura S, Zhu Y, Kawabata K, Furutani M, Nishikawa T, Tanaka T, Masaki T, Matsuoka R, Kiyama R. Brefeldin A is an estrogenic, Erk1/2-activating component in the extract of *Agaricus blazei* mycelia. *J Agric Food Chem*. 2013 Jan 9;61(1):128-36. doi: 10.1021/jf304546a.
41. Dong S, Terasaka S, Kiyama R. Bisphenol A induces a rapid activation of Erk1/2 through GPR30 in human breast cancer cells. *Environ Pollut*. 2011 Jan;159(1):212-218. doi: 10.1016/j.envpol.2010.09.004.
42. Shen W, Le S, Li Y, Hu F. SeqKit: A Cross-Platform and Ultrafast Toolkit for FASTA/Q File Manipulation. *PLoS One*. 2016 Oct 5;11(10):e0163962. doi: 10.1371/journal.pone.0163962.
43. Marcel M. Cutadapt removes adapter sequences from high-throughput sequencing reads. *EMBnet J*. 2011;17(1):10–12. doi: 10.14806/ej.17.1.200.
44. Kim D, Langmead B, Salzberg SL. HISAT: a fast spliced aligner with low memory requirements. *Nat Methods*. 2015 Apr;12(4):357-60. doi: 10.1038/nmeth.3317.
45. Trapnell C, Williams BA, Pertea G, Mortazavi A, Kwan G, van Baren MJ, Salzberg SL, Wold BJ, Pachter L. Transcript assembly and quantification by RNA-Seq reveals unannotated transcripts and isoform switching during cell differentiation. *Nat Bio-technol*. 2010 May;28(5):511-5. doi: 10.1038/nbt.1621.
46. Weidenfeld K, Schiff-Zuck S, Abu-Tayeh H, Kang K, Kessler O, Weissmann M, Neufeld G, Barkan D. Dormant tumor cells expressing LOXL2 acquire a stem-like phenotype mediating their transition to proliferative growth. *Oncotarget*. 2016 Nov 1;7(44):71362-71377. doi: 10.18632/oncotarget.12109.
47. Duong NT, Morris GE, Lam le T, Zhang Q, Sewry CA, Shanahan CM, Holt I. Nesprins: tissue-specific expression of epsilon and other short isoforms. *PLoS One*. 2014 Apr 9;9(4):e94380. doi: 10.1371/journal.pone.0094380.
48. Wang J, Yu H, Yili A, Gao Y, Hao L, Aisa HA, Liu S. Identification of hub genes and potential molecular mechanisms of chickpea isoflavones on MCF-7 breast cancer cells by integrated bioinformatics analysis. *Ann Transl Med*. 2020 Feb;8(4):86. doi: 10.21037/atm.2019.12.141.

49. Liao Y, Wang J, Jaehnig EJ, Shi Z, Zhang B. WebGestalt 2019: gene set analysis toolkit with revamped UIs and APIs. *Nucleic Acids Res.* 2019 Jul 2;47(W1):W199-W205. doi: 10.1093/nar/gkz401.
50. Oki S, Ohta T, Shioi G, Hatanaka H, Ogasawara O, Okuda Y, Kawaji H, Nakaki R, Sese J, Meno C. ChIP-Atlas: a data-mining suite powered by full integration of public ChIP-seq data. *EMBO Rep.* 2018 Dec;19(12):e46255. doi: 10.15252/embr.201846255.
51. Inoue A, Omoto Y, Yamaguchi Y, Kiyama R, Hayashi SI. Transcription factor EGR3 is involved in the estrogen-signaling pathway in breast cancer cells. *J Mol Endocrinol.* 2004 Jun;32(3):649-61. doi: 10.1677/jme.0.0320649.
52. Tourtellotte WG, Keller-Peck C, Milbrandt J, Kucera J. The transcription factor Egr3 modulates sensory axon-myotube interactions during muscle spindle morphogenesis. *Dev Biol.* 2001 Apr 15;232(2):388-99. doi: 10.1006/dbio.2001.0202.
53. Transcription factor early growth response 3 is associated with the TGF- β 1 expression and the regulatory activity of CD4-positive T cells in vivo. Sumitomo S, Fujio K, Okamura T, Morita K, Ishigaki K, Suzukawa K, Kanaya K, Kondo K, Yamasoba T, Furukawa A, Kitahara N, Shoda H, Shibuya M, Okamoto A, Yamamoto K. *J Immunol.* 2013 Sep 1;191(5):2351-9. doi: 10.4049/jimmunol.1202106.
54. Suehiro J, Hamakubo T, Kodama T, Aird WC, Minami T. Vascular endothelial growth factor activation of endothelial cells is mediated by early growth response-3. *Blood.* 2010 Mar 25;115(12):2520-32. doi: 10.1182/blood-2009-07-233478.
55. Vilarinho S, Sari S, Mazzacuva F, Bilgüvar K, Esendagli-Yilmaz G, Jain D, Akyol G, Dalgiç B, Günel M, Clayton PT, Lifton RP. ACOX2 deficiency: A disorder of bile acid synthesis with trans-aminase elevation, liver fibrosis, ataxia, and cognitive impairment. *Proc Natl Acad Sci U S A.* 2016 Oct 4;113(40):11289-11293. doi: 10.1073/pnas.1613228113.
56. Baes M, Van Veldhoven PP. Mouse models for peroxisome biogenesis defects and β -oxidation enzyme deficiencies. *Biochim Biophys Acta.* 2012 Sep;1822(9):1489-500. doi: 10.1016/j.bbadis.2012.03.003.
57. Lentjes MH, Niessen HE, Akiyama Y, de Bruïne AP, Melotte V, van Engeland M. The emerging role of GATA transcription factors in development and disease. *Expert Rev Mol Med.* 2016 Mar 8;18:e3. doi: 10.1017/erm.2016.2.
58. Güemes M, Garcia AJ, Rigueur D, Runke S, Wang W, Zhao G, Mayorga VH, Atti E, Tetradis S, Péault B, Lyons K, Miranda-Carboni GA, Krum SA. GATA4 is essential for bone mineralization via ER α and TGF β /BMP pathways. *J Bone Miner Res.* 2014 Dec;29(12):2676-87. doi: 10.1002/jbmr.2296.
59. Miranda-Carboni GA, Guemes M, Bailey S, Anaya E, Corselli M, Peault B, Krum SA. GATA4 regulates estrogen receptor-alpha-mediated osteoblast transcription. *Mol Endocrinol.* 2011

Jul;25(7):1126-36. doi: 10.1210/me.2010-0463.

60. Yu Z, Jiang E, Wang X, Shi Y, Shangguan AJ, Zhang L, Li J. Sushi Domain-Containing Protein 3: A Potential Target for Breast Cancer. *Cell Biochem Biophys*. 2015 Jun;72(2):321-4. doi: 10.1007/s12013-014-0480-9.

61. IL-20 receptor cytokines in autoimmune diseases. Chen J, Caspi RR, Chong WP. *J Leukoc Biol*. 2018 Nov;104(5):953-959. doi: 10.1002/JLB.MR1117-471R.

62. Su CH, Lin IH, Tzeng TY, Hsieh WT, Hsu MT. Regulation of IL-20 Expression by Estradiol through KMT2B-Mediated Epigenetic Modification. *PLoS One*. 2016 Nov 2;11(11):e0166090. doi: 10.1371/journal.pone.0166090.

63. Lee JY, Park YJ, Oh N, Kwack KB, Park KS. A transcriptional complex composed of ER(α), GATA3, FOXA1 and ELL3 regulates IL-20 expression in breast cancer cells. *Oncotarget*. 2017 Jun 27;8(26):42752-42760. doi: 10.18632/oncotarget.17459.

64. Chiarella E, Aloisio A, Scicchitano S, Bond HM, Mesuraca M. Regulatory Role of microRNAs Targeting the Transcription Co-Factor ZNF521 in Normal Tissues and Cancers. *Int J Mol Sci*. 2021 Aug 6;22(16):8461. doi: 10.3390/ijms22168461.

65. Bond HM, Scicchitano S, Chiarella E, Amodio N, Lucchino V, Aloisio A, Montalcini Y, Mesuraca M, Morrone G. ZNF423: A New Player in Estrogen Receptor-Positive Breast Cancer. *Front Endocrinol (Lausanne)*. 2018 May 18;9:255. doi: 10.3389/fendo.2018.00255.

66. Wang D, Fang J, Lv J, Pan Z, Yin X, Cheng H, Guo X. Novel polymorphisms in PDLIM3 and PDLIM5 gene encoding Z-line proteins increase risk of idiopathic dilated cardiomyopathy. *J Cell Mol Med*. 2019 Oct;23(10):7054-7062. doi: 10.1111/jcmm.14607.

67. Joustra SD, van Trotsenburg AS, Sun Y, Losekoot M, Bernard DJ, Biermasz NR, Oostdijk W, Wit JM. IGSF1 deficiency syndrome: A newly uncovered endocrinopathy. *Rare Dis*. 2013 May 2;1:e24883. doi: 10.4161/rdis.24883.

68. Wardell SE, Kazmin D, McDonnell DP. Research resource: Transcriptional profiling in a cellular model of breast cancer reveals functional and mechanistic differences between clinically relevant SERM and between SERM/estrogen complexes. *Mol Endocrinol*. 2012 Jul;26(7):1235-48. doi: 10.1210/me.2012-1031.

69. Moon HJ, Finney J, Xu L, Moore D, Welch DR, Mure M. MCF-7 cells expressing nuclear associated lysyl oxidase-like 2 (LOXL2) exhibit an epithelial-to-mesenchymal transition (EMT) phenotype and are highly invasive in vitro. *J Biol Chem*. 2013 Oct 18;288(42):30000-30008. doi: 10.1074/jbc.C113.502310.

70. Cano A, Eraso P, Mazón MJ, Portillo F. LOXL2 in Cancer: A Two-Decade Perspective. *Int J Mol Sci*. 2023 Sep 21;24(18):14405. doi: 10.3390/ijms241814405.

71. Bretschneider N, Kangaspeska S, Seifert M, Reid G, Gannon F, Dengler S. E2-mediated cathepsin D (CTSD) activation involves looping of distal enhancer elements. *Mol Oncol*. 2008

- Aug;2(2):182-90. doi: 10.1016/j.molonc.2008.05.004.
72. Cheng L, Li J, Han Y, Lin J, Niu C, Zhou Z, Yuan B, Huang K, Li J, Jiang K, Zhang H, Ding L, Xu X, Ye Q. PES1 promotes breast cancer by differentially regulating ER α and ER β . *J Clin Invest*. 2012 Aug;122(8):2857-70. doi: 10.1172/JCI62676.
 73. Rui X, Li Y, Jin F, Li F. TMPRSS3 is a novel poor prognostic factor for breast cancer. *Int J Clin Exp Pathol*. 2015 May 1;8(5):5435-42.
 74. Antony J, Dasgupta T, Rhodes JM, McEwan MV, Print CG, O'Sullivan JM, Horsfield JA. Cohe-sin modulates transcription of estrogen-responsive genes. *Biochim Biophys Acta*. 2015 Mar;1849(3):257-69. doi: 10.1016/j.bbagr.2014.12.011.
 75. Ha NT, Lee CH. Roles of farnesyl-diphosphate farnesyltransferase 1 in tumour and tumour mi-croenvironments. *Cells*. 2020 Oct 25;9(11):2352. doi: 10.3390/cells9112352.
 76. Dahlman-Wright K, Qiao Y, Jonsson P, Gustafsson JÅ, Williams C, Zhao C. Interplay between AP-1 and estrogen receptor α in regulating gene expression and proliferation networks in breast cancer cells. *Carcinogenesis*. 2012 Sep;33(9):1684-91. doi: 10.1093/carcin/bgs223.
 77. Uezu A, Kanak DJ, Bradshaw TW, Soderblom EJ, Catavero CM, Burette AC, Weinberg RJ, Soderling SH. Identification of an elaborate complex mediating postsynaptic inhibition. *Science*. 2016 Sep 9;353(6304):1123-9. doi: 10.1126/science.aag0821.
 78. Yue C, Bai Y, Piao Y, Liu H. DOK7 Inhibits Cell Proliferation, Migration, and Invasion of Breast Cancer via the PI3K/PTEN/AKT Pathway. *J Oncol*. 2021 Jan 22;2021:4035257. doi: 10.1155/2021/4035257.
 79. Liang J, Zhao H, Hu J, Liu Y, Li Z. SPOCD1 promotes cell proliferation and inhibits cell apop-tosis in human osteosarcoma. *Mol Med Rep*. 2018 Feb;17(2):3218-3225. doi: 10.3892/mmr.2017.8263.
 80. Chen PD, Liao YY, Cheng YC, Wu HY, Wu YM, Huang MC. Decreased B4GALT1 promotes hepatocellular carcinoma cell invasiveness by regulating the laminin-integrin pathway. *Oncogenesis*. 2023 Oct 31;12(1):49. doi: 10.1038/s41389-023-00494-y.
 81. Choi HJ, Chung TW, Kim CH, Jeong HS, Joo M, Youn B, Ha KT. Estrogen induced β -1,4-galactosyltransferase 1 expression regulates proliferation of human breast cancer MCF-7 cells. *Biochem Biophys Res Commun*. 2012 Oct 5;426(4):620-5. doi: 10.1016/j.bbrc.2012.08.140.
 82. Stevens TA, Meech R. BARX2 and estrogen receptor-alpha (ESR1) coordinately regulate the production of alternatively spliced ESR1 isoforms and control breast cancer cell growth and invasion. *Oncogene*. 2006 Aug 31;25(39):5426-35. doi: 10.1038/sj.onc.1209529.
 83. Harbin LM, Lin N, Ueland FR, Kolesar JM. SYNE1 mutation is associated with increased tumor mutation burden and immune cell infiltration in ovarian cancer. *Int J Mol Sci*. 2023 Sep 18;24(18):14212. doi: 10.3390/ijms241814212.
 84. Rodriguez-Acevedo AJ, Smith RA, Roy B, Sutherland H, Lea RA, Frith A, MacGregor EA,

- Griffiths LR. Genetic association and gene expression studies suggest that genetic variants in the SYNE1 and TNF genes are related to menstrual migraine. *J Headache Pain*. 2014 Oct 14;15(1):62. doi: 10.1186/1129-2377-15-62.
85. Liu H, Zhou Y, Qiu H, Zhuang R, Han Y, Liu X, Qiu X, Wang Z, Xu L, Tan R, Hong W, Wang T. Rab26 suppresses migration and invasion of breast cancer cells through mediating autophagic degradation of phosphorylated Src. *Cell Death Dis*. 2021 Mar 17;12(4):284. doi: 10.1038/s41419-021-03561-7.
86. Pei H, Wang W, Zhao D, Su H, Su G, Zhao Z. G Protein-Coupled Estrogen Receptor 1 Inhibits Angiotensin II-Induced Cardiomyocyte Hypertrophy via the Regulation of PI3K-Akt-mTOR Signaling and Autophagy. *Int J Biol Sci*. 2019 Jan 6;15(1):81-92. doi: 10.7150/ijbs.28304.
87. Schwidetzky U, Haendler B, Schleuning WD. Isolation and characterization of the andro-gen-dependent mouse cysteine-rich secretory protein-3 (CRISP-3) gene. *Biochem J*. 1995 Aug 1;309:831-6. doi: 10.1042/bj3090831.
88. Pathak BR, Breed AA, Deshmukh P, Mahale SD. Androgen receptor mediated epigenetic regulation of CRISP3 promoter in prostate cancer cells. *J Steroid Biochem Mol Biol*. 2018 Jul;181:20-27. doi: 10.1016/j.jsbmb.2018.02.012.
89. Piecha D, Hartmann K, Kobbe B, Haase I, Mauch C, Krieg T, Paulsson M. Expression of matrilin-2 in human skin. *J Invest Dermatol*. 2002 Jul;119(1):38-43. doi: 10.1046/j.1523-1747.2002.01789.x.
90. Avino S, De Marco P, Cirillo F, Santolla MF, De Francesco EM, Perri MG, Rigracciolo D, Dolce V, Belfiore A, Maggiolini M, Lappano R, Vivacqua A. Stimulatory actions of IGF-I are mediated by IGF-IR cross-talk with GPER and DDR1 in mesothelioma and lung cancer cells. *Oncotarget*. 2016 Aug 16;7(33):52710-52728. doi: 10.18632/oncotarget.10348.
91. Gao N, Nester RA, Sarkar MA. 4-Hydroxy estradiol but not 2-hydroxy estradiol induces expression of hypoxia-inducible factor 1alpha and vascular endothelial growth factor A through phosphatidylinositol 3-kinase/Akt/FRAP pathway in OVCAR-3 and A2780-CP70 human ovarian carcinoma cells. *Toxicol Appl Pharmacol*. 2004 Apr 1;196(1):124-35. doi: 10.1016/j.taap.2003.12.002.
92. Radulovich N, Leung L, Ibrahimov E, Navab R, Sakashita S, Zhu CQ, Kaufman E, Lockwood WW, Thu KL, Fedyshyn Y, Moffat J, Lam WL, Tsao MS. Coiled-coil domain containing 68 (CCDC68) demonstrates a tumor-suppressive role in pancreatic ductal adenocarcinoma. *Oncogene*. 2015 Aug 6;34(32):4238-47. doi: 10.1038/onc.2014.357.
93. Hua T, Ding J, Xu J, Fan Y, Liu Z, Lian J. Coiled-coil domain-containing 68 promotes non-small cell lung cancer cell proliferation in vitro. *Oncol Lett*. 2020 Dec;20(6):356. doi: 10.3892/ol.2020.12220. Epub 2020 Oct 14.
94. Wu Q, Cai C, Ying X, Zheng Y, Yu J, Gu X, Tu W, Lou X, Yang G, Li M, Jiang S. Electro-

- acu-puncture inhibits dendritic spine remodeling through the srGAP3-Rac1 signaling pathway in rats with SNL. *Biol Res.* 2023 May 22;56(1):26. doi: 10.1186/s40659-023-00439-0.
95. A Lahoz I, A Hall. A tumor suppressor role for srGAP3 in mammary epithelial cells. *Oncogene.* 2013 Oct;32(40):4854-60. doi: 10.1038/onc.2012.489.
96. John Mary DJS, Sikarwar G, Kumar A, Limaye AM. Interplay of ER α binding and DNA meth-ylation in the intron-2 determines the expression and estrogen regulation of cystatin A in breast cancer cells. *Mol Cell Endocrinol.* 2020 Mar 15;504:110701. doi: 10.1016/j.mce.2020.110701.
97. Irie K, Nagai T, Mizuno K. Furry protein suppresses nuclear localization of yes-associated protein (YAP) by activating NDR kinase and binding to YAP. *J Biol Chem.* 2020 Mar 6;295(10):3017-3028. doi: 10.1074/jbc.RA119.010783.
98. Liu Y, Chen X, Gong Z, Zhang H, Fei F, Tang X, Wang J, Xu P, Zarbl H, Ren X. Fry Is required for mammary gland development during pregnant periods and affects the morphology and growth of breast cancer cells. *Front Oncol.* 2019 Nov 21;9:1279. doi: 10.3389/fonc.2019.01279.
99. Tanji M, Kiyama R. Expression profiling of estrogen responsive genes using genomic and pro-teomic techniques for the evaluation of endocrine disruptors *Curr. Pharmacogenomics.* 2004 2:255-66. doi: 10.2174/1570160043377529.
100. Korpos É, Deák F, Kiss I. Matrilin-2, an extracellular adaptor protein, is needed for the re-generation of muscle, nerve and other tissues. *Neural Regen Res.* 2015 Jun;10(6):866-9. doi: 10.4103/1673-5374.158332.
101. Erasmus M, Samodien E, Lecour S, Cour M, Lorenzo O, Dlodla P, Pheiffer C, Johnson R. Linking LOXL2 to cardiac interstitial fibrosis. *Int J Mol Sci.* 2020 Aug 18;21(16):5913. doi: 10.3390/ijms21165913.
102. Barker HE, Chang J, Cox TR, Lang G, Bird D, Nicolau M, Evans HR, Gartland A, Erler JT. correction: LOXL2-mediated matrix remodeling in metastasis and mammary gland involution. *Cancer Res.* 2019 Oct 1;79(19):5123. doi: 10.1158/0008-5472.CAN-19-2420.
103. He M, Yu W, Chang C, Miyamoto H, Liu X, Jiang K, Yeh S. Estrogen receptor alpha promotes lung cancer cell invasion via increase of and cross-talk with infiltrated macrophages through the CCL2/CCR2/MMP9 and CXCL12/CXCR4 signaling pathways. *Mol Oncol.* 2020 Aug;14(8):1779-1799. doi: 10.1002/1878-0261.12701.
104. Liu J, Yu L, Castro L, Yan Y, Sifre MI, Bortner CD, Dixon D. A nongenomic mechanism for "metalloestrogenic" effects of cadmium in human uterine leiomyoma cells through G protein-coupled estrogen receptor. *Arch Toxicol.* 2019 Oct;93(10):2773-2785. doi: 10.1007/s00204-019-02544-0.
105. Hsu LH, Chu NM, Lin YF, Kao SH. G-protein coupled estrogen receptor in breast cancer. *Int J Mol Sci.* 2019 Jan 14;20(2):306. doi: 10.3390/ijms20020306.
106. García M, Barrio R, García-Lavandeira M, Garcia-Rendueles AR, Escudero A, Díaz-Rodríguez

- E, Gorbenko Del Blanco D, Fernández A, de Rijke YB, Vallespín E, Nevado J, Lapunzina P, Matre V, Hinkle PM, Hokken-Koelega AC, de Miguel MP, Cameselle-Teijeiro JM, Nistal M, Alvarez CV, Moreno JC. The syndrome of central hypothyroidism and macroorchidism: IGSF1 controls TRHR and FSHB expression by differential modulation of pituitary TGFbeta and Activin pathways. *Sci Rep*. 2017 Mar 6;7:42937. doi: 10.1038/srep42937.
107. Zheng Q, Gao J, Yin P, Wang W, Wang B, Li Y, Zhao C. CD155 contributes to the mesenchymal phenotype of triple-negative breast cancer. *Cancer Sci*. 2020 Feb;111(2):383-394. doi: 10.1111/cas.14276.
108. Li S, Ma YM, Zheng PS, Zhang P. GDF15 promotes the proliferation of cervical cancer cells by phosphorylating AKT1 and Erk1/2 through the receptor ErbB2. *J Exp Clin Cancer Res*. 2018 Apr 10;37(1):80. doi: 10.1186/s13046-018-0744-0.
109. Ikeda M, Chiba S, Ohashi K, Mizuno K. Furry protein promotes aurora A-mediated Polo-like kinase 1 activation. *J Biol Chem*. 2012 Aug 10;287(33):27670-81. doi: 10.1074/jbc.M112.378968.
110. Feng Y, Spezia M, Huang S, Yuan C, Zeng Z, Zhang L, Ji X, Liu W, Huang B, Luo W, Liu B, Lei Y, Du S, Vuppapapati A, Luu HH, Haydon RC, He TC, Ren G. Breast cancer development and progression: Risk factors, cancer stem cells, signaling pathways, genomics, and molecular pathogenesis. *Genes Dis*. 2018 May 12;5(2):77-106. doi: 10.1016/j.gendis.2018.05.001.
111. Zhao C, Tao T, Yang L, Qin Q, Wang Y, Liu H, Song R, Yang X, Wang Q, Gu S, Xiong Y, Zhao D, Wang S, Feng D, Jiang WG, Zhang J, He J. Loss of PDZK1 expression activates PI3K/AKT signaling via PTEN phosphorylation in gastric cancer. *Cancer Lett*. 2019 Jul 1;453:107-121. doi: 10.1016/j.canlet.2019.03.043.
112. Bacon C, Endris V, Rappold GA. The cellular function of srGAP3 and its role in neuronal morphogenesis. *Mech Dev*. 2013 Jun-Aug;130(6-8):391-5. doi: 10.1016/j.mod.2012.10.005.
113. Lee DH, Asare BK, Rajnarayanan RV. Discovery at the interface: Toward novel anti-proliferative agents targeting human estrogen receptor/S100 interactions. *Cell Cycle*. 2016 Oct 17;15(20):2806-18. doi: 10.1080/15384101.2016.1220460.
114. Sabe H, Hashimoto S, Morishige M, Ogawa E, Hashimoto A, Nam JM, Miura K, Yano H, On-odera Y. The EGFR-GEP100-Arf6-AMAP1 signaling pathway specific to breast cancer invasion and metastasis. *Traffic*. 2009 Aug;10(8):982-93. doi: 10.1111/j.1600-0854.2009.00917.x.
115. Huang M, Anand S, Murphy EA, Desgrosellier JS, Stupack DG, Shattil SJ, Schlaepfer DD, Cheresch DA. EGFR-dependent pancreatic carcinoma cell metastasis through Rap1 activation. *On-cogene*. 2012 May 31;31(22):2783-93. doi: 10.1038/onc.2011.450.
116. Shukla A, Yang Y, Madanikia S, Ho Y, Li M, Sanchez V, Cataisson C, Huang J, Yuspa SH. Evaluating CLIC4 in multiple cell types reveals a TGF-dependent induction of a dominant negative smad7 splice variant. *PLoS One*. 2016 Aug 18;11(8):e0161410. doi: 10.1371/journal.pone.0161410.
117. Yang T, Zhang H, Qiu H, Li B, Wang J, Du G, Ren C, Wan X. EFEMP1 is repressed by estro-

gen and inhibits the epithelial-mesenchymal transition via Wnt/beta-catenin signaling in endometrial carcinoma. *Oncotarget*. 2016 May 3;7(18):25712-25. doi: 10.18632/oncotarget.8263.

118. Simpson NE, Lambert WM, Watkins R, Giashuddin S, Huang SJ, Oxelmark E, Arju R, Hochman T, Goldberg JD, Schneider RJ, Reiz LF, Soares FA, Logan SK, Garabedian MJ. High levels of Hsp90 cochaperone p23 promote tumor progression and poor prognosis in breast cancer by increasing lymph node metastases and drug resistance. *Cancer Res*. 2010 Nov 1;70(21):8446-56. doi: 10.1158/0008-5472.CAN-10-1590.

119. Ghosh D, Egbuta C, Kanyo JE, Lam TT. Phosphorylation of human placental aromatase CYP19A1. *Biochem J*. 2019 Nov 15;476(21):3313-3331. doi: 10.1042/BCJ20190633.

120. Viedma-Rodríguez R, Baiza-Gutman L, Salamanca-Gómez F, Diaz-Zaragoza M, Mar-tínez-Hernández G, Ruiz Esparza-Garrido R, Velázquez-Flores MA, Arenas-Aranda D. Mechanisms associated with resistance to tamoxifen in estrogen receptor-positive breast cancer (review). *Oncol Rep*. 2014 Jul;32(1):3-15. doi: 10.3892/or.2014.3190.

121. Blanchet E, Van de Velde S, Matsumura S, Hao E, LeLay J, Kaestner K, Montminy M. Feed-back inhibition of CREB signaling promotes beta cell dysfunction in insulin resistance. *Cell Rep*. 2015 Feb 24;10(7):1149-57. doi: 10.1016/j.celrep.2015.01.046.

122. Bar-Sadeh B, Amichai OE, Pnueli L, Begum K, Leeman G, Emes RD, Stöger R, Bentley GR, Melamed P. Epigenetic regulation of 5alpha reductase-1 underlies adaptive plasticity of reproductive function and pubertal timing. *BMC Biol*. 2022 Jan 7;20(1):11. doi: 10.1186/s12915-021-01219-6.

123. Pranjol MZI, Gutowski NJ, Hannemann M, Whatmore JL. Cathepsin D non-proteolytically induces proliferation and migration in human omental microvascular endothelial cells via activation of the ERK1/2 and PI3K/AKT pathways. *Biochim Biophys Acta Mol Cell Res*. 2018 Jan;1865(1):25-33. doi: 10.1016/j.bbamcr.2017.10.005.

124. Suzuki YJ. Cell signaling pathways for the regulation of GATA4 transcription factor: Implications for cell growth and apoptosis. *Cell Signal*. 2011 Jul;23(7):1094-9. doi: 10.1016/j.cellsig.2011.02.007.

125. Xie K, Colgan LA, Dao MT, Muntean BS, Sutton LP, Orlandi C, Boye SL, Boye SE, Shih CC, Li Y, Xu B, Smith RG, Yasuda R, Martemyanov KA. NF1 is a direct G protein effector essential for opioid signaling to Ras in the striatum. *Curr Biol*. 2016 Nov 21;26(22):2992-3003. doi: 10.1016/j.cub.2016.09.010.

126. Moy I, Todorović V, Dubash AD, Coon JS, Parker JB, Buranapramest M, Huang CC, Zhao H, Green KJ, Bulun SE. Estrogen-dependent sushi domain containing 3 regulates cytoskeleton organization and migration in breast cancer cells. *Oncogene*. 2015 Jan 15;34(3):323-33. doi: 10.1038/onc.2013.553.

127. Harder L, Puller AC, Horstmann MA. ZNF423: Transcriptional modulation in development and cancer. *Mol Cell Oncol*. 2014 Dec 23;1(3):e969655. doi: 10.4161/23723548.2014.969655.

128. Zhang J, Chen QM. Far upstream element binding protein 1: a commander of transcription, translation and beyond. *Oncogene*. 2013 Jun 13;32(24):2907-16. doi: 10.1038/onc.2012.350.
129. Akman BH, Can T, Erson-Bensan AE. Estrogen-induced upregulation and 3'-UTR shortening of CDC6. *Nucleic Acids Res*. 2012 Nov;40(21):10679-88. doi: 10.1093/nar/gks855.
130. Xu ZW, Wang FM, Gao MJ, Chen XY, Hu WL, Xu RC. Targeting the Na(+)/K(+)-ATPase α 1 subunit of hepatoma HepG2 cell line to induce apoptosis and cell cycle arresting. *Biol Pharm Bull*. 2010;33(5):743-51. doi: 10.1248/bpb.33.743.
131. Cheng CT, Qi Y, Wang YC, Chi KK, Chung Y, Ouyang C, Chen YR, Oh ME, Sheng X, Tang Y, Liu YR, Lin HH, Kuo CY, Schones D, Vidal CM, Chu JC, Wang HJ, Chen YH, Miller KM, Chu P, Yen Y, Jiang L, Kung HJ, Ann DK. Arginine starvation kills tumor cells through aspartate exhaustion and mitochondrial dysfunction. *Commun. Biol*. 2018 Oct 26;1:178. doi: 10.1038/s42003-018-0178-4.
132. Baek A, Yoon S, Kim J, Baek YM, Park H, Lim D, Chung H, Kim DE. Autophagy and KRT8/keratin 8 protect degeneration of retinal pigment epithelium under oxidative stress. *Autophagy*. 2017 Feb;13(2):248-263. doi: 10.1080/15548627.2016.1256932.
133. Zhang S, Xia C, Xu C, Liu J, Zhu H, Yang Y, Xu F, Zhao J, Chang Y, Zhao Q. Early growth response 3 inhibits growth of hepatocellular carcinoma cells via upregulation of Fas ligand. *Int J Oncol*. 2017 Mar;50(3):805-814. doi: 10.3892/ijo.2017.3855.
134. Mauny A, Faure S, Derbré S. Phytoestrogens and breast cancer: should french recommendations evolve? *cancers (basel)*. 2022 Dec 14;14(24):6163. doi: 10.3390/cancers14246163.
135. Alshehri MM, Sharifi-Rad J, Herrera-Bravo J, Jara EL, Salazar LA, Kregiel D, Uprety Y, Akram M, Iqbal M, Martorell M, Torrens-Mas M, Pons DG, Daştan SD, Cruz-Martins N, Ozdemir FA, Kumar M, Cho WC. Therapeutic potential of isoflavones with an emphasis on daidzein. *Oxid Med Cell Longev*. 2021 Sep 9;2021:6331630. doi: 10.1155/2021/6331630.
136. Chen LR, Chen KH. Utilization of isoflavones in soybeans for women with menopausal syn-drome: an overview. *Int. J. Mol. Sci*. 2021 Mar 22;22(6):3212. doi: 10.3390/ijms22063212.
137. Zaheer K, Humayoun Akhtar M. An updated review of dietary isoflavones: nutrition, processing, bioavailability and impacts on human health. *Crit. Rev. Food Sci. Nutr*. 2017 Apr 13;57(6):1280-1293. doi: 10.1080/10408398.2014.989958.
138. Nagata C, Takatsuka N, Shimizu H, Hayashi H, Akamatsu T, Murase K. Effect of soymilk consumption on serum estrogen and androgen concentrations in Japanese men. *Cancer Epidemiol Bi-omarkers Prev*. 2001 10(3):179-84.
139. Wang Q, Ge X, Tian X, Zhang Y, Zhang J, Zhang P. Soy isoflavone: The multipurpose phyto-chemical. *Biomed. Rep*. 2013 1:697–701. doi: 10.3892/br.2013.129.
140. Ohba T, Iwata I, Takezaki C, Kudo N, Igita K, Shodai T, Hara M, Ikeda M, Taka-yanagi S, Shimotsu M, Hashimoto T, Shiga K, Tomita S. A new soybean cultivar FU-KUYUTAKA. *Bull*.

Kyushu Agr. Expt. Sta., 1982 22(3):405-432.

141. Nakazawa Y, Takahashi M, Komatsu K, Matsunaga K, Hajika M, Sakai S, Igita K. A new soybean cultivar Kurodamaru. Bull. of the NARO Kyushu Okinawa Agr. Res. Center. 2007 48:11-30. doi: 10.24514/00001980

142. Nishi K, Imamura I, Takemoto T, Iga K, Kiyama R. Estrogenic activity of fermented soymilk extracts and soy compounds. Appl. Food Res. 2023 3(2):100341. doi: 10.1016/j.afres.2023.100341

143. Bordignon J.R, Nakahara K, Yoshihashi T, Nikkuni S. Hydrolysis of isoflavones and consumption of oligosaccharides during lactic acid fermentation of soybean milk. Jpn. Agric. Res. Q. 2004 38(4):259–265. doi: 10.6090/jarq.38.259.

144. Langa S, Peirotén Á, Curiel JA, de la Bastida AR, Landete JM. Isoflavone metabolism by lactic acid bacteria and its application in the development of fermented soy food with beneficial effects on human health. Foods. 2023 Mar 18;12(6):1293. doi: 10.3390/foods12061293.

145. Choi Y, Kim K, Rhee J. Hydrolysis of soybean isoflavone glucosides by lactic acid bacteria. Biotechnol. Lett. 2002 24:2113–2116. doi: 10.1023/A:1021390120400.

146. Sun Y, Xu J, Zhao H, Li Y, Zhang H, Yang B, Guo S. Antioxidant properties of fermented soymilk and its anti-inflammatory effect on DSS-induced colitis in mice. Front Nutr. 2023 Jan 6;9:1088949. doi: 10.3389/fnut.2022.1088949.

147. Han JS, Joung JY, Kim HW, Kim JH, Choi HS, Bae HJ, Jang JH, Oh NS. Enhanced cholesterol-lowering and antioxidant activities of soymilk by fermentation with *Lactiplantibacillus plantarum* KML06. J. Microbiol. Biotechnol. 2023 Nov 28;33(11):1475-1483. doi: 10.4014/jmb.2306.06036.

148. Kiyama R, Wada-Kiyama Y. Estrogenic endocrine disruptors: Molecular mechanisms of action. Environ Int. 2015 Oct;83:11-40. doi: 10.1016/j.envint.2015.05.012.

149. Kiyama R. Estrogenic flavonoids and their molecular mechanisms of action. J Nutr Biochem. 2023 Apr;114:109250. doi: 10.1016/j.jnutbio.2022.109250.

150. Ruiz-Larrea MB, Mohan AR, Paganga G, Miller NJ, Bolwell GP, Rice-Evans CA. Antioxidant activity of phytoestrogenic isoflavones. Free Radic Res. 1997 Jan;26(1):63-70. doi: 10.3109/10715769709097785.

151. Arora A, Nair MG, Strasburg GM. Antioxidant activities of isoflavones and their biological metabolites in a liposomal system. Arch Biochem Biophys. 1998 Aug 15;356(2):133-41. doi: 10.1006/abbi.1998.0783.

152. Zhao J, Liu H, Qin R, Ho-Young C, Yang X. Ethnomedicinal uses, phytochemistry and bioactivities of *Sophora flavescens* Ait.: A review. J. Holist. Integr. Pharm. 2021 Sep;2(3):163-195. doi: 10.1016/S2707-3688(23)00077-8.

153. Chen M, Ding Y, Tong Z. Efficacy and Safety of *Sophora flavescens* (Kushen) Based Traditional Chinese Medicine in the Treatment of Ulcerative Colitis: Clinical Evidence and Potential Mecha-

- nisms. *Front Pharmacol*. 2020 Dec 10;11:603476. doi: 10.3389/fphar.2020.603476.
154. Wu J, Ma X, Wang X, Zhu G, Wang H, Li J. Efficacy and safety of compound kushen injection for treating advanced colorectal cancer: A protocol for a systematic review and meta-analysis. *Heliyon*. 2024 Feb 28;10(5):e26981. doi: 10.1016/j.heliyon.2024.e26981.
155. Chen X, Mukwaya E, Wong MS, Zhang Y. A systematic review on biological activities of prenylated flavonoids. *Pharm Biol*. 2014 May;52(5):655-60. doi: 10.3109/13880209.2013.853809.
156. Nishi K, Imamura I, Hoashi K, Kiyama R, Mitsuiki S. Estrogenic Prenylated Flavonoids in *Sophora flavescens*. *Genes* 2024 Feb 4;15(2):204. doi: 10.3390/genes15020204.
157. Chen L, Cheng X, Shi W, Lu Q, Go VL, Heber D, Ma L. Inhibition of growth of *Streptococcus mutans*, methicillin-resistant *Staphylococcus aureus*, and vancomycin-resistant enterococci by kurarinone, a bioactive flavonoid isolated from *Sophora flavescens*. *J Clin Microbiol*. 2005 Jul;43(7):3574-5. doi: 10.1128/JCM.43.7.3574-3575.2005.
158. Yim D, Kim MJ, Shin Y, Lee SJ, Shin JG, Kim DH. Inhibition of Cytochrome P450 Activities by *Sophora flavescens* Extract and Its Prenylated Flavonoids in Human Liver Microsomes. *Evid Based Complement Alternat Med*. 2019 Mar 13;2019:2673769. doi: 10.1155/2019/2673769.
159. De Naeyer A, Vanden Berghe W, Pocock V, Milligan S, Haegeman G, De Keukeleire D. Estrogenic and anticarcinogenic properties of kurarinone, a lavandulyl flavanone from the roots of *Sophora flavescens*. *J Nat Prod*. 2004 Nov;67(11):1829-32. doi: 10.1021/np040069a.